UNIVERSITY OF THE
WITWATERSRAND,
JOHANNESBURG

Agricultural pest management: Identification, characterisation, and stress tolerance of entomopathogenic nematodes

By

Kavisha Naidoo
(1517690)

A dissertation

Submitted in fulfilment of the requirements for the degree of
Master of Science

In

Molecular and Cell Biology

In the Faculty of Science, University of the Witwatersrand, Johannesburg, South Africa

Supervisor: Dr. Tiisetso Elizabeth Lephoto

June 2025

DECLARATION

I, Kavisha Naidoo, hereby declare that this dissertation is my own, unaided work. It is being submitted in fulfilment of the requirements for the degree of Master of Science at the University of the Witwatersrand, Johannesburg. This work has not been submitted previously for any degree or examination at any other university.

09th June 2025 in Johannesburg, Gauteng.

ABSTRACT

Sustainable agriculture faces increasing challenges from insect pests as climate change and pesticide resistance reduce the efficacy of conventional pest control methods. This study evaluated the biocontrol potential of two new nematode strains, *Oscheius* sp. k KN-2024 isolate kv-2022 and *Cruznema* sp. NTM-2021. Using insect-baiting and modified White-trap techniques, the nematodes and their symbiotic bacteria were isolated, with DNA extraction performed using E.Z.N.A kits followed by sequencing and bioinformatic identification. Laboratory experiments assessed the efficacy and environmental tolerance of these potential entomopathogenic nematodes (EPNs) under varying temperature and desiccation conditions to enhance their application as eco-friendly alternatives to chemical pesticides. *Cruznema* sp. NTM-2021 demonstrated efficacy across a broad temperature range (5-30°C), exhibiting opportunistic pathogenic characteristics, while *O.* sp. k KN-2024 displayed true entomopathogenic behaviour with optimal efficacy at 25°C. At elevated temperatures (37°C), insect mortality occurred independently of nematode infection, indicating complex temperature-host-pathogen interactions. Desiccation trials revealed superior survival rates for both strains at higher relative humidity levels (75-85%), with *O.* sp. k KN-2024 demonstrating significantly greater desiccation tolerance than *C.* sp. NTM-2021. Peak survival was observed at 85% relative humidity over 24 hours. Four-way ANOVA confirmed statistically significant differences in performance across experimental conditions. These findings provide critical insights for optimising strain-specific EPN deployment in diverse agricultural settings, potentially reducing chemical pesticide dependence. By characterising the environmental tolerances of these novel nematode strains, this research advances the development of targeted, sustainable biological control strategies for integration into environmentally conscious pest management systems.

Keywords: Entomopathogenic nematodes, eco-friendly biocontrol, sustainable, temperature tolerance, desiccation resistance, *Cruznema, Oscheius, Cruznema* sp. NTM-2021, *Oscheius* sp. k KN-2024.

Presentations arising from this Dissertation:

Naidoo, K. (2024). Enhancing Biocontrol Efficacy: Temperature and Desiccation Tolerance of Entomopathogenic Nematodes for Sustainable Agriculture. Oral presentation at the 15th Cross Faculty Symposium, University of the Witwatersrand, Johannesburg, South Africa.

In loving memory of my father

Krishna George Naidoo

1957 – 2015.

Forever my inspiration and guide.

And my beloved sister

Nikita Jenece Naidoo

2001 – 2024.

Forever in my heart, guiding my way.

ACKOWLEDGEMENTS

I would like to express my most sincere gratitude to my supervisor, Dr. Tiisetso Elizabeth Lephoto, for her invaluable guidance throughout my master's research.

I am deeply grateful to my colleague, Pusang King Sekobela, from the Nematology Laboratory for his guidance and support.

To my partner, Meelan Lakhoo, family and friends - thank you for your unwavering encouragement and support throughout this journey.

Special thanks to Mr. Michael Tobin and Ms. Naledi Nkabinde, from the Microbiology and Biotechnology department at the University of the Witwatersrand, for their extensive technical support and assistance.

Special thanks to Dr. Deran Reddy from the Microscopy and Microanalysis Unit at the University of the Witwatersrand for microscopy training and sharing his expertise.

I would like to acknowledge the National Research Foundation (NRF) and the Research Office at the University of the Witwatersrand for funding, which made this research possible.

TABLE OF CONTENTS

LIST OF FIGURES

LIST OF TABLES

ABBREVIATIONS

ABC	Augmentative biological control
A	Adenine
BF	Bright-field microscopy
BOD	Bio Oxygen Demand
Bt	*Bacillus thuringensis*
C	Cytosine
ddH_20	Double-distilled water
DIC	Differential interference contrast microscopy
EPBs	Entomopathogenic bacteria
EPNs/ EPN	Entomopathogenic nematodes
EMB	Eosin methylene blue
EtBr	Ethidium bromide
G	Guanine
HSPs	heat shock proteins
IJ	Infective juvenile
IPM	Integrated Pest Management
ITS	Internal transcribed spacer region
J (J1 – J4)	Juvenile stages 1-4 (entomopathogenic nematode larval stages)
L (L1 – L4)	Larval stages 1-4 (nematode developmental stages)
LB	Luria-Bertani
NB	Nutrient agar
NBTA	Nutrient Bromothymol Blue Triphenyltetrazolium Agar
RD	Rapid desiccation
RH	Relative humidity
SEM	Scanning electron microscope
T	Thymine
UN	United Nations
US/ USA	United states / United states of America

Chapter 1

Introduction

1.1 Current international crisis

The need for food, feed, biofuel, and fibre is rising globally. Projections by the International Food and Agricultural Trade Policy Council (IPC) in 2007 and the United Nations (UN) in 2012 estimated that by 2050, there would be a 50% increase in demand for food stocks to sustain the growing worldwide population which is expected to reach 9.73 billion (Godfray *et al.,* 2010; FAO, 2011; Fleming *et al.*, 2016). However, there are major challenges that are negatively impacting global food security. These include natural resource limitations, environmental pollution, ecological degradation, climate change and more importantly crop pests (FAO, 2011; Alexandratos and Bruinsma, 2012; Mc Carthy *et al.,* 2018).

According to Zhou *et al.* (2025), insect attacks cause the loss of over 45% of agricultural crop annually worldwide, costing the global economy approximately seventy billion US dollars. This challenge has led to extensive use of chemical pesticide since the early 20th century, resulting in dependence on these compounds to sustain agriculture. However, chemical pesticides negatively impact the environment, resulting in soil degradation, water contamination and disruption of beneficial insect populations, particularly pollinators such as honeybees *(Apis* spp.). Additionally, epidemiological studies have documented toxicity to humans, ranging from acute neurological to chronic conditions including neurodevelopmental disorders, carcinogenic effects, reproductive dysfunction, and potential disruption of immune and endocrine system function (Children, 1993; US EPA, 2015; Ahmad *et al.,* 2024).

1.2 Problem statement

The substantial crop loss experienced worldwide due to pest invasions and diseases spread by vectors, has driven the need for chemical pesticides for over 20 centuries. However, the vast negative impacts associated with their use, including human health disorders, the notable decline in biodiversity and the emergence of pesticide-resistant insects, has influenced the search for natural and sustainable alternatives (Aktar, Sengupta, and Chowdhury, 2009;

Nicolopoulou-Stamati *et al,* 2016; Koppenhöfer, Shapiro-Ilan, and Hiltpold, 2020; van der Linden, Fatouros and Kammenga, 2022).

The demand for sustainable alternatives has led to augmentative biological control (ABC) development. Within ABC strategies, entomopathogenic nematodes (EPNs) have emerged as a promising option, offering environmental sustainability and reduced risk of insect resistance compared to conventional chemical pesticides (Ehlers, 2005; Van der Linden, Fatouros and Kammenga, 2022).

However, EPNs show major limitations due to their susceptibility to unfavourable environmental conditions, particularly high temperatures and desiccation. These limitations are primarily due to their small size, and limited water regulation mechanisms, and lack of specialised water conservation structures (Shapiro-Ilan *et al.,* 2012). Open field applications further worsen the risk of desiccation. Therefore, investigating EPN temperature and desiccation tolerance is crucial for understanding their survival capacity in different environments.

1.3 Research motivation

EPNs represent a promising alternative to chemical pesticides, though their efficacy remains lower in comparison. Understanding how abiotic factors, particularly temperature and desiccation, influence EPNs performance and identifying their optimal conditions is crucial for advancing their large-scale agricultural applications. This knowledge would enable agricultural practitioners to select appropriate nematode species based on their regional temperature and rainfall patterns, thereby optimising biocontrol efficacy in diverse climatic zones. Additionally, these insights would contribute to the development of improved storage formulations—an important consideration for commercial viability.

1.4 Aims and objectives

Aim 1

Isolation, morphological, and molecular identification of nematodes

Objectives

- To isolate nematodes from soil collected in Gauteng, South Africa using insect baiting techniques
- To collect nematodes using White traps for subsequent analysis and experiments
- To perform morphological characterisation of the isolated nematode species using microscopy
- To extract DNA from the isolated nematode species
- To perform 18S rDNA sequencing
- To identify and classify the isolated nematode species using bioinformatics tools

Aim 2

Isolation and identification of symbiotic bacteria isolated from the *Oscheius sp.* k KN-2024

Objectives

- To isolate the symbiotic bacteria from the nematodes gut using sterile techniques
- To isolate pure bacterial colonies using non-selective and selective agar: nutrient agar, NBTA, and MacConkey agar
- To characterise the isolated bacteria through morphological and biochemical tests
- To extract the genomic DNA from the purified bacterial isolates
- To identify and classify the bacteria through 16S rDNA sequencing analysis

Aim 3

To investigate the efficacy of nematodes after exposure to temperature-dependent stress

Objectives

- To analyse the efficacy of the isolated nematodes under a range of temperature conditions (5, 25, 30 and 37°C)
- To statistically analyse the interaction effects of temperature, and strain-specific traits using four-way ANOVA to inform optimal deployment strategies

Aim 4

To investigate the survival and tolerance of nematodes after exposure to desiccation-dependent stress

Objectives

- To assess the survival of nematodes after exposure to varying desiccation conditions: (33, 53, 75 and 85% relative humidity)
- To analyse the efficacy of the nematodes in controlling insect pests following desiccation stress
- To statistically analyse the interaction effects of relative humidity, and strain-specific traits using four-way ANOVA to inform optimal deployment strategies

1.5 References

Aktar, Md.W., Sengupta, D. and Chowdhury, A., 2009. Impact of pesticides use in agriculture: their benefits and hazards, *Interdisciplinary Toxicology*, 2(1), pp. 1–12. doi:10.2478/v10102-009-0001-7

Ahmad, M.F., Ahmad, F.A., Alsayegh, A.A., Zeyaullah, Md., AlShahrani, A.M., Muzammil, K., Saati, A.A., Wahab, S., Elbendary, E.Y., Kambal, N., Abdelrahman, M.H., Hussain, S., 2024. Pesticides impacts on human health and the environment with their mechanisms of action and possible countermeasures. Heliyon 10, e29128. https://doi.org/10.1016/j.heliyon.2024.e29128

Children, N.R.C. (US) C. on P. in the D. of I. and, 1993. Background and Approach to the Study, in: Pesticides in the Diets of Infants and Children. National Academies Press (US).
Ehlers, R.U. 2005. Forum on safety and regulation', *Nematodes as Biocontrol Agents*, eds P. S. Grewal, R. -U. Ehlers, and D. I. Shapiro-Ilan (Wallingford: CABI Publishing), 107–114. doi: 10.1079/9780851990170.0107.

FAO. 2011. Land tenure, climate change mitigation and agriculture', *Mitigation of Climate Change in Agriculture (MICCA) Programme.* Rome.

Fleming, T.R., McGowan, N.E., Maule, A.G., Fleming, C.C., 2016. Prevalence and diversity of plant parasitic nematodes in Northern Ireland grassland and cereals, and the influence of soils and rainfall. Plant Pathology 65, 1539–1550. https://doi.org/10.1111/ppa.12525

Godfray, H.C.J., Beddington, J.R., Crute, I.R., Haddad, L., Lawrence, D., Muir, J.F., Pretty, J., Robinson, S., Thomas, S.M., Toulmin, C., 2010. Food Security: The Challenge of Feeding 9 Billion People. Science 327, 812–818. https://doi.org/10.1126/science.1185383

Koppenhöfer, A.M., Shapiro-Ilan, D.I., Hiltpold, I., 2020. Entomopathogenic Nematodes in Sustainable Food Production, *Frontiers in Sustainable Food Systems* 4.

Mc Carthy, U., Uysal, I., Badia-Melis, R., Mercier, S., O'Donnell, C., Ktenioudaki, A., 2018. Global food security – Issues, challenges and technological solutions. Trends in Food Science & Technology 77, 11–20. https://doi.org/10.1016/j.tifs.2018.05.002

Nicolopoulou-Stamati, P., Maipas, S., Kotampasi, C., Stamatis, P., Hens, L., 2016. Chemical Pesticides and Human Health: The Urgent Need for a New Concept in Agriculture, *Frontiers in Public Health 4*

Shapiro-Ilan, D.I., Bruck, D.J. and Lacey, L., 2012. Principles of Epizootiology and Microbial Control. In: Vega, F.E. and Kaya, H.K., Eds., Insect Pathology, 2nd Edition, Elsevier, London, 29-72. https://doi.org/10.1016/B978-0-12-384984-7.00003-8

US EPA, O., 2015. Human Health Issues Related to Pesticides [WWW Document]. URL https://www.epa.gov/pesticide-science-and-assessing-pesticide-risks/human-health-issues-related-pesticides (accessed 2.17.24).

van der Linden, C.F.H., Fatouros, N.E. and Kammenga, J.E., 2022. The potential of entomopathogenic nematodes to control moth pests of ornamental plantings, *Biological Control*, 165, p. 104815. Available at: https://doi.org/10.1016/j.biocontrol.2021.104815

Zhou, W., Li, M., Achal, V., 2025. A comprehensive review on environmental and human health impacts of chemical pesticide usage. Emerging Contaminants 11, 100410. https://doi.org/10.1016/j.emcon.2024.100410

Chapter 2
Literature review

2.1 Pesticides in agriculture

2.1.1 Pesticides

Pesticides are important for preventing substantial agricultural losses due to pest attack and in protecting crops against diseases caused by vectors (Abhilash and Singh., 2009; Zhou *et al.*, 2025). They are chemical or biological substances used to control, repel or eliminate unwanted organisms in agricultural and domestic settings (Children, 1993; Nicolopoulou-Stamati *et al.*, 2016; Sharma *et al.*, 2019; Pathak *et al.*, 2022; Kaur *et al.*, 2024). Pesticides consist of a wide range of agents including insecticides for controlling insects, fungicides for fungi, herbicides for weeds, rodenticides for rodents, molluscicides for molluscs, and nematicides for nematodes. Some pesticides also serve specialised agricultural functions as plant growth regulators, defoliants, or desiccants (Ball., 1996).

Modern agriculture is heavily dependent on pesticides to protect crops, improve produce yield and quality, and maintain food security for the growing population. This is as the reliance on agricultural systems for food production have become more intensive and industrialised (Boxall, 2001; Narayanasamy, 2005; Aktar *et al.*, 2009; Fenik, Tankiewicz and Biziuk, 2011; Strassemeyer *et al.*, 2017; Sharma *et al.*, 2019).

2.1.2 The history of pesticide use

Pesticides have been used for centuries, progressing from natural remedies to chemical substances (Mason, 1928; McCallan, 1967; Children, 1993; Tudi *et al.*, 2021; "National Institute of Environmental Health Sciences: Pesticides," n.d.). Pesticide use unfolds across three distinct periods. Initially, before 1870, natural pesticides, such as sulfur, were predominant in pest control practices. However, there was a major shift during the second period, spanning from 1870 to 1945, with synthetic chemical pesticides becoming increasingly common and widely adopted in agriculture (Abubakar *et al.*, 2020; Tudi *et al.*, 2021). There was a rise in the global production of synthetic pesticides, increasing by approximately 11%

annually, from 0.2 million tons in the 1950s to global output of over 3 million tons by the early 2000s (Bernardes *et al.,* 2015). Over three billion kgs of synthetic pesticides are used every year, however, only 1% of these are effective in controlling the target pests (Bernardes *et al.,* 2015; Tudi *et al.,* 2021). In the third period, after 1945, the harmful effects of synthetic pesticides were discovered, leading to the need for more sustainable, eco-friendly alternatives like genetically engineered crops and biological control agents (BCA) arose.

Synthetic pesticides are produced by modifying natural substances through chemical manufacturing processes and provide longer-lasting protection against pests. Some synthetic pesticides, such as copper sulfate and peracetic acid, meet organic farming standards and are permitted by regulatory bodies like the USDA in organic farming. However, many persist in the environment for prolonged periods of time, negatively impacting the ecosystem ("Natural vs. Chemical Pesticide," n.d; Stoate *et al.,* 2001; Power., 2010; McCoy, 2020).

2.1.3 The negative effects of chemical pesticides

While chemical pesticides provide essential pest control benefits in agriculture, they are known for their persistence and bioaccumulation. Their widespread use causes substantial risks to human health, ecosystems stability, and agricultural sustainability (Damalas and Koutroubas, 2016; Kaur *et al.,* 2024; Zhou *et al.,* 2025). Clinical and epidemiological studies have established strong associations between chemical pesticides exposure and a range of human health conditions, including reproductive dysfunction, endocrine disruption, neurological disorders, gastrointestinal complications and various forms of cancers (Bassil *et al.,* 2007; Alewu and Nosiri., 2011; Thakur *et al.,* 2014; "How pesticides impact human health and ecosystems in Europe,"., 2023). Research highlights that pregnant women and children are at higher risks, with pregnant women experiencing adverse birth outcomes and children showing increased vulnerability to developmental disorders and certain childhood cancers (Witczak and Abdel-Gawad., 2014; Nicolopoulou-Stamati *et al.,* 2016; CDC, 2025).

Chemical pesticides greatly impact the environment by causing disruption of ecosystems function and biodiversity. These substances lead to the decrease of populations of beneficial insects like bees and other pollinators, parasitoids, as well as birds, mammals and aquatic organisms (Aktar *et al.,* 2009; Harwood and Dolezal, 2020). Chemical pesticide runoff

contaminates water sources, harming soil microorganisms and aquatic ecosystems (Mahmood *et al.*, 2016; Tudi *et al.*, 2021; Zhou *et al.*, 2025).

According to Tang *et al.* (2021), an estimated 64% of the global agricultural land is at risk of pollution by pesticides. The initial effectiveness for short-term pest control masks the long-term effects of chemical pesticides. These chemicals may lead to pest resistance, secondary pest outbreaks, and reduced soil fertility over time. They may also negatively impact beneficial soil nematodes and microorganisms that are crucial for maintaining soil health and plant productivity (Zhou *et al.*, 2025). Furthermore, the economic costs not only include direct application costs, but also societal burdens, including healthcare expenses from exposure-related illnesses and lost productivity.

2.1.4 Alternatives to chemical pesticides

Natural pesticides are extracted from natural sources like minerals, plants, or animals and non-target organisms. These substances degrade quickly due to weather conditions or soil microbial activity. Some common examples of organic pesticides include diatomaceous earth, neem oil, and pyrethrins **Figure 1** (McCoy, 2020; Souto *et al.*, 2021; Pathak *et al.*, 2022).

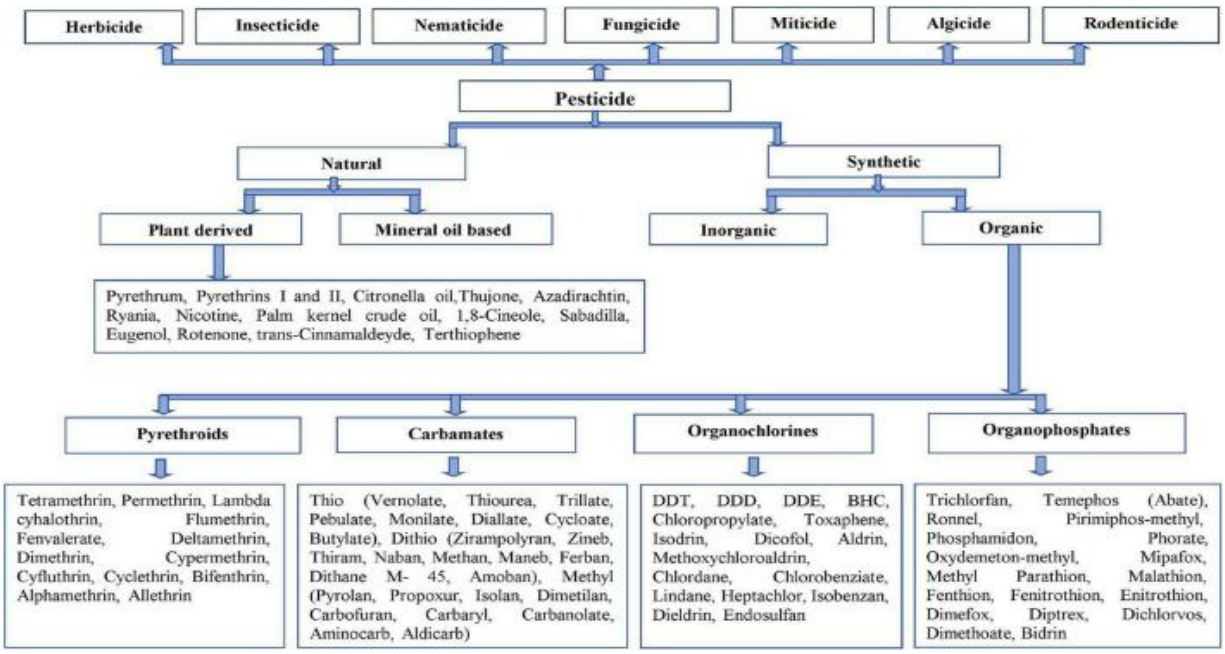

Figure 2.1 | Classification of pesticides (adapted from Pathak *et al.*, 2022).

2.1.5 Biological control agents

Among these alternatives, BCA emerged as a promising pest management strategy (Tudi *et al.*, 2021). Biological agents use as pesticides began in the 17th century with the observations of Italian naturalists Antonio Vallisnieri on insect parasitism (Tremblay and Masutti, 2005). Initially noted by Aldrovandi in 1602 and visually depicted by Goedart in 1662, these early records laid the basis for understanding parasitic behaviour. Van Leeuwenhoek's description in 1700 provided further insight, followed by Vallisnieri's accurate interpretation in 1706. Cestoni's contributions expanded taxonomic knowledge, while Darwin's discourse emphasised the ecological role of parasitoids in pest regulation (Tudi *et al.*, 2021).

These events show a progression from early observations to present understandings, shaping current pest management strategies with a focus on ecological sustainability. In November 2022, the rule facilitating the use of microorganisms as active substances in plant protection products was approved by the European Commission. This has made agriculture and plant protection practices more sustainable. This rule was passed as farmers across the European Union currently have better access to BCA (*Micro-organisms - European Commission*, no date).

Microorganisms such as viruses, bacteria, fungi as well as protozoa can be utilised as biocontrol agents as they can either be parasites or pathogens of insects that feed on or cause disease in plant (*Micro-organisms - European Commission*, no date). The use of bacteria, specifically species of *Bacillus thuringiensis* (Bt) has been safely used as biocontrol agents in many countries for over 30 years, including against the invasive pest *Spodoptera frugiperda* (fall armyworm), which has spread to South Africa (Nester *et al.*, 2002; Kumar *et al.*, 2021). Bt produces crystal proteins (Cry) that is toxic to insects of the orders Lepidoptera (moths and butterflies), Coleoptera (Weevils and beetles) and Diptera (mosquitos and flies). However, reports have stated that Bt is toxic to beneficial insects as well, particularly those of the order Hymenoptera (bees and wasps) (Bravo *et al.,* 2007). Despite this, Bt remains a part of the Integrated Pest Management (IPM) due to their efficiency (Kumar *et al.,* 2021). However, due to these concerns, the development of more targeted biocontrol agents emerged, giving way for other microorganism such as entomopathogenic nematodes to be used as BCA.

2.2 Nematodes as biocontrol agents

2.2.1 Nematodes

Nematodes are non-segmented, soft-bodied, invertebrate roundworms in the phylum Nematoda (Elsen *et al.*, 2007). They are the world's most diverse organisms and are naturally found living in a variety of environments, including deserts, mountains, arctic regions, oceans, diverse soils, open water bodies, as well as on other living organisms (Singh *et al.*, 2021; Tarasco *et al.*, 2023). With an evolutionary history dating back over 500 million years, nematodes represent one of the earliest and most successful animal groups on Earth. Their adaptability is evidenced by their estimated species diversity of 100,000 to 1 million species, though fewer than 25,000 have been formally described to date (Morand *et al.*, 2015). Most nematode species are free-living, feeding on bacteria and other microorganisms, while others are parasitic to plants and animals (Elsen *et al.*, 2007). A major proportion of nematodes, including the insect parasitic nematodes, are microscopic with the most common nematode, *Caenorhabditis elegans*, having a diameter of around fifty μm and length of around 1 mm except for the animal parasitic nematodes, which are large, about 33 mm long (Wyk and Mayhew, 2013; Andrews, 2019). Nematodes fall under many trophic positions within the soil food web, making them crucial in soil ecosystems. These organisms play crucial ecological roles in almost all ecosystem functions. They act as decomposers, predators, and prey, contributing greatly to nutrient cycling, carbon cycling, and soil health across terrestrial and marine ecosystems (Ferris., 2010; Zhang *et al.*, 2024). Their anatomical adaptations, including a protective collagenous cuticle, specialised digestive systems, and efficient osmoregulatory mechanisms, have enabled them to thrive in nearly every ecological niche (McSorley, 2003).

2.2.2 Life cycle of nematodes

Free-living nematode members of the *Rhabditidae* family progress through four larval stages (L1 to L4) prior to reaching reproductive maturity in favourable conditions (Golden and Riddle, 1984; Mata-Cabana *et al.*, 2021). The complete developmental cycle, including both normal and alternative pathways, is illustrated in **Figure 2.2**. The Dauer larvae is a specialised, non-feeding larval form adapted for dispersal and survival after exposure to adverse conditions. This stage is an alternative to the normal nematode life cycle and is triggered by environmental stressors—such as food scarcity, high population density, or high temperatures—allowing the

nematode to enter a state of arrested development (Golden and Riddle, 1984). It is characterised by a thickened cuticle, reduced metabolic activity and reliance on stored energy reserves. In free-living species like *C. elegans* and most *Cruznema*, the Dauer larvae persists until favourable conditions are restored. Nematodes in this stage are resilient, enabling their persistence and survival.

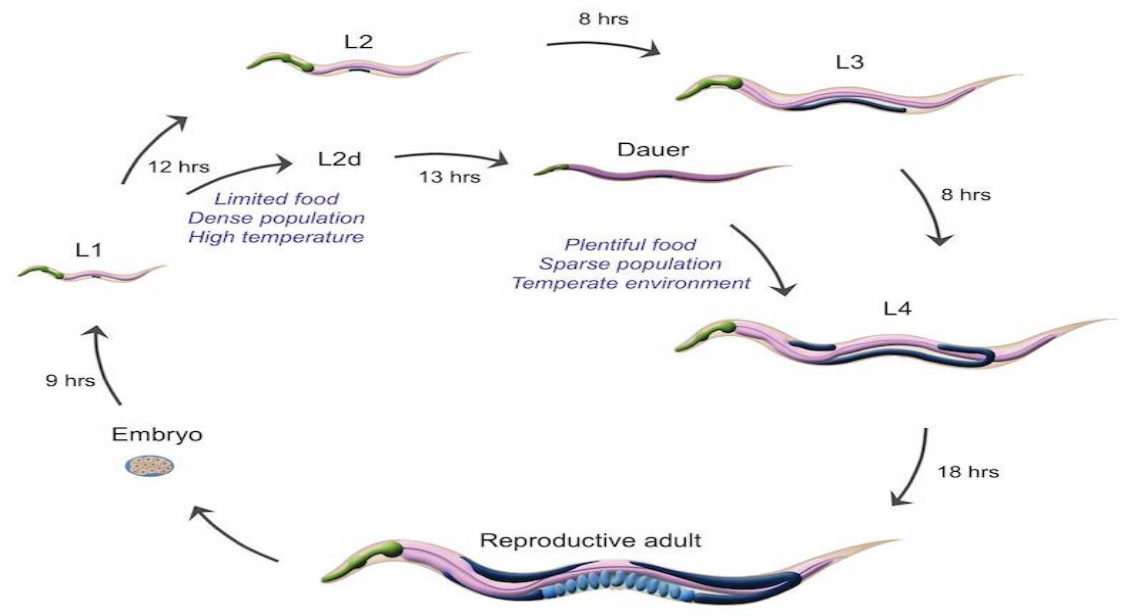

Figure 2.2 | Life cycle of nematodes. The cycle shows the developmental stages, environmental adaptations, and the potential for alternative developmental pathways in response to external conditions. The diagram details the progression through larval stages L1 to L4, highlighting the morphological changes and environmental influences that shape each developmental transition. Adapted from ("Dauer Introduction Overview," n.d.).

2.2.3 Entomopathogenic nematodes

Entomopathogenic nematodes or EPNs are soil-dwelling parasites of insects that have been effectively used globally as biocontrol agents against more than two hundred economically important insect crop pests (Grewal, Ehlers & Shapiro-Ilan 2006; Kaya & Gaugler 1993; Shapiro-Ilan, Gouge & Koppenhofer 2002). These beneficial nematodes thrive in moist soil environments and have been isolated from diverse habitats across all continents except Antarctica (Campos–Herrera *et al.*, 2012, Sharma *et al.*, 2021). The EPNs primarily utilised in biological control are those of the genus *Heterorhabditis* and *Steinernema*, along with the

recently characterised insectivorous members of the *Oscheius* genus (Ley & Blaxter, 2002; Lephoto *et al.*, 2016; Sharma *et al.*, 2021). The pros and cons of EPNs are listed in **Table 2.1** below.

Despite belonging to different taxonomic families (Steinernematidae for *Steinernema*, Heterorhabditidae for *Heterorhabditis* and Rhabditidae for *Oscheius*), these nematodes exhibit similarities in their parasitotic life cycle and host associations – a result of convergent evolution influenced by their predatory lifestyles, rather than shared ancestry (Koppenhöfer, Shapiro-Ilan & Hiltpold, 2020; Lillis, Griffin and Carolan, 2022). **Figure 2.3** illustrates IJs emerging from depleted wax moth insect cadavers following successful parasitism. The morphology under both a light and scanning electron microscope is also shown as well as the organisation of its internal structures.

Table 2.1 The pros and cons of EPNs (modified from Lacey and Georgis, 2012).

Pros	**Cons**
Highly effective against various insect pests.	Vulnerable to conditions such as temperature, desiccation, UV radiation and soil chemistries (pH and soil salinity).
Eliminates pests rapidly.	Production is costly.
Environmentally friendly.	Require specific storage and handling conditions for optimum viability.
Can be applied easily using standard spraying equipment.	Possesses a shorter shelf-life compared to chemical pesticides.
Short life cycle.	
Simple rearing requirements.	
Simple molecular manipulation.	
Safe for non-host organisms (invertebrates, and vertebrate - humans, plants, and animals).	

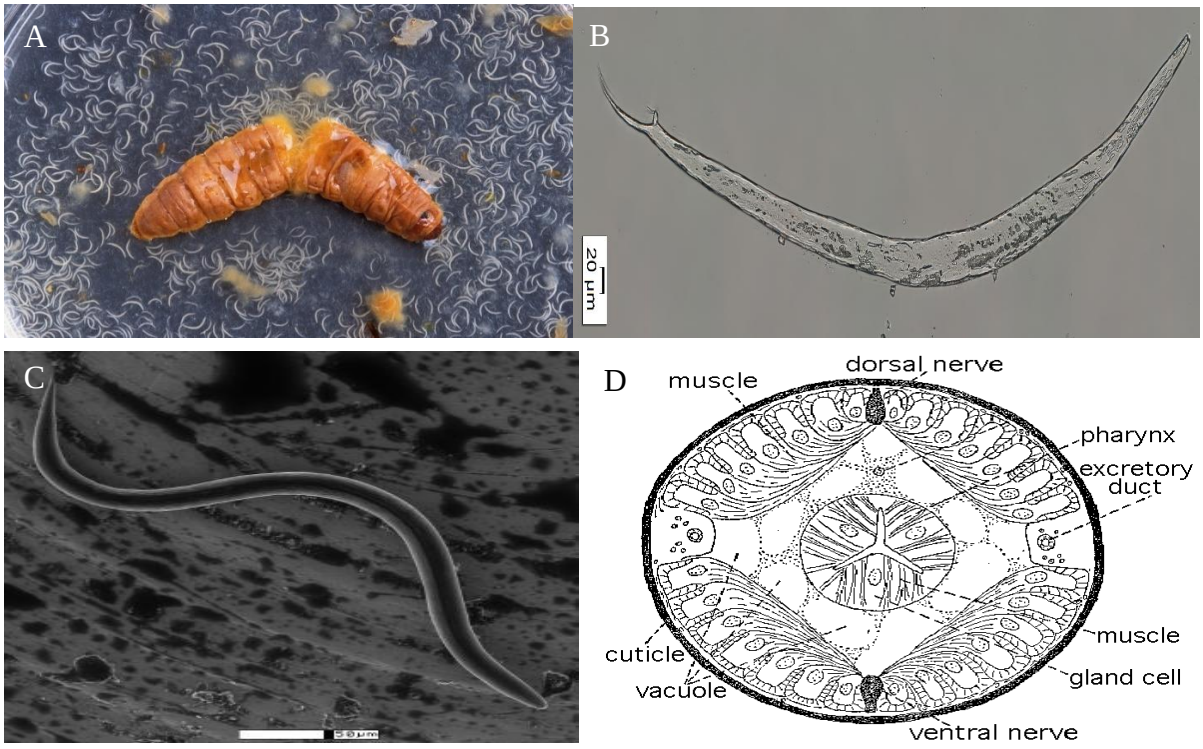

Figure 2.3 | EPNs A) IJs emerging from a depleted *Galleria mellonella* (wax moth) cadaver following successful parasitism (Greb, P., USDA Agricultural Research Service); **B)** Light microgram showing the morphology of the *Oscheius* sp. k KN-2024 nematode (Microscopy and Microanalysis Unit; University of the Witwatersrand); **C)** Nematode approximately 1 mm long viewed under an environmental scanning electron microscope (SEM); **D)** Diagrammatic view of nematode internal anatomy showing the organisms simplified organisational structure.

2.2.4 Bacteria

2.2.4.1 Proteobacteria

Proteobacteria is the largest and most diverse phylum in the domain bacteria. It encompasses a significant portion of known bacteria with ecological importance depicted in **Figure 4.2** (Maheshwari and Sankar, 2023). The phylum is divided into six classes, primarily: Alphaproteobacteria, Betaproteobacteria, Gammaproteobacteria, Deltaproteobacteria, Epsilonproteobacteria and the more recently recognised class, Zetaproteobacteria (Verma and Melcher, 2012; Rizzatti *et al.*, 2017; Maheshwari and Sankar, 2023). It is made up of a wide range of species that inhabit diverse environments like soil, water, and the guts of animals (Rizzatti *et al.*, 2017).

Proteobacteria perform a key role in the ecosystem as they are part of the biogeochemical cycles which includes the carbon, nitrogen, and sulphur cycles. They decompose organic matter, are involved in nitrogen fixation, as well as the mineralisation of various compounds, thus affecting the overall health and functioning of the ecosystem (Zhou., *et al.* 2020). Proteobacteria also interacts either mutualistically or parasitically with other organisms in the ecosystem, that is, plants, animals and other organisms. Alphaproteobacteria is well known for its nitrogen fixation function ("Proteobacteria - an overview | ScienceDirect Topics," n.d.). Betaproteobacteria is known for oxidising ammonia, and some have other biochemical compounds that make them resistant to other soil bacteria. Gammaproteobacteria on the other hand is divided into various families such as *Xanthamonas, Enterobacter* and *Proteobacter* which decomposes organic matter. This function is beneficial to plants and possesses ecological functions to soil. However, in this study we are more interested in Enterobacter because they are known to be associated with EPN symbiosis.

The characterisation and classification of bacteria is done by molecularly analysing the 16S rDNA gene sequence. These 1,550 base pair sequences consist of both conserved and variable sections. The 16S gene has sufficient interspecific polymorphisms to enable reliable differentiation of strains. With over 34 trillion base pairs from 4.7 billion sequences available in GenBank, and a large portion of this being the 16S rDNA gene sequences, comparisons with previously deposited sequences can effectively identify unknown strains (Clarridge, 2004; Sayers *et al.,* 2025). The evolutionary associations between species are inferred from the construction of a phylogenetic tree. Hence, members within each class do not share morphological or physical traits (Rizzatti *et al.,* 2017).

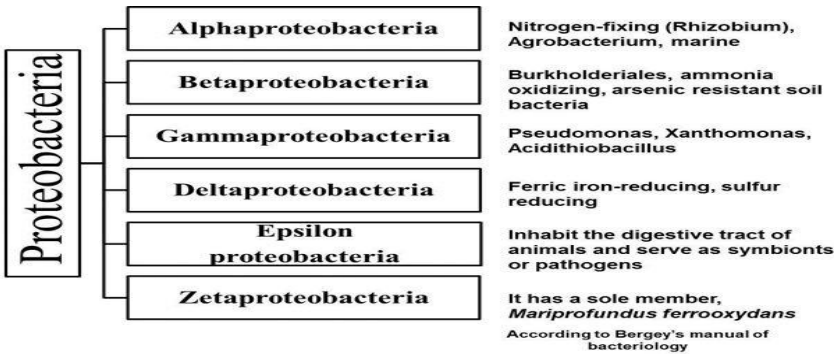

Figure 2.4 | Classification of bacteria into its sister bacteria groups and the ecological functions. Classification of Proteobacteria into major subclasses (Alpha, Beta, Gamma, Delta, Epsilon, Zeta) and their ecological roles, adapted from (Verma and Melcher, 2012).

2.2.4.2 The role of bacteria in EPN infectivity

Infectivity refers to the ability of an organism such as a pathogen or parasite to infect or invade a host organism and induce disease or harm (Silva and Jacintho, 1997; Barreto, Teixeira and Carmo, 2006). **Figure 2.5** depicts the major pathogenic bacterial species known to target and infect insect hosts.

For EPNs, infectivity refers to their ability to successfully cause infection and mortality in insect hosts with the assistance of symbiotic bacteria (Ruiz-Vega, Cortés-Martínez and García-Gutiérrez, 2018). Other microbial control, like *Bt*, causes passive infection, that is, when toxins produced by the bacteria are ingested by the insect hosts. However, the symbiotic bacteria of EPNs cause an active infection and hence have a broader host range (Pervez, Lone and Pattnaik, 2020).

All symbiotic bacteria of EPNs are non-spore forming, Gram-negative, facultative anaerobes that are rod shaped. Their phenotypic traits, particularly in their inability to convert nitrate to nitrite, a defining trait of bacteria in the Enterobacteriaceae, set them apart from other bacteria in this family (Boemare 2002; Imhoff 2005). Additionally, these bacteria exhibit phenotypic variability, existing in primary and secondary forms. However, the environmental cues triggering this variation and its significance in the life cycle of EPN symbionts remain ambiguous (Boemare and Akhurst 1988). They produce several secondary metabolites, including insect killing and antimicrobial compounds, like benzylideneacetone, phenethylamines. Their pathogenicity depends on their ability to reproduce within the hemocoel of the insect host and release toxic substances that leads to septicaemia, and eventually death (Ruiu, 2015).

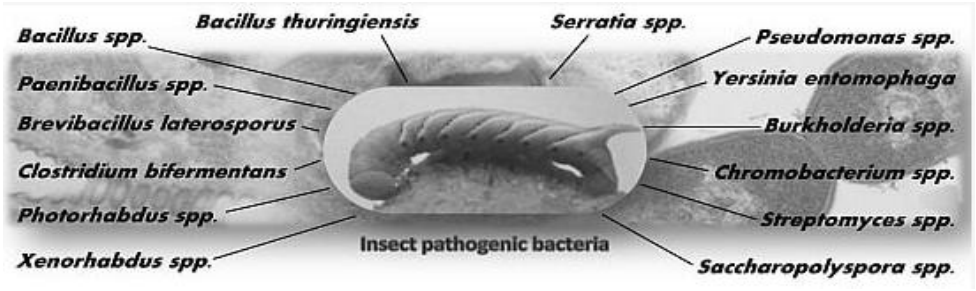

Figure 2.5 | Depicts the major pathogenic bacterial species known to target and infect insects through the production of various metabolites adapted from (Ruiu, 2015).

2.2.4.3 Noncognate bacteria in EPNs

Noncognate bacteria are bacterial species that coexist with EPNs but may not be their primary symbionts. These including members of the genera *Pseudomonas*, *Acinetobacter*, *Staphylococcus*, *Stenotrophomonas*, *Ochrobactrum*, and *Achromobacter* (Poinar., 1966; Mangowa and Serepa-Dlamini, 2020). However, very little information is available on these bacteria, and their role within the EPNs, and contributions to their infectivity is not well understood, requiring further research.

2.2.5 EPNs use as pesticides

EPNs were first identified by Gotthold Steiner in 1923 and then formally characterised by Poinar (1976) as suitable biocontrol agents (Kaya and Stock, 1997; Serepa-Dlamini and Gray, 2018; Shakeel *et al.*, 2022). Their efficacy as BCAs was first proven in 1931, when they were used to control the invasive pests like, *Popillia japonica*, the Japanese beetle in the United States (Birhan *et al.*, 2017). While EPNs are distributed worldwide, most of the characterised species originate from Asia (Abate *et al.*, 2017). Taxonomic records from Nemys Eds. (2025) document approximately 113 identified species within the genus *Steinernema* and 21 within *Heterorhabditis*. The commercialisation of EPNs, which occurred in the 1980s, has been selective, with only 13 species from *Steinernema* and *Heterorhabditis* genera being successfully developed for industrial-scale production and distribution (Lacey *et al.*, 2015; Helmberger *et al.*, 2017). In contrast, 23 of the recently characterised EPN species of the *Oscheius* genus have been presently isolated, but none have been commercialised (Serepa-Dlamini and Gray, 2018).

2.2.6 Life cycle of EPNs

2.2.6.1 Infective juveniles

EPNs such as *Steinernema*, *Heterorhabditis*, and some *Oscheius* species have evolved their free-living stage to support a specialised parasitic lifestyle. This developmental stage is known as the infective juvenile (IJ) which represents the only free-living stage of EPNs. Unlike typical nematodes with L1 to L4 larval stages, EPNs progress through J1 to J4 juvenile stages before becoming IJs. They enter this durable stage in the absence of insect hosts (Akhurst and Boemare, 1990; O'Leary *et al.*, 1998; Oliveira-Hofman *et al.*, 2019).

IJs form a symbiotic relationship with bacteria inhabiting their digestive system (Sharma *et al.*, 2021). The symbiotic bacteria of *Heterorhabditis* are found in the anterior intestine, while in most *Steinernema* species, they inhabit specialised intestinal vesicles (Campos-Herrera *et al*., 2013; Pervez *et al.*, 2020). Together, the EPNs and their symbiotic bacteria play a crucial role in successfully targeting and causing mortality in insect hosts. The life cycle is depicted in **Figure 2.6** below.

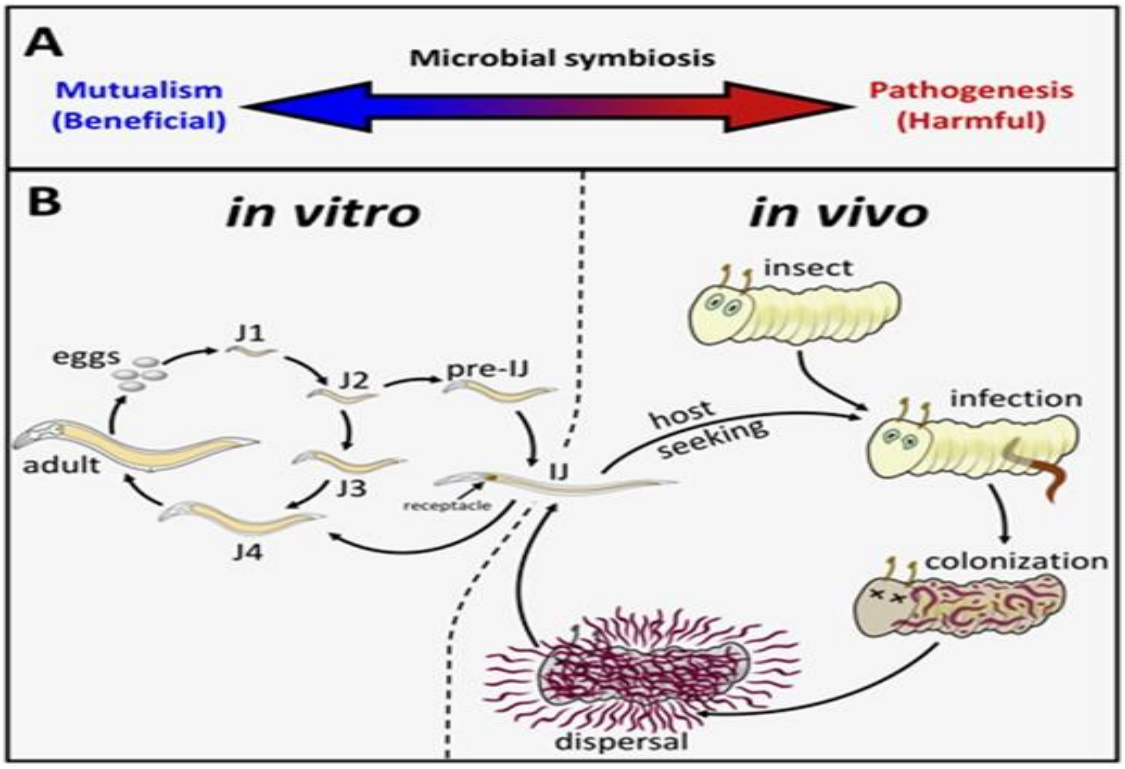

Figure 2.6 | EPNs life cycle adapted from (Cao *et al.,* 2022). **(a)** A spectrum of microbial symbiosis illustrating the continuum from mutualism (beneficial interactions) to pathogenesis (harmful interactions). **(b)** Developmental stages and infection cycle of entomopathogenic nematodes (EPNs) in vitro and in vivo. The in vitro panel shows the progression through J1-J4 juvenile stages from eggs to adults, including pre-IJ and IJ stages. The in vivo panel depicts the host-seeking behaviour, infection process, and colonisation of an insect host, highlighting the nematodes' ability to disperse and establish a symbiotic relationship. The EPNs undergo three generations within the host before emerging from the cadaver.

2.2.6.2 Foraging strategies of EPNs

The foraging strategies of parasitic nematodes, including EPNs, and the infection of hosts, are informed by olfactory and mechanosensory cues (Zhang *et al.,* 2019). The IJ stage of EPNs use host-seeking behaviours to locate suitable insect hosts to infect. IJs respond to various environmental cues when host-seeking (Baiocchi *et al.,* 2017; Zhang *et al.,* 2021). They detect chemical signals like carbon dioxide gradients, which helps them locate biological activity, along with plant volatiles released after herbivore damage, and insect-derived compounds. Physical factors also influence their foraging behaviour, and these include soil conditions (texture and moisture), temperature, host movement vibrations and sometimes light (Jones 2002; Matuska-Łyżwa *et al.,* 2024). EPNs employ two primary mechanisms to find hosts: chemotaxis - their directed movement in response to chemical gradients – and nictating, where they stand on their tails to attach to passing insect hosts (Campbell and Gaugler, 1997; Zhang *et al.,* 2021). By sensing these combined cues, EPNs can not only find hosts but also evaluate their quality, such as whether they are already infected or their diet composition.

EPNs employ two main foraging strategies: ambushing and cruising. Ambushers remain stationary, using nictating behaviour to attach to mobile hosts. In contrast, cruisers actively move through soil to find inactive prey. Cruisers may travel up to 90 cm horizontally and vertically in search of hosts and generally infect the less mobile hosts.

Once an insect host is located through foraging, EPNs begin their parasitic life cycle. This cycle is characterised by distinct developmental stages, beginning with the infective juvenile (IJ). Upon successful host location, IJs utilise foraging strategies to track and infect insect hosts,

transitioning from their free-living environmental stage to the parasitic phase of their life cycle (Ramakrishnan *et al.*, 2022).

2.2.6.3 Life cycle

IJs actively search for uninfected or newly infected insect hosts within the soil and enter through their natural openings (mouth, anus, or spiracles) or occasionally directly through the cuticle (Koppenhöfer *et al*., 2020; Ruiu *et al.*, 2022). Upon entering, their symbiotic bacteria are released into the insect's hemocoel through regurgitation (Dziedziech, Shivankar and Theopold, 2020). These bacteria multiply rapidly, producing toxins and secondary metabolites that suppress the host's immune system, causing mortality in 24-48 hours (Mollah and Kim, 2020; Koppenhöfer, Shapiro-Ilan and Hiltpold, 2020; Ashish *et al*, 2021). The bacteria then multiply within the cadaver, creating an ideal nutrient environment for nematode development and reproduction while preventing other organisms and microorganisms from feeding on the cadaver (Koppenhöfer *et al.*, 2020; Ashish *et al*, 2021; Cao *et al.*, 2021; Lillis, Griffin and Carolan, 2022). The nematodes then feed on bacterial cells and decomposing host tissues, developing through juvenile stages (J1-J4) to adulthood (Cao *et al.*, 2022). Adults reproduce within the insect cadaver, with females laying eggs that hatch into juveniles. As resources deplete, second-stage juveniles (J2) associate with the symbiotic bacteria and divert from normal development, forming new IJs instead of third-stage juveniles (J3). These new IJs, carrying symbiotic bacteria in their intestines, emerge from the depleted insect cadaver to seek new hosts, thus completing the cycle that spans 7-14 days based on the temperature and host size (Baiocchi *et al.*, 2017; Půža and Machado, 2024).

EPNs of *Steinernema, Heterorhabditis* and *Oscheius* display similar traits and life cycles despite lacking close genetic relationships (Blaxter *et al.*, 1998). The specific mechanisms of host killing vary between nematode genera. In *Heterorhabditis-Photorhabdus* partnerships, the bacteria contribute predominantly to host mortality (Koppenhöfer *et al*., 2020). On the other hand, in *Steinernema-Xenorhabdus* interactions, the nematodes perform a more active role by releasing venom proteins that damage tissues and modulate the host's immune response (Lu *et al*., 2017; Chang *et al*., 2019). Some members of the *Oscheius* genus, such as *O. insectivorus*, lack entomopathogenic traits entirely, possibly due to the absence of symbiotic relationships with pathogenic bacteria (Lephoto *et al.*, 2016).

2.2.7 Types of EPNs and their associated symbiotic bacteria

Steinernema and *Heterorhabditis* are obligate parasites that rely on their symbiotic bacteria *Xenorhabdus* and *Photorhabdus* respectively to complete their life cycle. Their life cycle is completed within an insect host (Castillo *et al.,* 2011). In contrast, facultative parasites such as *Cruznema* and non-EPN *Oscheius* species can complete their lifecycle without insect hosts, but when present, show opportunistic parasitism. Nematodes of *Oscheius* and *Cruznema* associate with various bacteria rather than specific symbionts. *Oscheius* often associates with *Serratia* and *Cruznema* forms opportunistic associations without a fixed bacterial symbiont.

EPNs have evolved symbiotic relationships with bacteria that plays important roles in both the life cycle as well as the pathogenic abilities of EPNs. The parasitic abilities of EPNs are due to the associated mutualistic gram-negative Enterobacteriacea; *Xenorhabdus*, *Photorhabdus* and *Serratia* which are associated with the genera *Steinernema*, *Heterorhabditis* and *Oscheius,* respectively (Lephoto *et al*., 2016; Orozco, Lee, & Stock, 2014). This symbiosis is essential for the effectiveness of EPNs as BCA. The bacterial symbionts produce and release a wide variety of metabolites and toxic protein compounds, including cytotoxins, insecticides, antiparasitic and antimicrobials, that causes insect mortality in hosts. (Fukruksa *et al.,* 2017; Zhang *et al.,* 2022).

2.2.7.1 *Steinernema*

The genus *Steinernema* consists of the most diverse group of EPNs with over 113 species identified (Bhat *et al.,* 2020). They form symbiotic relationships with the bacteria of the genus *Xenorhabdus* which is harboured in the bacterial receptacle located in the anterior portion of the intestine (Kim *et al.,* 2012). They are characterised by their amphimictic reproduction, that is, they require the union of both males and female gametes from separate individuals to reproduce (Půža and Machado, 2024). They have distinctive morphological features including the presence of six labial papillae and a prominent excretory pore positioned anterior to the nerve ring (Fayyaz *et al.,* 2001). They exhibit both cruising and ambushing host-finding strategies. Species like *S. carpocapsae*, *S. feltiae*, and *S. glaseri* have been highly commercialised and show differential efficacy against various insect pests depending on their foraging behaviour and host preference (Abate *et al.,* 2017). *Steinernematids* are closely associated with *Strongyloididae* (Lillis, Griffin and Carolan, 2022).

The genus *Xenorhabdus* comprises of Gram-negative bacteria from the family *Enterobacteriaceae* and is primarily associated with nematodes of the genus *Steinernema*. This association is characterised by a high degree of species specificity, where *Xenorhabdus* species form symbiotic relationships with specific *Steinernema* species (Akhurst and Boemare, 1988). *Xenorhabdus* are enclosed within a specialised vesicle in the intestine. The *Xenorhabdus* bacteria play multiple critical roles in the EPN life cycle, including rapid killing of the host by producing toxins, bioconversion of host tissues into nutrients accessible to the nematodes, production of antibiotics to prevent competition from other microorganisms, and support of nematode reproduction (Forst and Clarke, 2002). For instance, in the case of *Steinernematids*, like *Steinernema carpocapsae*, the obligate symbiont *Xenorhabdus nematophila* releases a wide range of proteins which supresses immunity in the host and leads to death within 24 to 48 hours (Lillis, Griffin and Carolan, 2022; Zhang *et al.*, 2022).

2.2.7.2 *Heterorhabditis*

The genus *Heterorhabditis* consist of over 21 identified species that associate with bacteria of the genus *Photorhabdus* (Nemys Eds., 2025). Unlike *Steinernema, Heterorhabditis* species reproduce through self-fertilising hermaphroditism in their first generation, followed by amphimictic reproduction in subsequent generations (Půža and Machado, 2024). This reproductive flexibility provides an adaptive advantage during the initial colonisation of insect hosts. Morphologically, they possess distinctive features such as an external sheath over the infective juvenile and a dorsal tooth in the buccal cavity used to penetrate the insect cuticle. *Heterorhabditis* species primarily employ a "cruiser" foraging strategy, actively searching through soil for hosts, which makes them effective against sedentary and soil-dwelling pests. Commercially important species include *H. bacteriophora*, *H. megidis*, and *H. indica*. *Heterorhabditis* shows close relationships with the vertebrate parasites *Strongylida* and *C. elegans* (Lillis, Griffin and Carolan, 2022).

Similarly, the genus *Photorhabdus*, also part to the *Enterobacteriaceae* family, forms a mutualistic relationship with nematodes of the genus *Heterorhabditis*. *Photorhabdus* species are unique among terrestrial bacteria due to their bioluminescent properties and are found to inhabit the entire nematode intestine (Boemare *et al.*, 1993). A well-studied example of this symbiosis is the relationship between *Photorhabdus luminescens* and *Heterorhabditis bacteriophora*. Like *Xenorhabdus, Photorhabdus* bacteria are essential for the pathogenicity

and reproductive success of their nematode hosts. They produce difference virulence factors, including hydrolytic enzymes and toxins that result in rapid death of the host and the subsequent bioconversion of its tissues.

2.2.7.3 *Oscheius*

The genus *Oscheius* is the most recent described group of EPNs that belongs to the family *Rhabditidae*. *Oscheius* species are facultative insect parasites, capable of completing their life cycles both as free-living organisms (clade: Dolichura) and as insect parasites (clade: Insectivora) (Sudhaus and Hooper 1994). The entomopathogenic members of this genus primarily occur in the Insectivora group, with few exceptions (Torrini *et al.,* 2015). By 2019, 30 species within the subgenus Insectivora group and 14 species in the Dolichura group have been identified (Kumar *et al.,* 2019; Abolafia and Peña-Santiago, 2019; Ghavamabad *et al.,* 2021). Some identified entomopathogenic species include *O. chongmingensis, O. carolinensis,* and *O. safricana,* the latter discovered in South Africa and demonstrating great potential against indigenous pest species (Lephoto *et al.,* 2016; Campos-Herrera *et al.,* 2019; Torres-Barragan *et al.,* 2011).

Oscheius spp. associate with various bacterial genera, including *Bacillus*, *Klebsiella*, *Acinetobacter*, *Comamonas*, *Achromobacter*, *Providencia*, *Enterobacter*, *Proteus*, *Pseudomonas*, *Enterococcus*, *Serratia*, and *Staphylococcus*. Some of these bacteria, such as *Bacillus cereus*, *Flavobacterium* sp., *Serratia marcescens*, and *Serratia nematodiphila*, are known for their ability to infect a wide range of insects and ability to enhance nematode reproduction (Grimont and Grimont, 1978; Lephoto *et al.,* 2016; Fu and Liu, 2019).

Serratia sp. are mostly associated with *Oscheius* sp, and produce various virulence factors, including chitinases and proteases, which contribute to insect pathogenicity (Torres-Barragan *et al.,* 2011). However, the relationship between *Serratia* and nematodes is generally less specific compared to the *Xenorhabdus* - *Steinernema* and *Photorhabdus* - *Heterorhabditis* associations. *Oscheius* spp are effective biological control agents due their endosymbiotic bacteria which belongs to two genera *Serratia* and *Enterococcus* (Ghavamabad *et al.,* 2021). The lethality of EPNs and mortality rate is determined by the symbiotic bacteria associated with each species (Ghavamabad *et al.,* 2021). Unlike some EPNs that rely on specific host species, *Oscheius* spp. exhibit a broad host range, enabling them to target a wide range of

insects across various ecosystems (Sangeetha *et al.,* 2016). This makes the species valuable in integrated pest management programs, where they can be used to combat a wide range of agricultural and horticultural pests (Sangeetha *et al.,* 2016).

2.2.7.4 *Cruznema*

The species in genus *Cruznema* of the family *Rhabditidae* are free-living nematodes typically found in soil or decaying organic matters (Doucet, 1994; Du *et al.,* 2022). Despite their ecological presence, these nematodes have not been well defined and characterised. Through phylogenetic analysis, the genus has been identified as monophyletic and closely related to *C. elegans* (Du *et al.,* 2022; Guo *et al.,* 2023). *Cruznema* species are primarily saprophagous or bacterivorous – feeding on decaying material or bacteria respectively – and is key in improving the quality of the soil by assisting in the mineralisation of nitrogen through decomposition of organisms in the food web and by consuming bacteria and excreting excess nitrogen (Doucet, 1994; Ferris *et al.,* 1997). Species of *Cruznema* are not classified as EPNs, however, some species like *C. lincolnensis,* are parasitic to crickets and molluscs (Reboredo and Camino, 1998; Camino and Achinelly., 2011; Grewal *et al.,* 2011).

There are seven well described species of *Cruznema* to date, and these are *Cruznema campestris n. sp, Cruznema graciliformis* (Sudhaus, 1978), *Cruznema lincolnensis, Cruznema minimus, Cruznema scarabaeum, Cruznema tripartutum* and lastly, *Cruznema velatum* (Du *et al.*, 2022). Their limited direct economic importance compared to other nematode groups has resulted in knowledge gaps regarding their full ecological roles and potential applications.

C. campestris, discovered in Argentina, consist of 4 odontoplates with the males being distinguished by having 9 pairs of genital papillae, 5 postanal and 4 preanal (Reboredo and Camino, 2000). The nematode species *C. lincolnesis*, originating in Lincoln Buenos Aires, was found to be a parasitic nematode of the cricket *Gryllodes laplatae* (Orthoptera: Gryllidae). These nematodes can be differentiated by the presence of two pairs of preanal papillae, while the males consist of six pairs of postanal papillae and a single pair of adanal papillae (Reboredo and Camino, 1998).

C. minimus possesses a cuticle that is 2–3 μm thick, featuring clear punctations, six lateral lines, and a stoma that is 4–5 times longer than its width. The metastegostom is isomorphic,

and the pharynx has a pyriform bulb containing a single-chambered haustrulum (Sultana and Pervez, 2019). The post uterine sac is approximately half the size of the corresponding body diameter, and the uterus lacks eggs. The spermatheca is not well-defined, and in males, spicules measure between 19 and 23 μm, while the gubernaculum measures 17–18 μm. The bursa is rounded and half-closed, and there are eight pairs of genital papillae (Sultana and Pervez, 2019).

The bacterial associations of nematodes of the genus *Cruznema* provides contrast to symbioses. Unlike *Steinernema* or *Heterorhabditis*, *Cruznema* does not appear to have a specific obligate bacterial symbiont (Stock *et al.*, 2017). Instead, they may form more opportunistic associations with various soil bacteria. These potentially include members of the genera *Pseudomonas*, *Bacillus*, and *Serratia*, although the specific nature and consistency of these associations remain less well-characterised (Campos-Herrera *et al.,* 2015). The bacterial relationships in *Cruznema* appear to be more variable and environmentally dependent, which aligns with its facultative parasitic lifestyle.

2.2.8 Nematode host invasion characteristics

Table 2.2 Characteristics of host invasion characteristics among nematode genera adapted from (Kallali *et al.*, 2024).

Characteristics	*Heterorhabditis*	*Steinernema*	*Oscheius*	*Cruznema*
Parasitic nature	Obligate	Obligate	Facultative	Facultative
Primary entry	Intersegmental regions, natural openings	Natural openings	Natural openings	Natural openings
Specialised entry structures	Dorsal tooth	None	None	None
Host range	Broad	Broad	Narrow	Narrow
Virulence	High	High	Lower	Lower

Symbiotic bacteria relationship	Highly specialised	Highly specialised	Less specialised/ Variable	Less specialised/ Variable
Ability to complete lifecycle without insect	No	No	Yes	Yes

2.3 Factors influencing the development and efficacy of EPNs

The successful colonisation of all ecosystems by nematodes is a result of their ability to thrive in unfavourable environmental conditions at different stages of their life cycle (Perry *et al*., 2012). The prevalence and distribution of EPNs in soil, is dependent on both biotic and abiotic factors being optimal to support life, **Figure 2.7** (Matuska-Łyżwa *et al.*, 2024). Abiotic factors (temperature, humidity, texture, ultraviolet radiation, pH, heavy metals and pesticides) and biotic factors (host availability, competition like fungi and collembolans, and predators) affects the survival, population growth and development, host-seeking capabilities, infectivity and persistence of EPNs (Hominick and Briscoe, 1990; Kaya and Gaugler, 2002; Karthik Raja *et al*., 2021; Lalitha *et al.*, 2022; Matuska-Łyżwa *et al.*, 2024; Devi, 2024; Patil *et al.*, 2024). However, their ability to withstand extreme temperature and dehydration, the primary influencing factors, contributes to nematodes' evolutionary success and widespread distribution.

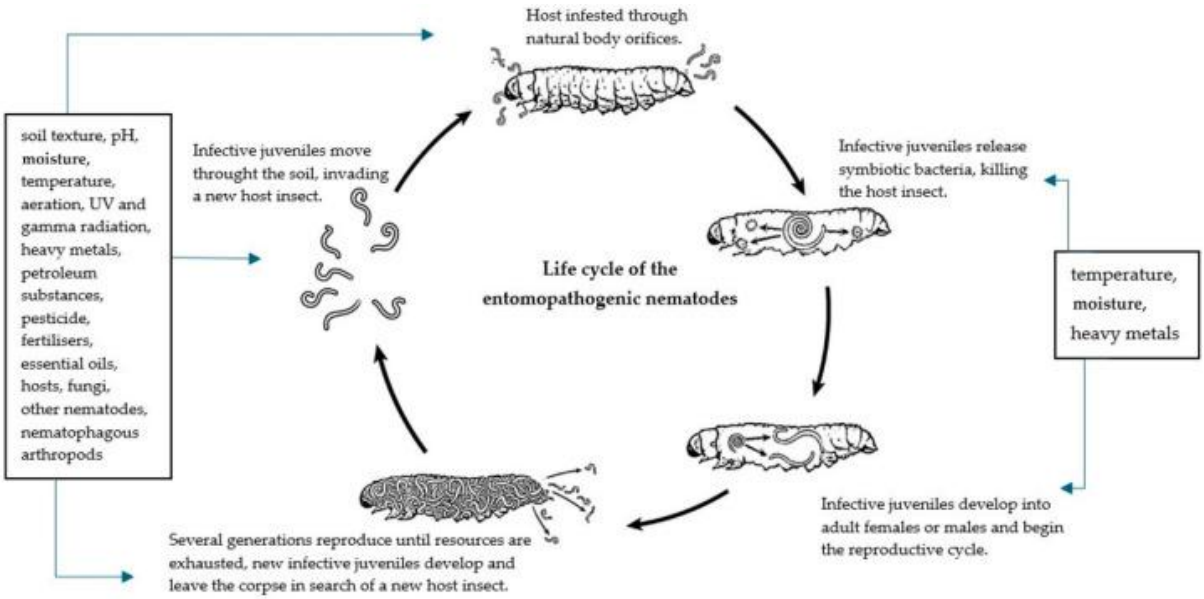

Figure 2.7 | Environmental factors influencing EPN development and efficacy adapted from (Matuska-Łyżwa *et al*., 2024). The effects of abiotic and biotic factors on the EPN life cycle at different stages is depicted. The blue arrows show important points in the life cycle where environmental conditions impact EPNs.

2.3.1 Temperature

Nematodes are extremotolerant organisms with the ability to enter a state of latent life known as cryptobiosis induced by freezing or anhydrobiosis induced by desiccation (Hvidepil and Møbjerg, 2023). Strategies employed by nematodes to survive harsh conditions like extreme temperatures and or desiccation allows them to remain in soil for long periods of time (Treonis and Wall, 2005; Watanabe, 2006).

Many nematodes show resilience against low temperatures in their environment. They employ three different strategies including freezing avoidance, cryoprotective dehydration and cold tolerance. Nematodes avoid ice formation in their bodies during freezing avoidance by maintaining body fluid below 0^{o}C. During cryoprotective dehydration the nematodes are protected from temperature drops caused by dehydration because of the surrounding ice. Cold tolerance is common in EPNs (Wu *et al.*, 2018).

2.3.1.1 Physiological and molecular responses to temperature stress

Temperature is a major factor affecting soil dwelling organisms like the IJs of EPNs. Temperature has lasting effects on the stress tolerance, chemotaxis as well as the proteome of EPNs (Lillis *et al.,* 2023). Exposure to extreme temperatures affects the physiological and molecular pathways in EPNs (Gulzar *et al.,* 2020; Matuska-Łyżwa *et al.,* 2024). Studies done by Lalitha *et al*, (2022) show that high temperatures result in increased pathogenicity as well as higher emergence, displaying that reproduction is not negatively impacted by rising temperatures. However, prolonged exposure to higher temperatures leads to lower infectivity, weakened immune suppression as symbiotic bacteria die, shorter life-span due to faster energy depletion, and population decline because of reproductive failure.

Temperature stress also leads to alterations in the EPN proteome, that is, all proteins expressed by the organism. These proteomic changes can affect enzyme function, membrane integrity, and cellular repair mechanisms (Lillis *et al.,* 2022). Heat stress specifically downregulates proteins involved in chemoreception while upregulating heat shock proteins (HSPs) that protect cellular components from thermal damage (Jagdale and Grewal, 2003). This protein reallocation, while offering short-term protection, impairs chemotaxis, the host-finding strategies of EPNs. These EPNs show reduced sensitivity to host volatiles and carbon dioxide gradients, lowering their ability to track down and infect insect hosts (Chen and Glazer, 2005). Studies done by Brown and Gaugler, (1997) showed that varying strains of EPNs tolerate temperature fluctuations differently. Ebssa *et al*, (2004) tested a range of temperatures for two species of EPNs, *H. indica* and *S. bicornutum*, isolated from tropical and temperate regions respectively, and found that *H. indica* performed better at high temperatures, while *S. bicornutum* performed better at lower temperatures. Both EPN strains showed optimal efficacy at 25^{o}C which is consistent with many other EPN strains (Trdan *et al.,* 2007).

IJs mostly rely on energy reserves to survive and cause infection. It was found that at room temperatures, IJs have a lower shelf-life since the physiological activity of the EPNs are higher (Ramakuwela *et al.*, 2015). Also, at high temperatures there is a higher consumption of the stored energy leading to higher mortality or a shorter shelf-life. Areas, like temperate regions, that experience low temperatures have lower emergence of IJs, negatively impacting their survival and efficacy. The EPNs storage temperatures may therefore differ from both the optimal effective pathogenicity temperature and the effective survival temperatures (Ramakuwela *et al.*, 2015).

IJs can survive extreme environments by staying within the host cadavers for about 50 days. In a study done by Glazer, (1996), it was found that *Steinernema carpocapsae* showed higher survival in the host cadaver in lower temperatures than higher temperatures. At 25°C, all the IJs were dead at 28 days, however, at 15°C, it was found that 28% of the IJs were still alive but only emerged from the cadaver upon submerging in water for 24 hours. Their survival is dependent on the conditions in which the cadaver is exposed, and the survival also varies based on individual species of the EPNs (Brown and Gaugler, 1997).

Studies done by (Lillis, Griffin and Carolan, 2022) showed that the stress tolerance and shelf life of IJs may be enhanced by storing them at lower temperatures. This study further showed that the proteome of both *Steinernema* and *Heterorhabditis* species was affected differently by low temperatures of 9°C and 20°C. At 20°C, there was an increased quantity of proteins related to cellular processes. Whereas there was a decrease in proteins related to metabolic activity.

2.3.2 Desiccation

A small number of organisms can survive nearly complete drying – desiccation. This survival strategy is found in taxonomically diverse groups including, some nematodes, fungi, lichens, brine shrimp, tardigrades, mosses, and protozoa to name a few (Rao, 2018). *C. elegans*, one of the most studied nematode species, can survive when low intracellular water of about 2 to 3% is retained in their active states (Hibshman, Clegg and Goldstein, 2020). The survival of nematodes after desiccation is highly dependent on their ability to repair all damages caused during the dehydration and rehydration process (Balakumaran *et al.*, 2022).

Studies done by Mason and Wright, (1997) show that EPNs tolerance to desiccation differs within and between species. The two species *Steinernema (SSL85/25)* and *Steinernema (M87/45)* showed marked but not statistically significance in survival rates at the same relative humidity (80%) with the *Steinernema (SSL85/25)* showing 51% survival and *Steinernema (M87/45)* showing 13%.

2.3.2.1 Anhydrobiosis

Anhydrobiosis, life without water, is the prolonged, reversible and ametabolic state that certain organisms may achieve to survive extreme desiccation conditions (Crowe and Madin, 1974;

McGill *et al.*, 2015). In this state, nematodes suspend activity, growth and development as well as reproduction, and upon rehydration, all life activities resume (Hoshino and Togashi, 2020). To enter the anhydrobiotic state, organisms loose both their free and bound water, almost 99% of their water content is lost from their cells (Danks, 2000; Rao, 2018). During anhydrobiosis, nematodes employ various behavioural responses like coiling or clumping (Crowe and Madin, 1974; Watanabe, 2006). They have adaptations involving a process where bound water is replaced and alternative pathways, like the glyoxylate pathway, are used to provide the energy required for the nematode to both enter and leave the state of anhydrobiosis (Madin *et al.*, 1985; Adhikari *et al.*, 2009). Biochemical adaptions are also used, and these include the accumulation of sugars like trehalose, synthesis of proteins including the heat-shock proteins (Hsps) and other proteins as well as the modifications in the metabolism of fatty acids (Browne *et al.*, 2004; Shannon *et al.*, 2005; Erkut *et al.*, 2013; Balakumaran *et al.*, 2022).

Anhydrobiosis involves a gradient of responses from quiescence to cryptobiosis (Treonis and Wall, 2005). Cryptobiosis is the term describing the state in which microorganisms whose metabolism has been reduced to undetectable levels is in (Hoshino and Togashi, 2020). The water loss during cryptobiosis may be due to two different causes. Firstly, evaporative dehydration and secondly, because of hypertonic osmotic pressure. These are termed anhydrobiosis and osmobiosis respectively (Hoshino and Togashi, 2020). Osmobiosis is a form of cryptobiosis that organisms enter when exposed to surrounding solution with an increased solute concentration, which lowers the water potential. The organism undergoes a cessation of metabolism. This adaptation allows certain life forms to withstand extreme osmotic stress by essentially "shutting down" until more favourable conditions return. Organisms in all three states, quiescence, anhydrobiosis and osmobiosis, can survive in long-lasting desiccation environmental and laboratory conditions (Watanabe, 2006).

The major differentiation between the states of anhydrobiosis and quiescence is the degree at which activity ceases in the organism (Treonis and Wall, 2005). At quiescence, biological processes are limited, that is, the organism’s ability to reproduce and feed is ceased. However, in cryptobiosis, otherwise called “latent life”, all processes including motility and metabolism is ceased (Treonis and Wall, 2005).

Some organisms in their anhydrobiotic state are resistant to freezing as the loss of water from their bodies means that tissue damaging ice crystal formation is prevented. Upon rehydration,

all life processes resume **Figure 2.8** (Mcgill *et al.*, 2015). Some Antarctic nematodes, including the bacterial feeding anhydrobiotic nematode, *Panagrolaimus davidi*, from Ross Island Antarctic, can survive intracellular ice formation in a fully hydrated state. Several other isolates from the genus *Panagrolaimus* were also found to be anhydrobiotic and free-tolerant. It was found to be a derived trait, and the genus lineages are strongly anhydrobiotic but show week freeze-tolerance (Mcgill *et al.*, 2015).

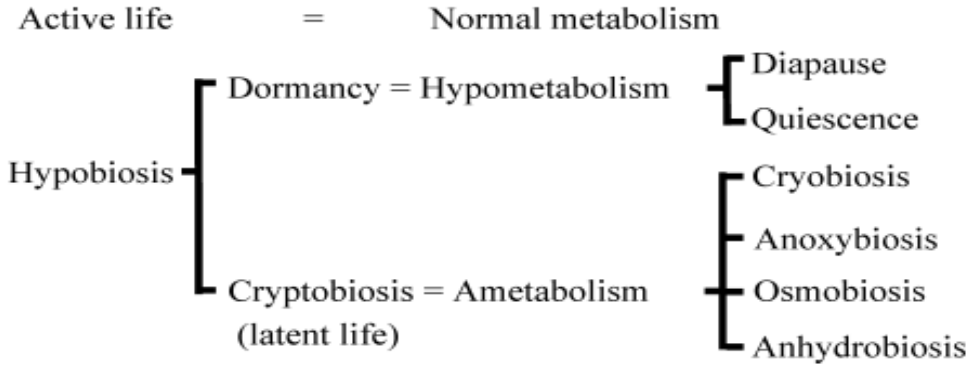

Figure 2.8 | Classification of hypobiosis based on the metabolic level adapted from Watanabe, (2006).

EPNs were first described and reported to undergo anhydrobiosis and survive desiccation in 1734 by John Needham upon observation of the larvae of the plant pathogenic nematode *Anguina tritici* emerging from blighted wheat grains. EPNs are defined as true anhydrobiotes, that is, surviving with close to no intracellular water, approximately 2 to 3% (Hibshman, Clegg and Goldstein, 2020). The traits of true anhydrobiotes includes increased resistance to low internal water percentages, as well as the ability to withstand extreme environmental conditions, vacuum, ionising radiation as well as metabolic poisons lethal to the active nematodes. They also exhibit no detectable metabolism resulting in higher energy conservation (Liu and Glazer, 2000).

EPNs are seen to withstand desiccation at multiple life stages. However, this differs among nematode species. *C. elegans*, the model nematode, was seen to only be able to withstand desiccation in the Dauer state, that is, a specialised stress-resistant larval stage where feeding stops (Hibshman, Clegg and Goldstein, 2020). Nematodes enter this stage because of declining environmental conditions. At this stage, the nematodes exhibit metabolic and morphological

changes which include but are not limited to radial constriction, the formation of a specialised cuticle and a plug over the mouth region (Hibshman, Clegg and Goldstein, 2020).

Studies by (Liu and Glazer, 2000) done on eleven isolated species of *Heterorhabditis* spp. show that the survival of nematodes is influenced by the rate at which the internal water from the nematodes body is lost as well as a minimal relative humidity level of greater than 93%.

2.3.2.2 Cellular adaptations to desiccation

Nematodes undergo several protective mechanisms to maintain the cellular integrity during anhydrobiosis and survive desiccation. These adaptations, as illustrated in **Figure 2.9,** include water replacement where, the protective disaccharide, trehalose substitute for water by forming hydrogen bonds with cellular components, preserving their structure and function in the absence of water (Hibshman, Clegg and Goldstein, 2020; Ramirez *et al.*, 2024). LEA proteins and other molecules facilitate a glass transition, resulting in a vitrified state that immobilises cellular constituents and prevent potential damage. Heat shock proteins (HSP40 and HSP70) and other molecular chaperones such as small heat shock proteins (sHSPs) provide molecular shielding, protecting proteins from misfolding and aggregation during dehydration (Gillan *et al.,* 2009). The process also involves metabolic restructuring, with shifts in pathways like gluconeogenesis that enable cellular adaptation to dried conditions. Additionally, antioxidant defence systems, including catalase, superoxide dismutase, and glutathione peroxidases, mitigates the increased oxidative stress associated with desiccation. These mechanisms collectively enable anhydrobiotic organisms to undergo nearly complete dehydration while maintaining the structural and functional integrity of their cells, allowing for successful revival upon rehydration.

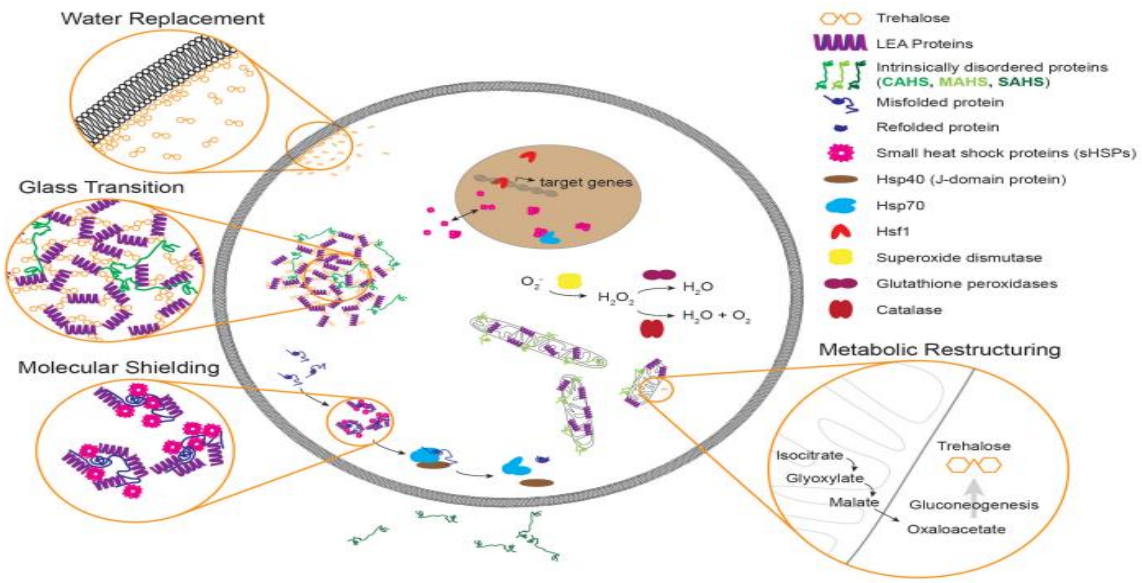

Figure 2.9 | Adapted from (Hibshman, Clegg and Goldstein, 2020) shows an illustration of molecular components and mechanisms involved in desiccation tolerance of nematodes

2.4 References

Abate, B.A., Wingfield, M.J., Slippers, B., Hurley, B.P., 2017. Commercialisation of entomopathogenic nematodes: should import regulations be revised? *Biocontrol Science and Technology* 27, 149–168. https://doi.org/10.1080/09583157.2016.1278200

Abubakar, Y., Tijjani, H., Egbuna, C., Adetunji, C.O., Kala, S., Kryeziu, T.L., Ifemeje, J.C., Patrick-Iwuanyanwu, K.C., 2020. Chapter 3 - Pesticides, History, and Classification, in: Egbuna, C., Sawicka, B. (Eds.), Natural Remedies for Pest, Disease and Weed Control. *Academic Press*, pp. 29–42. https://doi.org/10.1016/B978-0-12-819304-4.00003-8

Abhilash, P.C. and Singh, N., 2009. Pesticide use and application: an Indian scenario. *Journal of hazardous materials*, *165*(1-3), pp.1-12.

Adhikari, B.N., Wall, D.H., Adams, B.J., 2009. Desiccation survival in an Antarctic nematode: molecular analysis using expressed sequenced tags. *BMC Genomics* 10, 69. https://doi.org/10.1186/1471-2164-10-69

Abolafia, J., Peña-Santiago, R., 2019. Morphological and Molecular Characterization of *Oscheius saproxylicus* sp. n. (Rhabditida, Rhabditidae) From Decaying Wood in Spain, With New Insights into the Phylogeny of the Genus and a Revision of its Taxonomy. *J Nematol* 51, e2019-53. https://doi.org/10.21307/jofnem-2019-053

Akhurst R, Boemare N. Biology and taxonomy of *Xenorhabdus*. Entomopathogenic nematodes in biological control. *CRC;* 1990. pp. 75–90.

Aktar W., Paramasivam M., Sengupta D., Purkait S., Ganguly M., Banerjee S. 2008. Impact assessment of pesticide residues in fish of Ganga River around Kolkata in West Bengal. *Environ. Monit. Assess.* **157**: 97–104. Doi: 10.1007/s10661-008-0518-9.
Aktar, M.W., Sengupta, D., Chowdhury, A., 2009. Impact of pesticides use in agriculture: their benefits and hazards. *Interdisciplinary Toxicology* 2, 1. https://doi.org/10.2478/v10102-009-0001-7

Alewu, B. and Nosiri, C., 2011. Pesticides in the modern world–effects of pesticides exposure. *Pesticides and human health*, pp.231-250.

Andrássy, I., 1983. *A taxonomic review of the suborder Rhabditina (Nematoda: Secernentia)* (p. 241pp).

Andrews, D.G.H., 2019. A new method for measuring the size of nematodes using image processing. *Biology Methods & Protocols* 4, bpz020. https://doi.org/10.1093/biomethods/bpz020

Balakumaran, M., Chidambaranathan, P., Tej Kumar J P, J.P., Sirohi, A., Kumar Jain, P., Gaikwad, K., Iyyappan, Y., Rao, A.R., Sahu, S., Dahuja, A., Mohan, S., 2022. Deciphering the mechanism of anhydrobiosis in the entomopathogenic nematode Heterorhabditis indica through comparative transcriptomics. *PLoS One* 17, e0275342. https://doi.org/10.1371/journal.pone.0275342

Ball S.T., 1996. Defoliants, desiccators, and growth regulators. New Mexico Pesticide Applicator Training. Agricultural Pests and Agricultural Weeds. *New Mexico State University Cooperative Extension Service*. pp 1-14.

Baiocchi, T., Lee, G., Choe, D.-H., Dillman, A., 2017. Host seeking parasitic nematodes use specific odors to assess host resources. *Scientific Reports* 7. https://doi.org/10.1038/s41598-017-06620-2

Bassil, K.L., Vakil, C., Sanborn, M., Cole, D.C., Kaur, J.S., Kerr, K.J., 2007. Cancer health effects of pesticides. *Can Fam Physician* 53, 1704–1711.

Bhat, A.H., Chaubey, A.K., Askary, T.H., 2020. Global distribution of entomopathogenic nematodes, Steinernema and Heterorhabditis. *Egyptian Journal of Biological Pest Control* 30, 31. https://doi.org/10.1186/s41938-020-0212-y

Bernardes M.F.F., Pazin M., Pereira L.C., Dorta D.J. 2015. *Toxicology Studies—Cells, Drugs and Environment.* IntechOpen; London, UK. *Impact of Pesticides on Environmental and Human Health*; pp. 195–233.

Birhan A. Abate, Michael J. Wingfield, Bernard Slippers & Brett P. Hurley. 2017. Commercialisation of entomopathogenic nematodes: should import regulations be revised?, *Biocontrol Science and Technology*, doi: 10.1080/09583157.2016.1278200.

Blaxter, M.L., De Ley, P., Garey, J.R., Liu, L.X., Scheldeman, P., Vierstraete, A., Vanfleteren, J.R., Mackey, L.Y., Dorris, M., Frisse, L.M., Vida, J.T. & Thomas, W.K., 1998. A molecular evolutionary framework for the phylum Nematoda. *Nature* 392, 71-75.

Boxall R.A., 2001. Post-harvest losses to insects—a world overview. *Int. Biodeter. Biodegr*; **48**:137–152.

Bravo, A., Gill, S.S., Soberón, M., 2007. Mode of action of *Bacillus thuringiensis* Cry and Cyt toxins and their potential for insect control. Toxicon 49, 423–435. https://doi.org/10.1016/j.toxicon.2006.11.022

Browne, J.A., Dolan, K.M., Tyson, T., Goyal, K., Tunnacliffe, A., Burnell, A.M., 2004. Dehydration-specific induction of hydrophilic protein genes in the anhydrobiotic nematode *Aphelenchus avenae*. *Eukaryot Cell* 3, 966–975. https://doi.org/10.1128/EC.3.4.966-975.2004

Brzeski, M.W., 1989. *Cruznema velatum* sp. n. and observations on *C. tripartitum* (Linstow)(Nematoda: Rhabditidae).

Campos–Herrera, R., Barbercheck, M., Hoy, C.W., Stock, S.P., 2012. Entomopathogenic nematodes as a model system for advancing the frontiers of ecology. *Journal of nematology* 44, 162.

Cao, M., Schwartz, H.T., Tan, C.-H., Sternberg, P.W., 2021. The entomopathogenic nematode *Steinernema hermaphroditum* is a self-fertilizing hermaphrodite and a genetically tractable system for the study of parasitic and mutualistic symbiosis. *Genetics* 220, iyab170. https://doi.org/10.1093/genetics/iyab170

Camino, N.B. and Achinelly, M.F., 2011. Biodiversity of insect-parasitic nematodes in soil pest insect (Orthoptera, Gryllidae and Gryllotalpidae) in wheat fields of Buenos Aires, Argentina/Biodiversidad de nemátodos parásitos de insectos plaga del suelo (Orthoptera, Gryllidae y Gryllotalpidae) en áreas agrícolas de Buenos Aires, Argentina. In *Anales de biología* (No. 33, p. 15). Servicio de Publicaciones, Universidad de Murcia.

Campbell, J.F., Gaugler, R.R., 1997. Inter-specific variation in entomopathogenic nematode foraging strategy: Dichotomy or variation along a continuum? *Fundamental and Applied Nematology* 20, 393–398.

Castillo, J.C., Reynolds, S.E., Eleftherianos, I., 2011. Insect immune responses to nematode parasites. *Trends in Parasitology* 27, 537–547. https://doi.org/10.1016/j.pt.2011.09.001

CDC, 2025. About Pesticides and Reproductive Health [WWW Document]. Reproductive Health and The Workplace. URL https://www.cdc.gov/niosh/reproductive-health/prevention/pesticides.html (accessed 2.19.25).

Children, N.R.C. (US) C. on P. in the D. of I. and (1993) Background and Approach to the Study, in Pesticides in the Diets of Infants and Children. *National Academies Press (US)*. Available at: https://www.ncbi.nlm.nih.gov/books/NBK236265/ (Accessed: 17 September 2024).

Clarridge, J.E., 2004. Impact of 16S rRNA Gene Sequence Analysis for Identification of Bacteria on Clinical Microbiology and Infectious Diseases. *Clinical Microbiology Reviews* 17, 840–862. https://doi.org/10.1128/CMR.17.4.840-862.2004

Crowe, J.H., Madin, K.A., 1974. Anhydrobiosis in Tardigrades and Nematodes. *Transactions of the American Microscopical Society* 93, 513–524. https://doi.org/10.2307/3225155

Damalas, C.A. and Koutroubas, S.D. (2016) 'Farmers' Exposure to Pesticides: Toxicity Types and Ways of Prevention', *Toxics*, 4(1), p. 1. Available at: https://doi.org/10.3390/toxics4010001

Dauer Introduction Overview [WWW Document], n.d. URL https://www.wormatlas.org/dauer/introduction/DIntroframeset.html (accessed 3.24.25).

Devi, G., 2024. Influence of Abiotic Factors on Efficacy of Entomopathogenic Nematodes. International *Journal of Plant & Soil Science* 36, 283–290. https://doi.org/10.9734/ijpss/2024/v36i34425

Du, H., Guo, F., Gao, Y., Wang, X., Qing, X., Li, H., 2022. Complete Mitogenome of Cruznema tripartitum Confirms Highly Conserved Gene Arrangement within Family Rhabditidae. *Journal of Nematology* 54, 1–10. https://doi.org/10.2478/jofnem-2022-0029

Dziedziech, A., Shivankar, S. and Theopold, U. (2020) 'High-Resolution Infection Kinetics of Entomopathogenic Nematodes Entering Drosophila melanogaster', *Insects*, 11(1), p. 60. Available at: https://doi.org/10.3390/insects11010060.

Elsen, A., Vallterra, S.F., Van Wauwe, T., Thuy, T.T.T., Swennen, R., De Waele, D., Panis, B., 2007. Cryopreservation of *Radopholus similis*, a tropical plant-parasitic nematode. *Cryobiology* 55, 148–157. https://doi.org/10.1016/j.cryobiol.2007.06.006

Erkut, C., Vasilj, A., Boland, S., Habermann, B., Shevchenko, A., Kurzchalia, T.V., 2013. Molecular Strategies of the *Caenorhabditis elegans* Dauer Larva to Survive Extreme Desiccation. *PLOS ONE* 8, e82473. https://doi.org/10.1371/journal.pone.0082473

Fayyaz, S., Anis, M., Reid, A., Rowe, J., Maqbool, M., 2001. Steinernema pakistanense sp. N. (Rhabditida: Steinernematidae) from Pakistan. *International Journal of Nematology* 11.

Fenik, J., Tankiewicz, M., Biziuk, M., 2011. Properties and determination of pesticides in fruits and vegetables. *TrAC Trends in Analytical Chemistry* 30, 814–826. https://doi.org/10.1016/j.trac.2011.02.008

Ferris, H., Venette, R.C., Lau, S.S., 1997. Population energetics of bacterial-feeding nematodes: Carbon and nitrogen budgets. *Soil Biology and Biochemistry* 29, 1183–1194. https://doi.org/10.1016/S0038-0717(97)00035-7

Ferris, H., 2010. Contribution of nematodes to the structure and function of the soil food web. *Journal of nematology*, *42*(1), p.63.

Fu, J., Liu, Q., 2019. Evaluation and entomopathogenicity of gut bacteria associated with dauer juveniles of Oscheius chongmingensis (Nematoda: Rhabditidae). *MicrobiologyOpen* 8, e00823. https://doi.org/10.1002/mbo3.823

Ghavamabad, R.G., Talebi, A.A., Mehrabadi, M., Farashiani, M.E., Pedram, M., 2021. First record of *Oscheius myriophilus* () (Rhabditida: Rhabditidae) from Iran; and its efficacy against two economic forest trees pests, Cydalima perspectalis (Walker, 1859) (Lepidoptera: Crambidae) and Hyphantria cunea () (Lepidoptera: Erebidae) in laboratory condition. *J Nematol* 53, e2021-35. https://doi.org/10.21307/jofnem-2021-035

Gillan, V., Maitland, K., McCormack, G., Nik Him, N.A.I.I., Devaney, E., 2009. Functional genomics of hsp-90 in parasitic and free-living nematodes. *International Journal of Parasitology* 39, 1071–1081. https://doi.org/10.1016/j.ijpara.2009.02.024

Goffart, H., 1935. Rhabditis gracilis n. sp. (Rhabditidae, Nematoda) in decaying cacao fruit.

Golden, J.W., Riddle, D.L., 1984. The *Caenorhabditis elegans* dauer larva: Developmental effects of pheromone, food, and temperature. Developmental Biology 102, 368–378. https://doi.org/10.1016/0012-1606(84)90201-X

Grewal, P.S., Ehlers, R. & Shapiro-Ilan, D.I., 2006, Nematodes as biocontrol agents, CABI, Wallingford.

Guo, F., Slos, D., Du, H., Li, K., Li, H., Qing, X., 2023. Transcriptomics of Cruznema velatum (Nematoda: Rhabditidae) with a redescription of the species. *Journal of Helminthology* 97, e57. https://doi.org/10.1017/S0022149X23000342

Harwood, G.P., Dolezal, A.G., 2020. Pesticide–Virus Interactions in Honey Bees: Challenges and Opportunities for Understanding Drivers of Bee Declines. *Viruses* 12, 566. https://doi.org/10.3390/v12050566

Helmberger, M.S., Shields, E.J., Wickings, K.G., 2017. Ecology of belowground biological control: Entomopathogenic nematode interactions with soil biota. *Applied Soil Ecology* 121, 201–213. https://doi.org/10.1016/j.apsoil.2017.10.013

Homininck, W.M. and Briscoe, B.R., 1990. Occurrence of entomopathogenic nematodes (Rhabditida: Steinernematidae and Heterorhabditidae) in British soils. *Parasitology*, *100*(2), pp.295-302.

How pesticides impact human health and ecosystems in Europe [WWW Document], 2023. *European Environment Agency.* URL https://www.eea.europa.eu/publications/how-pesticides-impact-human-health/how-pesticides-impact-human-health (accessed 11.1.24).

Hvidepil, L.K.B. and Møbjerg, N. 2023. New insights into osmobiosis and chemobiosis in tardigrades, *Frontiers in Physiology*, 14, p. 1274522. Available at: https://doi.org/10.3389/fphys.2023.1274522.

Jones, J., 2002. 14. Nematode Sense Organs. *The biology of nematodes*, 353 pp 16.

Kallali, N.S., Ouijja, A., Goura, K., Laasli, S.-E., Kenfaoui, J., Benseddik, Y., Blenzar, A., Joutei, A.B., El Jarroudi, M., Mokrini, F., Lahlali, R., 2024. From soil to host: Discovering the tripartite interactions between entomopathogenic nematodes, symbiotic bacteria and insect pests and related challenges. *Journal of Natural Pesticide Research* 7, 100065. https://doi.org/10.1016/j.napere.2023.100065

Karthik Raja, R., Arun, A., Touray, M., Hazal Gulsen, S., Cimen, H., Gulcu, B., Hazir, C., Aiswarya, D., Ulug, D., Cakmak, I., Kaya, H.K., Hazir, S., 2021. Antagonists and defense mechanisms of entomopathogenic nematodes and their mutualistic bacteria. *Biological Control* 152, 104452. https://doi.org/10.1016/j.biocontrol.2020.104452

Kaya, H.K. & Gaugler, R., 1993, 'Entomopathogenic nematodes', *Annual Review of Entomology* 38, 181–206. https://doi.org/10.1146/annurev.en.38.010193.001145

Kaya HK, Stock SP. 1997. Entomopathogenic nematodes. In: Knowles BH, Blatt MR, Tester M, Horsnell JM, Carroll J, Menestrina G, Ellar DJ, editors. *Manual of techniques in insect pathology*. New York: Academic Press; p. 259–262.

Kaya, H.K. and Gaugler, R., 2002. Entomopathogenic nematology. *Entomopathogenic Nematology*, pp.189-200.

Kaur, R., Choudhary, D., Bali, S., Bandral, S.S., Singh, V., Ahmad, M.A., Rani, N., Singh, T.G., Chandrasekaran, B., 2024. Pesticides: An alarming detrimental to health and environment. *Science of The Total Environment* 915, 170113. https://doi.org/10.1016/j.scitotenv.2024.170113

Kim, S.K., Flores-Lara, Y., Patricia Stock, S., 2012. Morphology and ultrastructure of the bacterial receptacle in *Steinernema* nematodes (Nematoda: Steinernematidae). *Journal of Invertebrate Pathology, SIP Symposium on Resistance to Bt Crops* 110, 366–374. https://doi.org/10.1016/j.jip.2012.04.011

Koppenhöfer, A.M., Shapiro-Ilan, D.I., Hiltpold, I., 2020. Entomopathogenic Nematodes in Sustainable Food Production. Front. Sustain. Food Syst. 4. https://doi.org/10.3389/fsufs.2020.00125

Kumar, P., Jamal, W., Somvanshi, V.S., Chauhan, K., Mumtaz, S., 2019. Description of *Oscheius indicus* n. sp. (Rhabditidae: Nematoda) from India. *Journal of Nematology*. 51, e2019-04. https://doi.org/10.21307/jofnem-2019-004

Kumar, P., Kamle, M., Borah, R., Mahato, D.K., Sharma, B., 2021. Bacillus thuringiensis as microbial biopesticide: uses and application for sustainable agriculture. *Egyptian Journal of Biological Pest Control* 31, 95. https://doi.org/10.1186/s41938-021-00440-3

Lacey, L.A., Georgis, R., 2012. Entomopathogenic Nematodes for Control of Insect Pests Above and Below Ground with Comments on Commercial Production. *Journal of Nematology* 44, 218.

Lacey, L.A., Grzywacz, D., Shapiro-Ilan, D.I., Frutos, R., Brownbridge, M., Goettel, M.S., 2015. Insect pathogens as biological control agents: back to the future. *J. Invertebr. Pathol.* 132, 1–41. http://dx.doi.org/10.1016/j.jip.2015.07.009

Ley, P., Blaxter, M., 2002. Systematic Position and Phylogeny. pp. 1–30. https://doi.org/10.1201/b12614-2

Lillis, P.E., Kennedy, I.P., Carolan, J.C., Griffin, C.T., 2022. Low-temperature exposure has immediate and lasting effects on the stress tolerance, chemotaxis and proteome of entomopathogenic nematodes. *Parasitology* 150, 15–28. https://doi.org/10.1017/S0031182022001445

Linstow, O.V., 1906. Neue und bekannte Helminthen. *Zool. Jahrb*, *24*, pp.1-20.

Lephoto, T.E., Mpangase, P.T., Aron, S., Gray, V.M., 2016. Whole genome sequence of Oscheius sp. TEL-2014 entomopathogenic nematodes isolated from South Africa. *Genom Data* 7, 259–261. https://doi.org/10.1016/j.gdata.2016.01.017

Madin, K.A.C., Loomis, S.H., Crowe, J.H., 1985. Anhydrobiosis in nematodes: Control of carbon flow through the glyoxylate cycle. *Journal of Experimental Zoology* 234, 341–350. https://doi.org/10.1002/jez.1402340303

Maheshwari, P., Sankar, P.M., 2023. Chapter 42 - Culture-independent and culture-dependent approaches in symbiont analysis: in proteobacteria, in: Dharumadurai, D. (Ed.), Microbial Symbionts, Developments in Applied Microbiology and Biotechnology. *Academic Press*, pp. 743–763. https://doi.org/10.1016/B978-0-323-99334-0.00018-9

Mahmood, I., Imadi, S.R., Shazadi, K., Gul, A., Hakeem, K.R., 2016. Effects of Pesticides on Environment, in: Hakeem, K.R., Akhtar, M.S., Abdullah, S.N.A. (Eds.), Plant, Soil and Microbes: Volume 1: Implications in Crop Science. *Springer International Publishing*, Cham, pp. 253–269. https://doi.org/10.1007/978-3-319-27455-3_13

Mason, A.F. 1928. Spraying, Dusting, and Fumigating of Plants. New York: Macmillan.

Mata-Cabana, A., Pérez-Nieto, C., Olmedo, M., 2021. Nutritional control of postembryonic development progression and arrest in *Caenorhabditis elegans*, in: Kumar, D. (Ed.), Advances in Genetics. Academic Press, pp. 33–87. https://doi.org/10.1016/bs.adgen.2020.11.002

Matuska-Łyżwa, J., Duda, S., Nowak, D., Kaca, W., 2024. Impact of Abiotic and Biotic Environmental Conditions on the Development and Infectivity of Entomopathogenic Nematodes in Agricultural Soils. *Insects* 15, 421. https://doi.org/10.3390/insects15060421

McCallan, S.E.A. 1967. History of fungicides. In Fungicides: An Advanced Treatise, Vol. 1, D.C. Torgeson, editor., ed. New York: Academic.

McCoy, T., 2020. Organic vs. Conventional (Synthetic) Pesticides: Advantages and Disadvantages. *Virginia Cooperative Extension.* https://vtechworks.lib.vt.edu/server/api/core/bitstreams/95dbec81-43ad-4e41-94a1-551210fa543a/content (Accessed: 7 April 2024).

Mcgill, L., Shannon, A., Pisani, D., Félix, M.-A., Ramløv, H., Dix, I., Wharton, D., Burnell, A.M., 2015. Anhydrobiosis and Freezing-Tolerance: Adaptations That Facilitate the Establishment of Panagrolaimus Nematodes in Polar Habitats. *PloS one* 10, e0116084. https://doi.org/10.1371/journal.pone.0116084

McSorley, R., 2003. ADAPTATIONS OF NEMATODES TO ENVIRONMENTAL EXTREMES. flen 86, 138–142. https://doi.org/10.1653/0015-4040(2003)086[0138:AONTEE]2.0.CO;2

Micro-organisms - European Commission (no date). Available at: https://food.ec.europa.eu/plants/pesticides/micro-organisms_en (Accessed: 7 April 2024).

Mangowa, D., Serepa-Dlamini, M.H., 2020. Draft Genome Sequence of a Noncognate Bacterium, *Achromobacter* sp. Strain Bel, Associated with a Rhabditid Entomopathogenic Nematode. *Microbiology Resource Announcements* 9, e01247-20. https://doi.org/10.1128/MRA.01247-20

Morand, S., Nadler, S., Skorping, A., 2015. Nematode life-traits diversity in the light of their phylogenetic diversification. pp. 289–303. https://doi.org/10.1017/CBO9781139794749.017
Narayanasamy, P., 2005. *Postharvest pathogens and disease management*. John Wiley & Sons. New York, NY, USA.

National Institute of Environmental Health Sciences: Pesticides [WWW Document], n.d. URL https://www.niehs.nih.gov/health/topics/agents/pesticides (accessed 9.6.24).

Natural vs. Chemical Pesticide: Are They Both Effective at Removing Pests? [WWW Document], n.d. Foreverest Resources Ltd. URL https://foreverest.net/news-list/natural-vs-chemical-pesticide-are-they-both-effective-at-removing-pests (accessed 4.23.24).

Nemys Eds., 2025. Nemys: *World Database of Nematodes*. Accessed at https://nemys.ugent.be on 2025-01-20. https://doi.org/10.14284/366

Nester, E.W., Thomashow, L.S., Metz, M., Gordon, M., 2002. 100 Years of Bacillus thuringiensis: A Critical Scientific Assessment: This report is based on a colloquium, "100 Years of Bacillis thuringiensis, a Paradigm for Producing Transgenic Organisms: A Critical Scientific Assessment," sponsored by the American Academy of Microbiology and held November 16–18, in Ithaca, New York, American Academy of Microbiology Colloquia Reports. *American Society for Microbiology, Washington (DC).*

Nicolopoulou-Stamati, P., Maipas, S., Kotampasi, C., Stamatis, P., Hens, L., 2016. Chemical Pesticides and Human Health: The Urgent Need for a New Concept in Agriculture. *Front Public Health* 4, 148. https://doi.org/10.3389/fpubh.2016.00148

Oliveira-Hofman, C., Kaplan, F., Stevens, G., Lewis, E., Wu, S., Alborn, H.T., Perret-Gentil, A., Shapiro-Ilan, D.I., 2019. Pheromone extracts act as boosters for entomopathogenic

nematodes efficacy. *Journal of Invertebrate Pathology* 164, 38–42. https://doi.org/10.1016/j.jip.2019.04.008

Pathak, V.M., Verma, V.K., Rawat, B.S., Kaur, B., Babu, N., Sharma, A., Dewali, S., Yadav, M., Kumari, R., Singh, S., Mohapatra, A., Pandey, V., Rana, N., Cunill, J.M., 2022. Current status of pesticide effects on environment, human health and it's eco-friendly management as bioremediation: A comprehensive review. *Front Microbiol* 13, 962619. https://doi.org/10.3389/fmicb.2022.962619

Patil, J., Nekkanti, A., Gowda, M.T., Sushil, S.N., 2024. Effect of temperature and soil moisture on the infectivity of four species of entomopathogenic nematodes (*Steinernema* and *Heterorhabditis* spp.) to fall armyworm, *Spodoptera frugiperda* (Smith). *Journal of Agriculture and Food Research* 18, 101471. https://doi.org/10.1016/j.jafr.2024.101471

Perry, R.N., Ehlers, R.-U., Glazer, I., 2012. A Realistic Appraisal of Methods to Enhance Desiccation Tolerance of Entomopathogenic Nematodes. *Journal of Nematology* 44, 185–190.
Pervez, R., Lone, S.A., Pattnaik, S., 2020. Characterization of symbiotic and associated bacteria from entomopathogenic nematode Heterorhabditis sp. (nematode: Heterorhabditidae) isolated from India. *Egyptian Journal of Biological Pest Control* 30, 144. https://doi.org/10.1186/s41938-020-00343-9

Poinar GO Jr, Thomas GM., 1966. Significance of *Achromobacter nematophilus* Poinar and Thomas (Achromobacteraceae: Eubacteriales) in the development of the nematode, DD-136 (*Neoaplectana* sp. Steinernematidae). *Parasitology*. 56(2):385-90. doi: 10.1017/s0031182000070980. PMID: 4960247.

Poinar GO Jr. 1976. Description and biology of a new insect parasitic rhabditoid, *Heterorhabditis bacteriophora n. gen. n. sp.* (Rhabditida: Heterorhabditidae n. fam.). *Nematologica.* 21:463– 470.

Power, A.G., 2010. Ecosystem services and agriculture: tradeoffs and synergies. *Philosophical transactions of the royal society B: biological sciences*, *365*(1554), pp.2959-2971.

Proteobacteria - an overview | ScienceDirect Topics [WWW Document], n.d. URL https://www.sciencedirect.com/topics/immunology-and-microbiology/proteobacteria (accessed 3.24.25).

Půža, V., Machado, R.A.R., 2024. Systematics and phylogeny of the entomopathogenic nematobacterial complexes *Steinernema–Xenorhabdus* and *Heterorhabditis–Photorhabdus*. *Zoological Letters* 10, 13. https://doi.org/10.1186/s40851-024-00235-y

Ramakrishnan, J., Salame, L., Nasser, A., Glazer, I., Ment, D., 2022. Survival and efficacy of entomopathogenic nematodes on exposed surfaces. *Sci Rep* 12, 4629. https://doi.org/10.1038/s41598-022-08605-2

Reboredo, G.R., Camino, N.B., 1998. Two new species of nematodes (Rhabditida: Diplogasteridae and Rhabditidae) parasites of Gryllodes laplatae (Orthoptera: Gryllidae) in Argentina. *Mem Inst Oswaldo Cruz* 93, 763–766. https://doi.org/10.1590/s0074-02761998000600013

Reboredo, G.R., Camino, N.B., 2000. TWO NEW RHABDITIDA SPECIES (NEMATODA: RHABDITIDAE) PARASITES OF CYCLOCEPHALA SIGNATICOLLIS (COLEOPTERA: SCARABAEIDAE) IN ARGENTINA. *Journal of Parasitology* 86, 819–821. https://doi.org/10.1645/0022-3395(2000)086[0819:TNRSNR]2.0.CO;2

Rizzatti, G. *et al.* 2017. Proteobacteria: A common factor in human diseases. *BioMed Research International*, 2017, p. 9351507. Available at: https://doi.org/10.1155/2017/9351507

Ruiu, L., 2015. Insect pathogenic bacteria in integrated pest management. *Insects*, 6(2), pp. 352–367. Available at: https://doi.org/10.3390/insects6020352

Ruiu, L., Marche, M.G., Mura, M.E. and Tarasco, E., 2022. Involvement of a novel Pseudomonas protegens strain associated with entomopathogenic nematode infective juveniles in insect pathogenesis. *Pest Management Science*, *78*(12), pp.5437-5443.

Sayers, E.W., Cavanaugh, M., Frisse, L., Pruitt, K.D., Schneider, V.A., Underwood, B.A., Yankie, L., Karsch-Mizrachi, I., 2025. GenBank 2025 update. *Nucleic Acids Research* 53, D56–D61. https://doi.org/10.1093/nar/gkae1114

Sangeetha, B. G., Jayaprakas, C. A., Siji, J. V., Rajitha, M., Shyni, B. & Mohandas, C. 2016. Molecular characterization and amplified ribosomal DNA restriction analysis of entomopathogenic bacteria associated with *Rhabditis* (*Oscheius*) spp. 3 Biotech., 6: 32.
Serepa-Dlamini, M., Gray, V., 2018. A new species of entomopathogenic nematode Osch eius safricana n. sp. (Nematoda: Rhabditidae) from South Africa. Archives of Phytopathology and Plant Protection 1–13. https://doi.org/10.1080/03235408.2018.1475281

Shakeel, Q., Shakeel, M., Raheel, M., Ali, S., Ashraf, W., Iftikhar, Y., Bajwa, R.T., 2022. Entomopathogenic Nematodes (EPNs): A Green Strategy for Management of Insect-Pests of Crops, in: Mandal, S.D., Ramkumar, G., Karthi, S., Jin, F. (Eds.), *New and Future Development in Biopesticide Research: Biotechnological Exploration. Springer Nature, Singapore*, pp. 115–135. https://doi.org/10.1007/978-981-16-3989-0_4

Sharma, A., Kumar, V., Shahzad, B., Tanveer, M., Sidhu, G.P.S., Handa, N., Kohli, S.K., Yadav, P., Bali, A.S., Parihar, R.D., Dar, O.I., Singh, K., Jasrotia, S., Bakshi, P., Ramakrishnan, M., Kumar, S., Bhardwaj, R., Thukral, A.K., 2019. Worldwide pesticide usage and its impacts on ecosystem. SN Appl. Sci. 1, 1446. https://doi.org/10.1007/s42452-019-1485-1

Sharma, H., Rana, A., Bhat, A.H., Chaubey, A.K., Sharma, H., Rana, A., Bhat, A.H., Chaubey, A.K., 2021. Entomopathogenic Nematodes: Their Characterization, Bio-Control Properties and New Perspectives, in: Nematodes - Recent Advances, Management and New Perspectives. *IntechOpen.* https://doi.org/10.5772/intechopen.99319

Shannon, A.J., Browne, J.A., Boyd, J., Fitzpatrick, D.A., Burnell, A.M., 2005. The anhydrobiotic potential and molecular phylogenetics of species and strains of Panagrolaimus (Nematoda, Panagrolaimidae). *J Exp Biol* 208, 2433–2445. https://doi.org/10.1242/jeb.01629

Shapiro-Ilan, D.I., Gouge, D.H. & Koppenhofer, A.M., 2002, 'Factors affecting commercial success: Case studies in cotton, turf and citrus', in R. Gaugler (ed.), *Entomopathogenic nematology*, pp. 333–356, CABI, Wallingford.

Singh, A., Kumar, M., Ahuja, A., Vinay, B., Kumar, K., Thakur, S., PASCHAPUR, A., B., J., Mishra, K., Meena, R., Parihar, M., Chaudhary, D., Kumar, S., Pradesh, H., Vishvavidyalaya, K., 2021. Entomopathogenic nematodes: a sustainable option for insect pest management. pp. 73–87. https://doi.org/10.1016/B978-0-12-823355-9.00007-9

Souto, A.L., Sylvestre, M., Tölke, E.D., Tavares, J.F., Barbosa-Filho, J.M., Cebrián-Torrejón, G., 2021. Plant-Derived Pesticides as an Alternative to Pest Management and Sustainable Agricultural Production: Prospects, Applications and Challenges. *Molecules* 26. https://doi.org/10.3390/molecules26164835

Stoate, C., Boatman, N.D., Borralho, R.J., Carvalho, C.R., De Snoo, G.R. and Eden, P., 2001. Ecological impacts of arable intensification in Europe. *Journal of environmental management*, *63*(4), pp.337-365.

Stock, S. P., Kusakabe, A., & Orozco, R. A. (2017). Secondary metabolites produced by *Heterorhabditis* symbionts and their application in agriculture: what we know and what to do next. Journal of Nematology, 49(4), 373-383.

Strassemeyer J., Daehmlow D., Dominic A., Lorenz S., Golla B. SYNOPS-WEB, an online tool for environmental risk assessment to evaluate pesticide strategies on field level. *Crop. Prot.* 2017; **97:28**–44. doi: 10.1016/j.cropro.2016.11.036.

Sudhaus, W., 1974. ZUR SYSTEMATIK, VERBREITUNG, OEKOLOGIE UND BIOLOGIE NEUER UND WENIG BEKANNTER RHABDITIDEN (NEMATODA). 2TEIL.

Sudhaus, W., 1978. Systematik, Phylogenie und Ökologie der holzbewohnenden Nematoden-Gruppe Rhabditis (Mesorhabditis) und das Problem" geschlechtsbezogener" Artdifferenzierung.

Sudhaus, W., Hooper, D.J., 1994. Rhabditis (Oscheius) Guentheri1 Sp.N., an Unusual Species with Reduced Posterior Ovary, With Observations On the Dolichura and Insectivora Groups (Nematoda: Rhabditidae) in: Nematologica Volume 40 Issue 1-4 (1994) [WWW Document].

URL https://brill.com/view/journals/nema/40/1-4/article-p508_39.xml?language=en (accessed 12.13.24).

Sultana, R., Pervez, R., 2019. Description of *Cruznema minimus* sp. n. (Nematoda: Rhabditidae) and *Acrobeloides insignis* sp. n. (Nematoda; Cephalobidae) with a key to *Cruznema* species. *Ann. of Plan. Prote. Scien*. 27, 394. https://doi.org/10.5958/0974-0163.2019.00087.9

Tabassum K.A., Shahina F., Nasira K., and Erum Y.I.. 2016. Description of six new species of *Oscheius* Andrassy, 1976 (Nematoda: Rhabditida) from Pakistan with a key and diagnostic compendium to species of the genus. *Pakistan Journal of Nematology* 34: 109–61.

Tang, F.H.M., Lenzen, M., McBratney, A., Maggi, F., 2021. Risk of pesticide pollution at the global scale. *Nature Geoscience* 14, 206–210. https://doi.org/10.1038/s41561-021-00712-5

Tarasco, E., Fanelli, E., Salvemini, C., El-Khoury, Y., Troccoli, A., Vovlas, A., De Luca, F., 2023. Entomopathogenic nematodes and their symbiotic bacteria: from genes to field uses. *Frontiers in Insect Science*, 3, 1195254. https://doi.org/10.3389/finsc.2023.1195254

Thakur, D.S., Khot, R., Joshi, P.P., Pandharipande, M. and Nagpure, K., 2014. Glyphosate poisoning with acute pulmonary edema. *Toxicology international*, *21*(3), p.328.

Torrini, G., Mazza, G., Carletti, B., Benvenuti, C., Roversi, P.F., Fanelli, E., De Luca, F., Troccoli, A., Tarasco, E. 2015. Oscheius onirici sp. n. (Nematoda: Rhabditidae): a new entomopathogenic nematode from an Italian cave. *Zootaxa* 3937: 533-548. DOI: https://doi.org/10.11646/zootaxa.3937.3.6

Tremblay, E. and Masutti, L. 2005. History of insect parasitism in Italy, *Biological Control*, 32, pp. 34–39. Available at: https://doi.org/10.1016/j.biocontrol.2004.09.014

Tudi, M., Daniel Ruan, H., Wang, L., Lyu, J., Sadler, R., Connell, D., Chu, C., Phung, D.T., 2021. Agriculture Development, Pesticide Application and Its Impact on the Environment. *Int J Environ Res Public Health* 18, 1112. https://doi.org/10.3390/ijerph18031112

Verma, R., Melcher, U., 2012. A Support Vector Machine based method to distinguish proteobacterial proteins from eukaryotic plant proteins. *BMC bioinformatics* 13 Suppl 15, S9. https://doi.org/10.1186/1471-2105-13-S15-S9

Witczak, A. and Abdel-Gawad, H., 2014. Assessment of health risk from organochlorine pesticides residues in high-fat spreadable foods produced in Poland. *Journal of Environmental Science and Health, Part B*, *49*(12), pp.917-928.

Wu, X., Zhu, X., Wang, Y., Liu, X., Chen, L., Duan, Y., 2018. The cold tolerance of the northern root-knot nematode, Meloidogyne hapla. *PLoS One* 13, e0190531. https://doi.org/10.1371/journal.pone.0190531

Wyk, J.A. van, Mayhew, E., 2013. Morphological identification of parasitic nematode infective larvae of small ruminants and cattle: A practical lab guide. *Onderstepoort Journal of Veterinary Research* 80, 14.

Zhang, K., Baiocchi, T., Lu, D., Chang, D.Z., Dillman, A.R., 2019. Differentiating between scavengers and entomopathogenic nematodes: Which is *Oscheius chongmingensis*? Journal of Invertebrate Pathology 167, 107245. https://doi.org/10.1016/j.jip.2019.107245

Zhang, X., Li, L., Kesner, L., Robert, C.A.M., 2021. Chemical host-seeking cues of entomopathogenic nematodes. *Current Opinion in Insect Science* 44, 72–81. https://doi.org/10.1016/j.cois.2021.03.011

Zhang, C., Wright, I.J., Nielsen, U.N., Geisen, S., Liu, M., 2024. Linking nematodes and ecosystem function: a trait-based framework. Trends in Ecology & Evolution 39, 644–653. https://doi.org/10.1016/j.tree.2024.02.002

Zhou, Z., Tran, P.Q., Kieft, K. *et al.* Genome diversification in globally distributed novel marine Proteobacteria is linked to environmental adaptation. *ISME J* **14**, 2060–2077 (2020). https://doi.org/10.1038/s41396-020-0669-4

Zhou, W., Li, M., Achal, V., 2025. A comprehensive review on environmental and human health impacts of chemical pesticide usage. Emerging Contaminants 11, 100410. https://doi.org/10.1016/j.emcon.2024.100410

Chapter 3

The isolation and characterisation of nematodes: *Oscheius* sp. k KN-2024 isolate kv-2022

3.1 Introduction

EPNs have attracted attention in recent years for their potential as biocontrol agents (Shapiro-Ilan, Gouge, and Koppenhöfer 2002; Noosidum *et al.*, 2010; Lacey and Georgis, 2012). They are parasites of many soil-inhabiting insects, serving as natural regulators of insect populations. Many EPN formulations are used as effective biocontrol agents against a broad spectrum of economically important pests. In South Africa, 16 EPN species have been reported, with the first record being *Steinernema carpocapsae* isolated from the black maize beetle, *Heteronychus arator* Fabricius (Harington, 1953; Malan *et al.*, 2016). EPNs have been effectively commercialised as biocontrol agents in North America, Europe, Japan, China, and Australia, with potential applications against important South African pests like the mealybug species, including *Planococcus ficus*, *P. citri*, and *Pseudococcus viburni*, which threaten grapevine, deciduous fruit, and citrus (Ehlers, 1996; Kaya *et al*, 2006; Nxitywa and Malan, 2021).

The soil environment serves as the primary habitat for EPNs, with different ecological niches harbouring distinctive nematode populations adapted to specific conditions. The distribution and abundance of EPNs in soil are influenced by numerous factors including soil texture, organic matter content, pH, temperature, moisture, and the presence of suitable hosts (Stuart *et al.*, 2006; Campos–Herrera *et al.*, 2012). Consequently, isolation methods must account for these variables to effectively recover viable nematode specimens. The insect baiting technique, which exploits the natural host-seeking behaviour of EPNs, remains the most widely used approach for recovering these organisms from soil samples (Bedding and Akhurst 1975; Boff et al., 2000).

The isolation and characterisation of EPNs from their natural soil habitats is a critical process for advancing biological control applications. EPN populations are diverse in their morphological features, host-finding behaviours, environmental tolerances, and virulence - characteristics that can only be fully understood through systematic isolation and detailed characterisation techniques (Jaffuel *et al.*, 2018; Neira-Monsalve *et al.*, 2020). Traditional

morphological characterisation of the nematode structures includes the study of body dimensions, cuticle patterns, stoma morphology, pharyngeal features, and reproductive organs such as spicules in males (Handoo *et al.*, 2021). However, the conserved morphology among closely related nematode species is determined using molecular characterisation of the conserved rDNA regions such as the internal transcribed spacers (ITS), 18S rDNA, or mitochondrial genes, enabling more precise species delineation (Vanlalhlimpuia *et al.*, 2018; Khashaba *et al.*, 2020).

Comparative studies were performed with a second species, previously isolated and maintained in the laboratory, *Cruznema* sp. NTM-2021 (Accession number: OQ408141). *Cruznema* spp. is less extensively studied as biocontrol agents, however, they demonstrate both free-living and parasitic lifestyles (Reboredo and Camino, 1998; Grewal *et al.*, 2011).

Our understanding of indigenous EPN diversity and their adaptation to local environmental conditions is not well-understood. Hence, the need for continued isolation efforts to identify native strains with enhanced efficacy against region-specific pests is essential. Additionally, the environmental variability across South African agricultural regions requires locally adapted EPN strains that can withstand specific abiotic stressors while maintaining virulence. EPNs offer a promising pest control alternative as they actively seek pests while remaining environmentally safe. This chapter details the specific methodologies employed for isolation and characterisation of nematodes, presenting morphological and molecular findings. This research contributes to nematode diversity and provides information for developing effective, regionally adapted biocontrol.

3.2 Material and methods

3.2.1 Rearing and maintenance of *T. molitor* larvae

Late-instar *T. molitor* larvae were purchased commercially and maintained under controlled conditions prior to use in experiments. The larvae were received in ventilated plastic containers containing wheat bran substrate that acted as both a food source and a habitat for the larvae. The containers had perforated lids to ensure adequate aeration. To preserve the larvae and slow their metabolism prior to experimental use, they were stored in a cold room maintained at 5 ± 1°C. Under these conditions, larvae remained viable for approximately one month. For all

experiments, only healthy, active larvae of uniform size (approximately 2-3 cm in length) were selected. Prior to infectivity assays, larvae were removed from cold storage and allowed to acclimate to room temperature for 2-3 hours to restore normal physiological activity. This standardisation ensured consistency across experimental replicates. EPNs used in all subsequent experiments were cultured in last instar *T. molitor* larvae according to Kaya and Stock (1997).

3.2.2 Treatment of soil before experimentation

Soil samples were collected from different regions in Gauteng, South Africa to isolate EPNs. The collected soil samples were treated by sieving out debris (roots and stones) using a fine metal sieve (with approximately 3 mm holes). The soil was then rehydrated with distilled deionised water (ddH_2O) to about 10% moisture content to facilitates the movement of EPNs. The ddH_2O was lightly sprayed onto the soil and thoroughly mixed to ensure uniformity.

3.2.3 Nematode culturing using insect-baiting technique

Isolation of EPNs from previously treated soil was done using insect-baiting techniques as described by Bedding and Akhurst, (1975) with the setup shown in **Figure 3.1**. About 1 kg of the treated soil samples were placed in sterile 2 kg containers with six *T. molitor* larvae in each container. The containers were then closed, inverted and stored in the dark at room temperature. Every 24 to 48 hours, the containers were inspected, and dead larvae were removed and replaced with healthy larvae. The morphology of the cadavers was noted. This is as cadavers that turned brown, or brick red were more likely to have been infected with EPNs. The cadavers were rinsed with ddH_2O and placed in modified White trap to recover the EPNs.

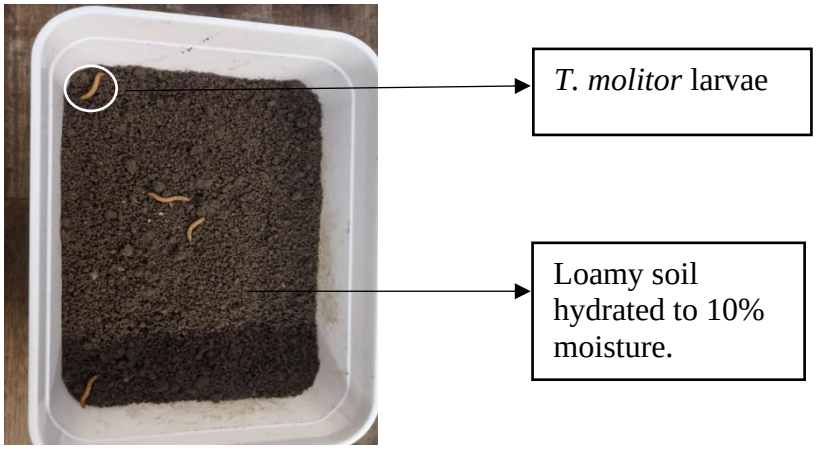

Figure 3.1 | Insect-baiting technique for EPN isolation from soil samples. Tub containing *T. molitor* larvae (n=6) in 1 kg of loamy soil with 10% moisture content monitored daily for infection.

3.2.4 Modified White trap technique to isolate EPNs

The nematodes at the IJ stage were recovered from the infected *T. molitor* third instar larvae using the modified White trap techniques that correspond to the design by S.P stock laboratories (White., 1927: Orozco, Lee, & Stock, 2014). White traps were setup as described by (Lee, Kim and Han., 2000) shown in **Figure 3.2**. The infected *T. molitor* cadavers were placed on top of a 55 mm #1 Whatman filter paper over a small, inverted petri dish (35 mm) which was placed in a larger petri dish (90 mm) with a shallow layer of water to create a continuous water bridge and the lid was replaced. The White traps were kept at room temperature and observed under a stereomicroscope every 24 to 48 hours to visually confirm the emergence of IJs. Emerging IJs were harvested from the ddH_2O surrounding the White traps within 10 days of their emergence (Lee, Kim and Han., 2000). This was done by pipetting the ddH_2O (with IJs) from the White traps into 50 ml falcon tubes. The EPNs were allowed to decant for an hour, after which the water was carefully pipetted out. The IJs were then rinsed twice and collected in 250 ml culture flask at the concentration of 1 000 – 3 000 EPNs/ ml. They were then stored at 20°C for use in subsequent experiments. This stock of IJs was stored for no more than 21 weeks in distilled water at room temperature 20°C before use to minimise the loss of infectivity (Park *et al.*, 1998).

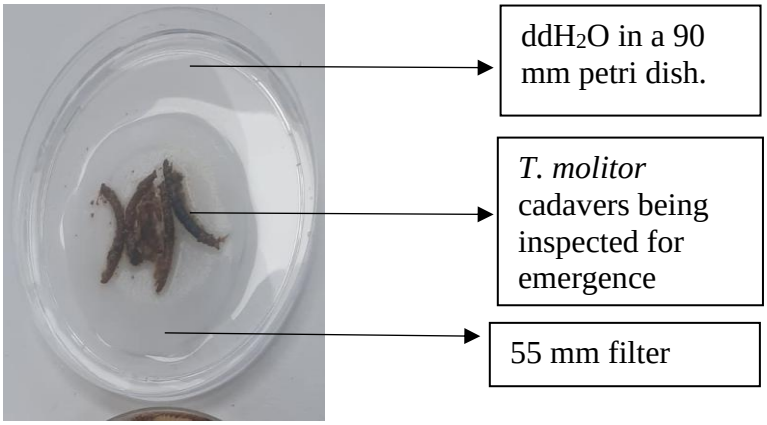

Figure 3.2 | White trap technique for isolation of mature IJs from infected insect cadavers. The setup was maintained at room temperature to facilitate IJ emergence and collection from the surrounding water.

3.2.5 Koch's postulate to re-isolate EPNs

Koch's postulate is important in determining a causal relationship between two organisms – the nematodes and the insect larvae. It is performed for re-isolation, to confirm that the observed mortality in insect hosts is directly caused by the isolated EPNs rather than by contaminants or other environmental factors. 45 grams of autoclaved sandy loam soil evenly rehydrated to 5% moisture content was added to sterile 90 mm petri dishes. To each petri dish, approximately 500 IJs from previous White traps were added. Ten *T. molitor* larvae were then placed on top of the soil, covered and stored in room temperature. The petri dishes were observed for larval mortality every 48 hours and hydrated back to 5% moisture at each check point. The EPNs were re-isolated from cadavers using the modified White traps as described in **3.2.4. Figure 3.3** shows a pathogenicity test in which Koch's postulate was performed.

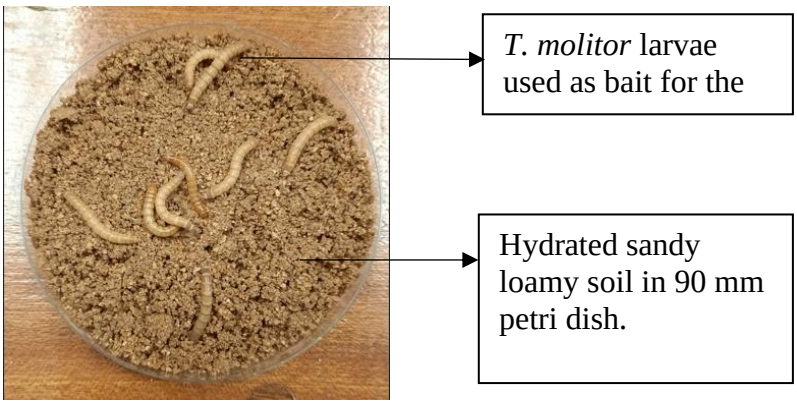

Figure 3.3 | Pathogenicity test for Koch's postulate confirmation and population increase of EPNs. *T. molitor* larvae were exposed to EPNs in sandy loam soil and monitored for mortality, with infected cadavers transferred to new White traps for IJ collection for subsequent experiments.

3.2.6 Morphological characterisation of EPNs

3.2.6.1 Semi-permanent slide mounting

For microscopic examination, semi-permanent slides were prepared using a modified glycerol mounting technique (Glime and Wagner, 2023). Nematode specimens were transferred to a clean microscope slide, and a single drop of 70% glycerol was placed directly over the specimens. Glycerol was selected as the mounting medium due to its optical clarity, appropriate refractive index, and ability to preserve specimen morphology while preventing rapid dehydration. To minimise air bubble formation, a coverslip was positioned at a 45° angle to the slide and gently lowered onto the mounting medium. Any trapped air bubbles were carefully eliminated by slightly lifting the edge of the coverslip with a toothpick. The edges of the coverslip were sealed with clear nail polish to prevent evaporation and specimen desiccation. The mounted slides were stored at 4°C overnight before microscopic examination.

3.2.6.2 Microscopic examination and imaging of EPN specimens

The mounted nematode slides were examined using an Olympus BX63 optical fluorescence microscope under bright-field illumination at 4X, 10X, and 40X magnifications. Images were captured at 1080K resolution. Z-stacking was employed for specimens where the entire nematode body could not be captured in focus within a single plane. Images of all specimens were captured, and subsequent morphometric measurements were performed and documented.

3.2.6.3 Differential interference contrast (DIC) microscopy of EPN specimens

DIC microscopy was performed using the same Olympus BX63 microscope system and following identical protocols for slide preparation, magnification settings (4X, 10X, and 40X), image capture (1080K resolution), and Z-stacking as described for bright-field microscopy.

This approach ensured consistent imaging conditions and comparability between both microscopy techniques.

3.2.6.4 Morphometric calculations

The full length and sub-sections of the isolated nematode were measured from the microscopic pictures taken in **3.2.6.2** and **3.2.6.3**. The total body length (L), distance from anterior end to excretory pore (EP), distance from anterior end base of basal bulb (ES), tail length (T), and maximum body width (W) were measured. The results were compared to the nematode readily available in the lab, *C.* sp. NTM-2021. Calculations previously published by Mabena and Lephoto. (2024), were used for comparative studies.

3.2.7 Molecular characterisation of EPNs

To obtain high-purity, contaminant-free genomic DNA for identification and further analysis, approximately 30 mg of nematodes were collected, and surface sterilised by rinsing with 0.1% hypochlorite solution, followed by three washes with ddH_2O. The sterilised nematodes were then transferred to a 1.5 ml microcentrifuge tube and crushed using an autoclaved small pestle. DNA extraction was performed using the E.Z.N.A. DNA kit, following the manufacturer's protocol detailed in **Appendix 7.1.** The concentration, purity, and integrity of the extracted DNA were assessed using a Nanodrop spectrophotometer (protocol detailed in **Appendix 7.2**). Samples failing to meet these thresholds were re-extracted. Samples meeting quality requirements were submitted to Inqaba Biotechnical Industries (Pretoria, South Africa) for sequencing of the 18S rDNA gene, specifically targeting the internal transcribed spacer (ITS) region. PCR to amplify the ITS region of the 18S rDNA was performed the forward primer TW81 (5'- GCGGATCCGTTTCCGTAGGTGAACCTGC-3') and reverse primer AB28 (5'-GCGGATCCATATGCTTAAGTTCAGCGGGT-3').

3.2.8 Phylogenetic analysis and identification of the nematode

3.2.8.1 Sequence processing and alignment

The FASTA sequences received from Inqaba Biotech were processed and analysed using BioEdit version 7.7.1.0. The raw sequence data were initially imported into the software for

examination and quality assessment. Sequence trimming was performed manually to remove low-quality or unidentified bases from both the 5' and 3' ends, with a quality threshold of Phred (Q) > 20. The sequences were visually inspected and trimmed to remove any ambiguous nucleotide positions and maintain greater than 500 base pairs per sequence. The forward and reverse sequences of each gene were uploaded, and the complement of the reverse was taken. Multiple sequence alignment was performed using muscle algorithm integrated within BioEdit.

3.2.8.2 Molecular identification and genetic characterisation

The resulting nucleotide sequences were then processed using BLAST. This was done to identify and compare the isolated species on a molecular level. The conserved gene regions, ITS region, of the rDNA were compared against reference sequences from GenBank using the built-in sequence comparison tools in BLAST. The identity of the sequence was determined by high percentage similarity, greater than 98%. The sequence was then submitted to NCBI to retrieve an accession number. The sequence was compared to other sequences and those with sequence identity threshold of ≥ 95% were considered significant for species-level identification. Genetic distances were calculated using the Kimura 2-parameter model, and a phylogenetic tree was generated using the Maximum likelihood method to visualise the genetic relationships between the studied sequences and reference taxa. Bootstrap analysis was performed with 2,000 replicates to assess the statistical reliability of the phylogenetic reconstructions (Zou *et al.*, 2024).

3.2.8.3 Phylogenetic trees of isolated nematode species

The aligned 18S rDNA sequences were used to construct a phylogenetic tree using MEGA12. For evolutionary analysis, fifteen reference sequences were obtained from the NCBI database to construct the phylogenetic tree. These included nine previously characterised species of *Oscheius*, four *Cruznema* (of which one was used for subsequent experiments), along with our newly isolated *Oscheius* strain. *Pristionchus pacificus* was used as the out-group. All sequences were aligned according to relatedness using muscle and misaligned areas were trimmed out. The final sequences were about 508 base pairs. The bootstrap parameters were set at 2,000. The tree was constructed using the Maximum Likelihood method and the Tamura-Nei model. The tree displaying the highest log likelihood was presented and used to infer relationships between the isolated nematode and other closely related species.

3.2.9 Assay to determine lethal dosage (LD80) of *O.* sp. k KN-2024

The LD50 of *O.* sp. k KN-2024 was determined using IJs cultured approximately 7 days before experimentation. The bioassay was conducted in filter paper-lined petri dishes moistened with 1 mL of ddH_2O. Four treatment concentrations were tested: 0 (control), 25, 50, and 100 IJs per insect larva. IJs were individually counted under stereomicroscope and pipetted onto dishes in their respective concentrations. Each treatment was replicated three times. Ten *T. molitor* larvae were introduced to each dish, after which dishes were sealed with parafilm to maintain humidity. Mortality assessments were conducted at 24- and 48-hours post-inoculation. To verify nematode infection as the cause of death, insect cadavers were transferred to White traps and monitored for IJ emergence. The proportion of cadavers producing IJs was recorded for each concentration to confirm successful parasitism and calculate the effective lethal dose for the nematode strain.

3.2.9.1 Statistical analysis for the LD80 assay

To assess the statistical significance in the LD80 assay, a two-sample Welch t-test (ttest_ind function with equal_var = False, from scipy.stats: version 1.10.1) was performed to compare the mortality of each of the experimental doses (25, 50, 100 IJs/larvae) against the control (0 IJs/larvae) at each time point, assuming unequal variances. The p-values for each comparison were generated and shown on the graph.

3.3 Results

3.3.1 Isolation of nematodes

An unknown nematode species was isolated from previously cultivated soil from the location (red GPS pin) shown on the map in **Figure 3.4** in Gauteng, South Africa. The coordinates were Latitude [-26.185.99°]: Longitude [28.02375833°]). The nematode species, *C.* sp. NTM-2021, used for comparative studies was previously isolated from agricultural land in Lesotho. The *T. molitor* larvae infected with the unknown nematode species exhibited characteristics of EPN infection, that is, the softening of the cadaver and colour change from brown to brownish black displayed in **Figure 3.5**.

Figure 3.4 | Map showing the region of isolation (red GPS pin) of the unknown nematode species from Gauteng, South Africa. The coordinates are latitude [-26.185.99°]: longitude [28.02375833°].

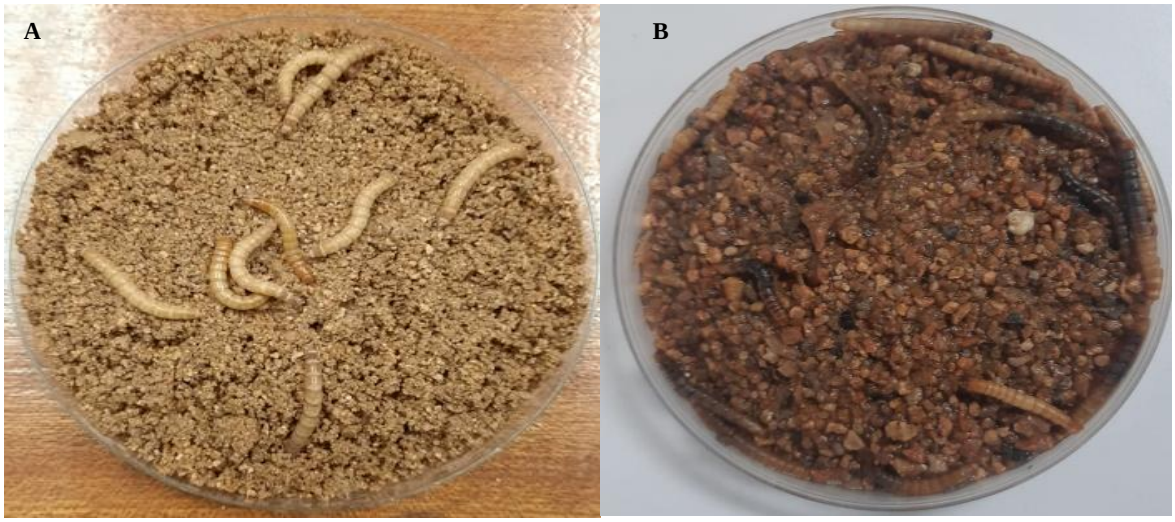

Figure 3.5 | Morphology of non-infected larvae and EPN-infected *T. molitor* cadavers. A) Uninfected larvae in a pathogenicity test; B) EPN infected cadaver change colour from brown (normal colour) to dark brown or black with softening of the cuticle.

3.3.2 Morphological characterisation

The isolated *O.* sp. k KN-2024 nematode was characterised morphologically through systematic examination of shape, size, and anatomical features. Initial bright-field microscopy provided an overview of multiple infective juveniles (IJs) in glycerol suspension, revealing their transparent bodies and internal structures **Figure 3.6**. Individual female specimens were then examined under higher magnification to observe complete anatomical characteristics **Figure 3.7**. Detailed DIC microscopy was used to analyse specific body regions of first-generation females, including head, mid-body, vulval area, and tail regions **Figure 3.8**. Morphometric measurements of *O.* sp. k KN-2024 were recorded and compared with *C.* sp. NTM-2021 species **Table 3.1**.

3.3.2.1 Microscope images of *O.* sp. k KN-2024

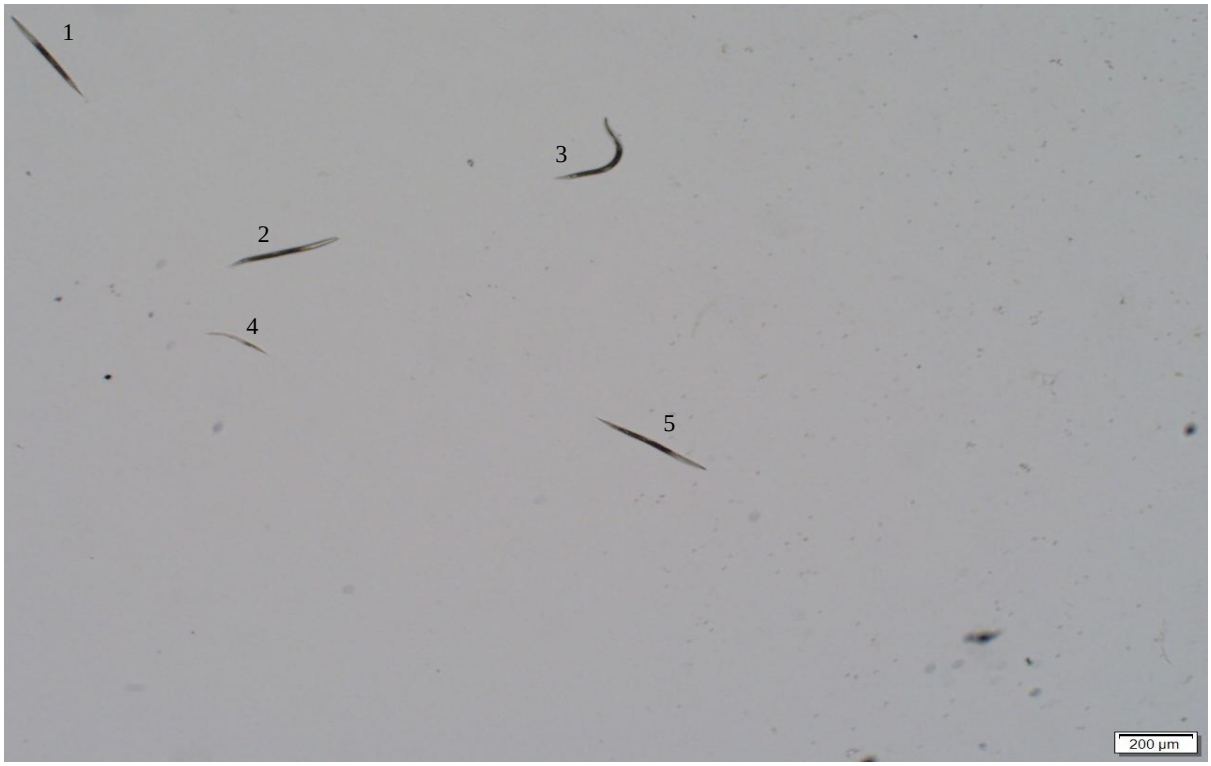

Figure 3.6 | Bright-field micrograph depicting IJs of *O.* sp k KN-2024. The image shows five IJs in glycerol suspension. Their transparent bodies show the intestinal tract (darker internal structure) through the bright-field illumination. The microgram was observed at 4X magnification. Scale bar: 200 µm.

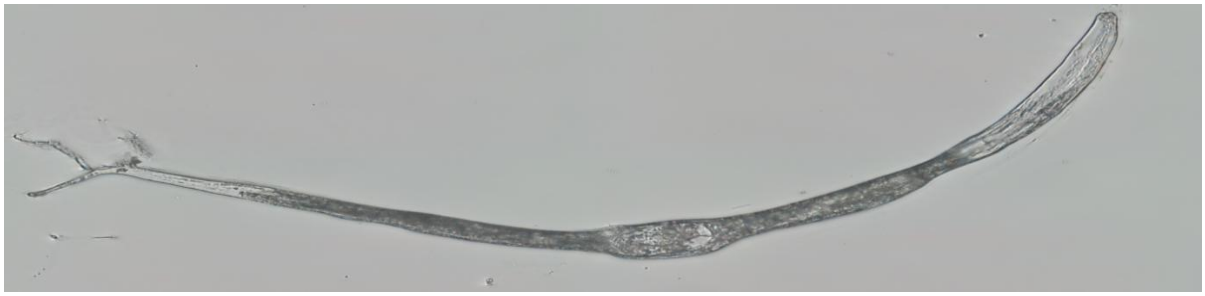

Figure 3.7 | Morphological features of female *O.* sp. k KN-2024 observed under BF microscopic examination. The image shows the anatomical characteristics of a female nematode of *O.* sp. k KN-2024. Micrograph captured at 40X magnification using an Olympus BX63 microscope.

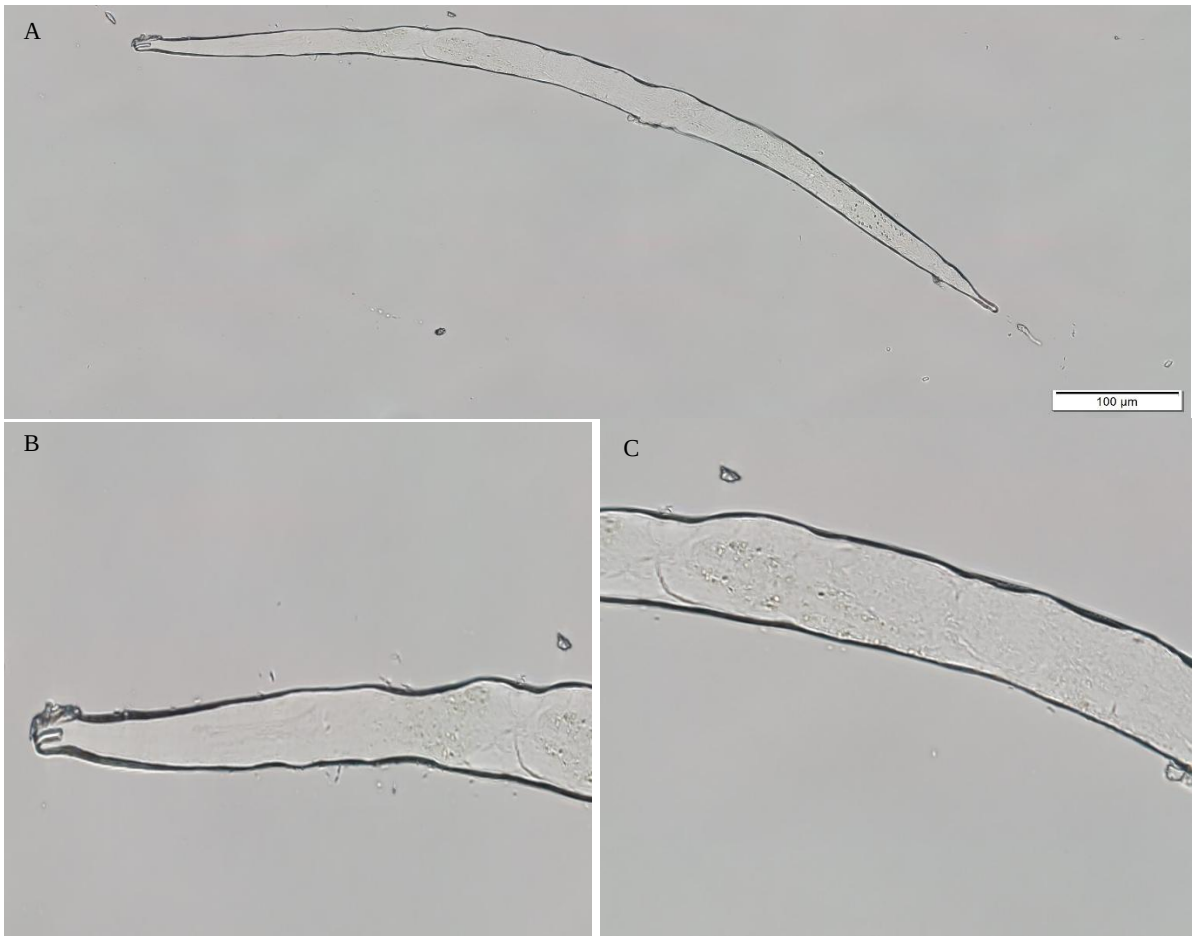

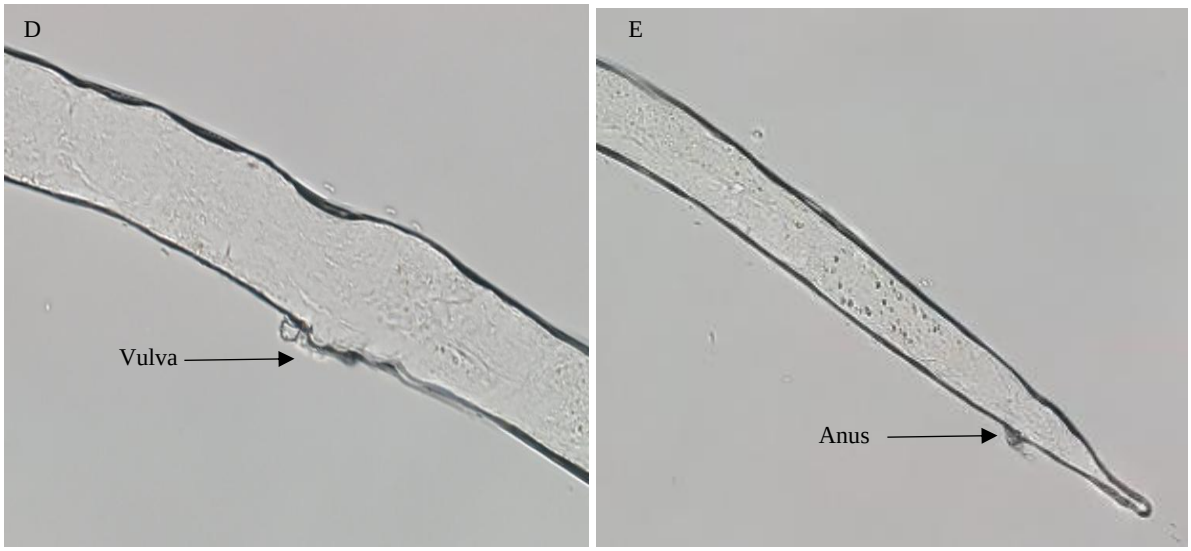

Figure 3.8 | DIC micrograph of 1st generation female *O.* sp. k KN-2024 observed at 40X under a microscope. A) Complete female with scale bar B) Head region showing open mouth; C) Mid-body region; D) Lateral field showing the vulval opening; E) Lateral field of tail region showing anal position. Scale bars: 100 µm.

3.3.2.2 Morphometric measurements

The entire *O.* sp k KN-2024 and sections are notably smaller in size than the *C.* sp. NTM-2021. The *O.* sp k KN-2024 species did not have any males in all 20 microscope slides prepared indicating hermaphrodism.

Table 3.1: Morphometrics of the IJ and female *O.* sp k KN-2024 compared to *C.* sp. NTM-2021. Measurements are in µm, data expressed in the form, mean ± SD (range).

Species	***Oscheius***			***Cruznema***		
	Male	**Female**	**IJ**	**Male**	**Female**	**IJ**
n	N/A	15	15	32	32	6
L		622.91 ± 155.42	355.01 ± 48.23	411.15 ± 188.40	1006.43 ± 210.95	868.31 ± 162.75
W		28.54 ± 16.32	18.96 ± 2.47	49.34 ± 16.65	81.95 ± 20.68	71.86 ± 13.06
EP		104.96 ± 44.65	N/A	N/A	N/A	N/A
ES		299.04 ± 16.40	N/A	87.65 ± 26.78	171.53 ± 27.37	164.58 ± 28.46
T		19.59 ± 6.39	N/A	59.13 ± 23.29	68.78 ± 18.42	28.75 ± 12.8
D%		35.10	N/A	21.32	17.04	18.95
E%		535.78	N/A	N/A	N/A	N/A

NA: not available, n: number of species, L: total body length, EP: distance from anterior end to excretory pore, ES: distance from anterior end base of basal bulb, T: tail length, W: maximum body width, a: L / W, b: L / ES, c: L / T, D%: (EP/ES) × 100, E%: (EP / T) × 100, f: W / T (1 Poinar, 1976; 2 Poinar, 1990; Malan, Knoetze and Moore, 2011; Mabena and Lephoto, 2024).

3.3.3 Molecular characterisation

To identify the isolated nematode at the species level, the ITS region of the 18S rDNA gene was trimmed and edited using BioEdit and saved as a FASTA format file. The resulting 768 base pair 18S rDNA sequence is provided in **Figure 3.9.** The sequence was submitted to NCBI and assigned the accession number PQ699765.1. The isolated nematode was identified as a new species within the *Oscheius* group, designated *O.* sp. k KN-2024.

3.3.3.1 Consensus sequence of isolated nematode

ATTCTTAGATCCAATAACAAGATTGAAACTACACCACAAGGGCAACCAAATAA
CAGATACCATTGTCAAGCTTTCATGGCAGTTATTTGGCAGTGCAGTTAAGCTCT
CGCCAGACCTATAGTTCGTATGAGTTTGTAGACTCGTACGATGTTGCAATTATT
ATTCTGAGCTAAGACGGGTATGGCACAAATAGGCCCTGCCATAGCCGTCCGAC
AGACCAGCATCCAGCTACTGGTAGTATTTAATACTTCCCTGATGCAGACGTACC
GTTAGCCGAAGCCAGCGGTGCTGTGCATTCAAGATTTTGCCACTCAAAGCGTTC
GCAATTCGTGGTAAATAACGGAGCTAGCTCCGCTTTTCATCGATTAAGGAAGCA
ACCGATCAATCCCTAAAGGTAGTCAAGGATCGTTACATTCAAAAAGAGAATAT
AAACGGTCAACGCAAAAATTAAACTTTAGATAGTTATATAGAATATAGCCGCC
AGTCAAAAAATGACCAGTCATTAAGACTCACTTTTTATTTCAAAAGTTGAAATA
ACCAGCTAAATCTATATGATTCGAGGTGAAACGGTATGCAGTTTCGTTATTTCC
CTACGTTCACGACTAAAGGTCGTAAGTTCTTTTGCTATTACGCTATTAAAAAAA
TAGCGACGGTCCAACCAGTGCCGCTAGCAAAACCTTTGGGAAACCTCGTGGTT
GTACATGCTGAGGTTGATCAAAGTCGCAGAAGTAAAGATCAAGAGCTCTACTT
CTATTGCGGCAACGACTG

Figure 3.9 | The 18S rDNA ITS region of the isolate *O.* sp. k KN-2024 (PQ699765.1). The NCBI BLAST results show high affinity to *Oscheius onirici* (LN613265).

Evolutionary analysis of the isolated *O.* sp. k KN-2024 using Maximum likelihood statistical method

3.3.3.2 Evolutionary relationship between *O.* sp. k KN-2024 and *C.* sp. NTM-2021

A phylogenetic tree of the order Rhabditida was created to show the evolutionary relationship between the isolated *O.* sp. k KN-2024 species and other previously characterised *Oscheius* species. The tree includes species of *Cruznema*, which falls under the order Rhabditida. *Cruznema* species are less extensively studied than *Oscheius*. By including both genera in the same tree, a direct comparison may be made, allowing their evolutionary relationship to be determined. A species of *Cruznema*, *C.* sp. NTM-2021, available in the laboratory was classified and added to the tree as well. It is seen to form a distinct clade with other *Cruznema* species.

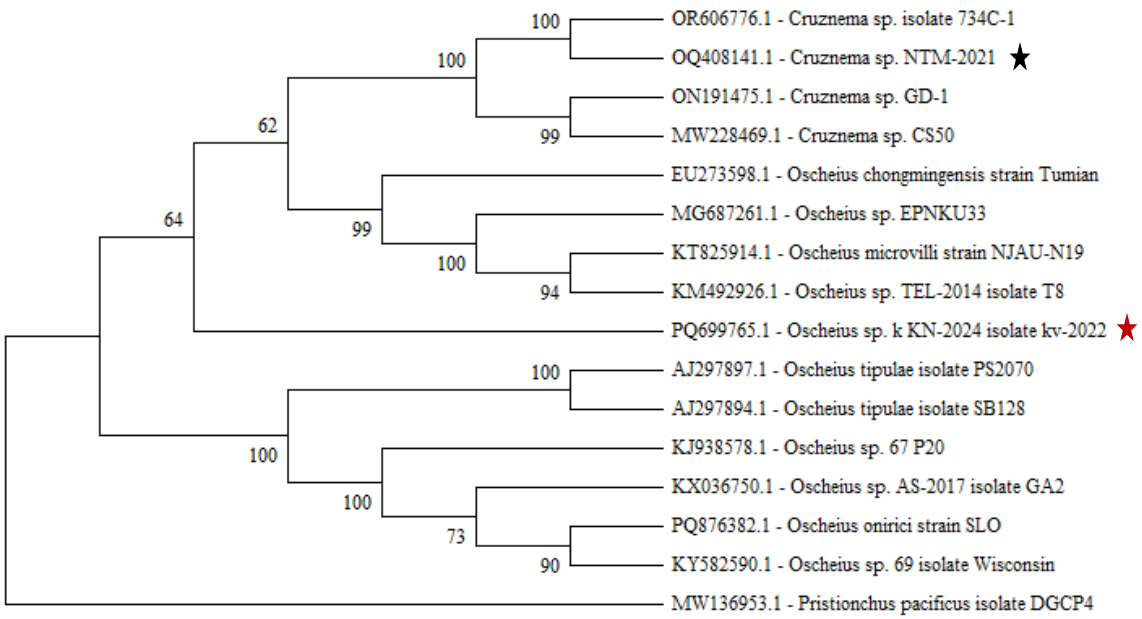

Figure 3.10 | Phylogenetic tree analysing the evolutionary relationship between 16 nucleotide sequences with 1516 positions in the final dataset of the order Rhabditida was performed on MEGA12. The phylogeny was determined using the Maximum Likelihood (ML) method and Tamura-Nei model (1993). The percentage of replicate trees in which the associated taxa cluster together is shown next to the branches. The tree was run at 2000 bootstraps with *Pristionchus pacificus* serving as the outgroup. The evolutionary relationships between the newly isolated *Oscheius* species, the *Cruznema* species available in the lab, and other species within their respective genera were compared. In the phylogenetic tree, *O.* sp. k KN-2024 is marked with a red star, while *C.* sp NTM-2021 is marked with a black star.

Table 3.2 | Estimates of evolutionary divergence between sequences conducted in MEGA12 (version 12.0.10). The number of base substitutions per site between sequences are depicted in the table. The standard error estimate(s) are shown above the diagonal and were obtained by a bootstrap procedure (2 000 replicates). The analyses were conducted using the Tamura-Nei model. The analytical procedure encompassed 16 nucleotide sequences. The pairwise deletion option was applied to all ambiguous positions for each sequence pair resulting in a final data set comprising 1 516 positions.

		1	2	3	4	5	6	7	8	9	10	11	12	13	14	15	16
1	PQ876382.1		0.179	0.071	0.068	0.091	0.077	0.069	0.057	0.000	0.002	0.057	0.059	0.003	0.051	0.018	0.019
2	PQ699765.1	1.207		0.239	0.182	0.238	0.177	0.551	0.248	0.166	0.173	0.130	0.174	0.158	0.136	0.340	0.401
3	OR606776.1	0.870	1.260		0.006	0.027	0.029	0.088	0.043	0.071	0.072	0.044	0.050	0.070	0.043	0.071	0.074
4	OQ408141.1	0.825	1.186	0.025		0.027	0.033	0.081	0.050	0.068	0.069	0.048	0.050	0.068	0.049	0.071	0.075
5	ON191475.1	0.736	1.118	0.215	0.218		0.017	0.129	0.047	0.093	0.096	0.051	0.053	0.088	0.054	0.091	0.075
6	MW228469.1	0.858	1.199	0.354	0.398	0.103		0.188	0.047	0.078	0.079	0.045	0.060	0.076	0.046	0.085	0.085
7	MW136953.1	0.788	1.444	0.937	0.883	0.827	1.030		0.074	0.070	0.070	0.080	0.085	0.068	0.066	0.077	0.079
8	MG687261.1	0.734	1.295	0.595	0.647	0.459	0.604	0.773		0.057	0.056	0.017	0.022	0.056	0.025	0.054	0.059
9	KY582590.1	0.000	1.185	0.856	0.828	0.740	0.841	0.791	0.721		0.002	0.058	0.059	0.003	0.051	0.018	0.019
10	KX036750.1	0.004	1.194	0.876	0.832	0.748	0.866	0.794	0.731	0.004		0.057	0.059	0.003	0.052	0.018	0.019
11	KT825914.1	0.747	1.104	0.596	0.635	0.496	0.590	0.806	0.200	0.733	0.745		0.021	0.058	0.026	0.056	0.062
12	KM492926.1	0.733	1.122	0.662	0.651	0.493	0.750	0.866	0.260	0.735	0.736	0.253		0.057	0.034	0.058	0.063
13	KJ938578.1	0.008	1.190	0.866	0.822	0.725	0.847	0.780	0.731	0.008	0.009	0.755	0.726		0.052	0.018	0.018
14	EU273598.1	0.682	1.175	0.576	0.631	0.524	0.634	0.729	0.316	0.668	0.686	0.349	0.455	0.689		0.053	0.059
15	AJ297897.1	0.200	1.316	0.861	0.831	0.725	0.901	0.834	0.719	0.200	0.197	0.727	0.740	0.194	0.708		0.003
16	AJ297894.1	0.177	1.245	0.806	0.787	0.536	0.841	0.812	0.675	0.177	0.173	0.692	0.695	0.169	0.677	0.007	

3.3.4 Lethal dosage (LD80) of *O.* sp. k KN-2024

The mortality of *T. molitor* larvae increased over time following exposure to IJs of *O.* sp. k KN-2024. At 24 hours, mortality remained low across all groups, including the highest IJ concentrations. By 48 hours, significant differences emerged, with the 25 IJs/larva treatment reaching approximately 83% mortality, indicating this dose is near the LD80 threshold. Higher concentrations (50 and 100 IJs/larva) did not result in higher mortality. Statistical analysis confirmed that all experimental groups experienced significantly higher mortality than the control (*$p < 0.05$, **$p < 0.01$).

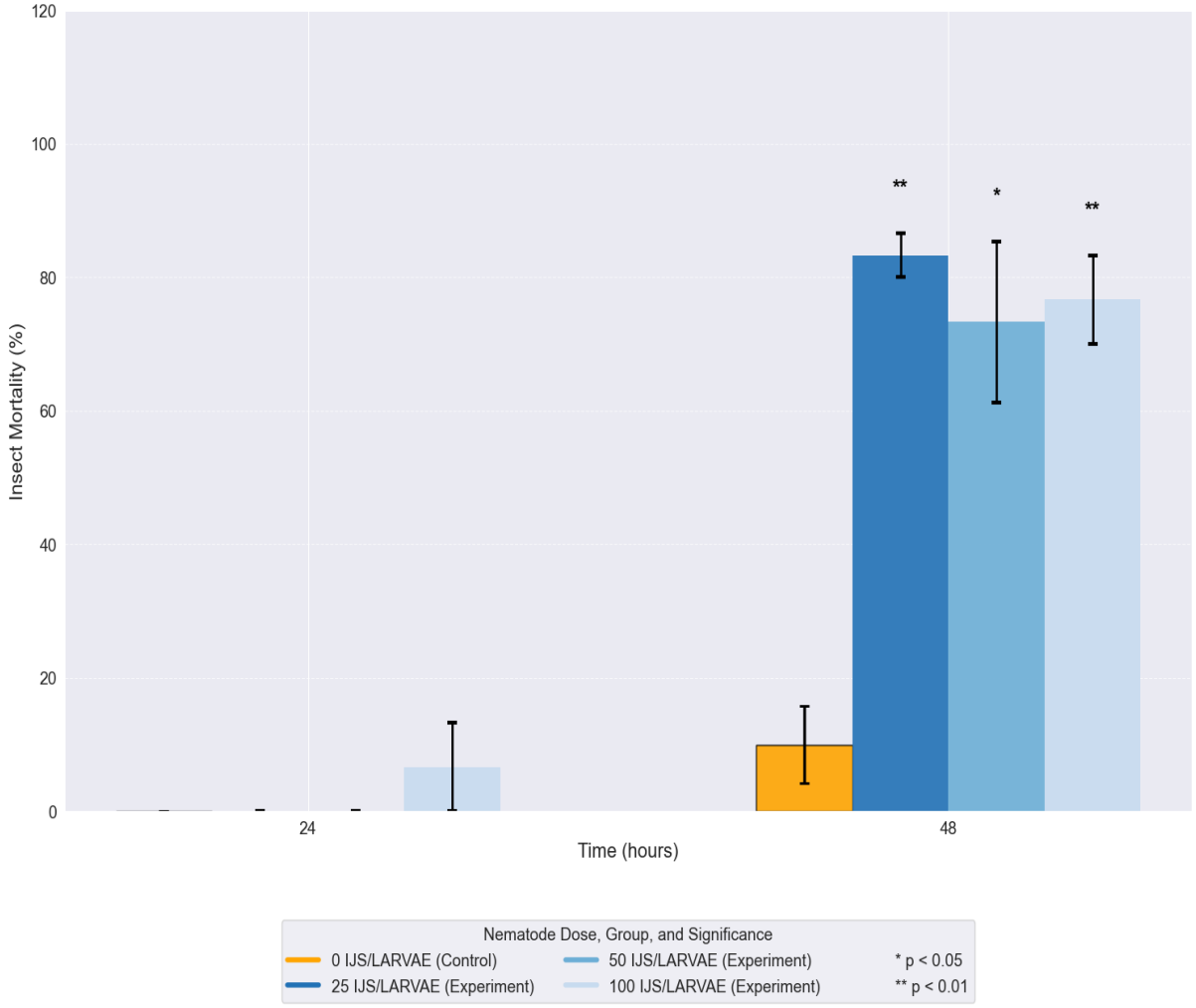

Figure 3.11 | Mortality rates of *T. molitor* in response to different concentrations of IJs of *O.* sp. k KN-2024. Insect mortality was assessed at 24- and 48-hours post-exposure to 0 (control), 25, 50, and 100 IJs per larva. Bars represent mean mortality percentage (n=3 replicates, 10 larvae per replicate) with error bars showing standard deviation. The 25 IJs/larva concentration achieved approximately 83% mortality at 48 hours, indicating this concentration approaches the LD80 for this nematode-host system. Statistical significance compared to control is indicated by asterisks (* for $p < 0.05$, ** for $p < 0.01$).

3.4 Discussion

The females and IJs of *O.* sp k KN-2024 were notably smaller than those of *C.* sp. NTM-2021. No males were isolated in all 20 microscope slides prepared indicating hermaphrodism which is in line with many *Oscheius* species isolated to date (Baïlle *et al.,* 2008).

The phylogenetic analysis **Figure 3.10** reveals clear evolutionary relationships among *Cruznema* and *Oscheius* species, with strong bootstrap support for most clades. The tree structure demonstrates distinct clustering of *Cruznema* species (bootstrap values of 99-100%), showing their close genetic relatedness. *Cruznema* sp. NTM-2021 forms a monophyletic clade with *Cruznema* sp. isolate 734C-1, showing close relatedness (Bootstrap (100%). The *Oscheius* genus appears more diverse, forming several well-supported clades that suggest potential species complexes or ongoing speciation events. *Oscheius* sp. k KN-2024 placement as a single branch between the *Cruznema* clade and other *Oscheius* species indicates that this isolate may represent an early-branching lineage within the genus, a cryptic species, or possibly even a distinct subgenus that has undergone substantial genetic differentiation (Brawn., 2008). This divergence could result from geographic isolation, ecological specialisation to specific niches or hosts, or long-term reproductive isolation. As such, this isolate might serve as an important transitional form or relict lineage that could provide valuable insights into the evolutionary history and diversification patterns of EPNs within this genus.

The genetic distance matrix **Table 3.2** quantifies the relationships depicted in the phylogenetic tree, with lower values indicating closer genetic relationships. Notable patterns include the very close relationship between OR606776.1 and OQ408141.1 (*Cruznema* sp. isolates) with a distance value of only 0.025, confirming their placement in the same tight clade. The outgroup, *Pristionchus pacificus* (MW136953.1), shows consistently high distance values from all other taxa (0.773-1.444), validating its position as an appropriate outgroup for rooting the phylogenetic tree.

The bioassay results **Figure 3.11** demonstrate a clear dose-dependent and time-dependent effect of the tested nematodes on insect mortality. At 24 hours post-exposure, minimal mortality was observed across all treatments, with only the 50 IJs/larvae treatment showing any measurable effect (~6%). The LD80 (lethal dose resulting in 80% mortality) is achieved by 25 IJs/larvae treatment, which produced approximately 83% insect mortality at 48 hours post-exposure. This indicates that approximately 25 infective juveniles (IJs) per target insect larva are sufficient to kill 80% of the treated larvae within a 48-hour period. This dose was the most effective among the tested concentrations, demonstrating greater efficacy than the higher doses of 50 and 100 IJs/larvae, which produced mortality rates of approximately 73-77%. The statistical significance ($p < 0.01$) of this result confirms the reliability of this finding.

The inverse relationship between dose and efficacy suggests that lower nematode concentrations may be more effective, possibly due to reduced competition among infective juveniles or more efficient host-finding behaviour when present in moderate numbers. This finding has important implications for optimising biological control applications, as it indicates that higher doses may not necessarily yield better results and could potentially reduce cost-effectiveness in field applications.

The strong statistical significance of the treatment effects ($p < 0.05$ and $p < 0.01$) confirms that these nematodes, particularly those from the *Oscheius* genus identified in the phylogenetic analysis, represent promising biological control agents. The genetic characterisation provided by the phylogenetic and distance data will be valuable for selecting specific isolates for further development and for tracking their performance and stability in field applications.

3.5 References

Abebe, E., Mekete, T., Thomas, W.K., 2011. A critique of current methods in nematode taxonomy. *African Journal of Biotechnology* 10, 312–323.

Akhurst, R.J. and Bedding, R., 1975. A simple technique for the detection of insect paristic rhabditid nematodes in soil', *Nematologica*, 21, pp. 109–110. Available at: https://doi.org/10.1163/187529275X00419

Alotaibi, S.S., Darwish, H., Zaynab, M., Alharthi, S., Alghamdi, A., Al-Barty, A., Asif, M., Wahdan, R.H., Baazeem, A., Noureldeen, A., 2022. Isolation, Identification, and Biocontrol Potential of Entomopathogenic Nematodes and Associated Bacteria against *Virachola livia* (Lepidoptera: Lycaenidae) and Ectomyelois ceratoniae (Lepidoptera: Pyralidae). *Biology* 11, 295. https://doi.org/10.3390/biology11020295

Aryal, S., Nielsen, U.N., Sumaya, N.H., De Faveri, S., Wilson, C., Riegler, M., 2022. Isolation and molecular characterization of five entomopathogenic nematode species and their bacterial symbionts from eastern Australia. *BioControl* 67, 63–74. https://doi.org/10.1007/s10526-021-10105-7

Baiocchi, T. *et al.* (2017) 'Host seeking parasitic nematodes use specific odors to assess host resources', *Scientific Reports*, 7. Available at: https://doi.org/10.1038/s41598-017-06620-2

Baiocchi, T., Li, C. and Dillman, A.R., 2020. EPNs Exhibit Repulsion to Prenol in Pluronic Gel Assays. *Insects*, 11(8), p. 457. Available at: https://doi.org/10.3390/insects11080457

Baïlle D, Barrière A, Félix MA. 2008 Oscheius tipulae, a widespread hermaphroditic soil nematode, displays a higher genetic diversity and geographical structure than Caenorhabditis elegans. Mol Ecol. ;17(6):1523-34. doi: 10.1111/j.1365-294X.2008.03697.x. Epub 2008 Feb 13. PMID: 18284567.

Bedding R, Akhurst R., 1975. A simple technique for the detection of insect paristic rhabditid nematodes in soil. *Nematologica* 21:109–110

Bhat, A.H., Gautum, S., Rana, A., Chaubey, A.K., Abolafia, J., Půža, V., 2021. Morphological, Morphometrical and Molecular Characterization of *Oscheius siddiqii* Tabassum and Shahina, 2010 (Rhabditida, Rhabditidae) from India with Its Taxonomic Consequences for the Subgenus *Oscheius Andrássy*, 1976. *Biology (Basel)* 10, 1239. https://doi.org/10.3390/biology10121239

Boff M, Wiegers G, Smits P., 2000. Influences of host size and host species on the infectivity and development of *Heterorhabditis megidis* (strain NLH-E87. 3). *BioControl* 45:469–482.

Bogale, M., Baniya, A., DiGennaro, P., 2020. Nematode Identification Techniques and Recent Advances. *Plants (Basel)* 9, 1260. https://doi.org/10.3390/plants9101260

Campos–Herrera, R., Barbercheck, M., Hoy, C.W., Stock, S.P., 2012. Entomopathogenic Nematodes as a Model System for Advancing the Frontiers of Ecology. *Journal of Nematology* 44, 162–176.

Baum, D. (2008) Reading a Phylogenetic Tree: The Meaning of Monophyletic Groups. *Nature Education* 1(1):190

Dillman AR, Sternberg PW., 2012. Entomopathogenic nematodes. *Curr Biol*. 5;22(11): R430-1. doi: 10.1016/j.cub.2012.03.047. PMID: 22677279; PMCID: PMC4662870.

Du, H. *et al.*, 2022. Complete Mitogenome of *Cruznema Tripartitum* Confirms Highly Conserved Gene Arrangement within Family Rhabditidae. *Journal of Nematology*, 54(1), p. 20220029. Available at: https://doi.org/10.2478/jofnem-2022-0029

Ghavamabad, R.G. *et al.*, 2021. First record of *Oscheius myriophilus* () (Rhabditida: Rhabditidae) from Iran; and its efficacy against two economic forest trees pests, *Cydalima perspectalis* (Walker, 1859) (Lepidoptera: Crambidae) and *Hyphantria cunea* () (Lepidoptera: Erebidae) in laboratory condition', *Journal of Nematology*, 53, pp. e2021-35. Available at: https://doi.org/10.21307/jofnem-2021-035

Grewel PS, Bai X, Jagdale GB. 2011 Longevity and stress tolerance of entomopathogenic nematodes. Pp. 157–181 *in* R.N. Perry, and D.A. Wharton, eds. Molecular and physiological basis of nematode survival. Wallingford, UK: CAB International.

Felsenstein J., 1985. Confidence limits on phylogenies: An approach using the bootstrap. *Evolution* 39:783-791.

Handoo, Z.A., Skantar, A.M., Subbotin, S.A., Kantor, M.R., Hult, M.N., Grabowski, M., 2021. Molecular and morphological characterization of a first report of Cactodera torreyanae Cid del Prado Vera & Subbotin, 2014 (Nematoda: Heteroderidae) from Minnesota, the United States of America. *Journal of Nematology*, 53, pp. e2021-93. https://doi.org/10.21307/jofnem-2021-093

Jaffuel, G., Blanco-Pérez, R., Hug, A.-S., Chiriboga, X., Meuli, R.G., Mascher, F., Turlings, T.C.J., Campos-Herrera, R., 2018. The evaluation of entomopathogenic nematode soil food web assemblages across Switzerland reveals major differences among agricultural, grassland and forest ecosystems. *Agriculture, Ecosystems & Environment* 262, 48–57. https://doi.org/10.1016/j.agee.2018.04.008

James M, Malan AP, Addison P., 2018. Surveying and screening South African entomopathogenic nematodes for the control of the Mediterranean fruit fly, *Ceratitis capitata* (Wiedemann). *Crop Prot* 105:41–48

Khashaba, E.H.K. *et al.*, 2020. Isolation, identification of entomopathogenic nematodes, and preliminary study of their virulence against the great wax moth, *Galleria mellonella* L.

(Lepidoptera: Pyralidae). *Egyptian Journal of Biological Pest Control*, 30(1), p. 55. Available at: https://doi.org/10.1186/s41938-020-00257-6

Koppenhöfer AM, Fuzy EM., 2003. *Steinernema scarabaei* for the control of white grubs. Biol Control 28:47–59.

Lacey, L.A. and Georgis, R. 2012. Entomopathogenic Nematodes for Control of Insect Pests Above and Below Ground with Comments on Commercial Production. *Journal of Nematology*, 44(2), pp. 218–225.

Lee, S., Kim, Y. and Han, S., 2000. An improved collecting method of the infective juveniles of the entomopathogenic nematode, Steinernema carpocapsae Weiser. *Korean J. Soil Zool*, *5*, pp.97-100.

Lewis, W.J. *et al.*, 1997. A total system approach to sustainable pest management. *Proceedings of the National Academy of Sciences*, 94(23), pp. 12243–12248.

Lephoto, T.E. *et al.* 2016. Whole genome sequence of *Oscheius* sp. TEL-2014 entomopathogenic nematodes isolated from South Africa. *Genomics Data*, 7, pp. 259–261. doi: 10.1016/j.gdata.2016.01.017

Lucena-Aguilar, G., Sánchez-López, A.M., Barberán-Aceituno, C., Carrillo-Ávila, J.A., López-Guerrero, J.A., Aguilar-Quesada, R., 2016. DNA Source Selection for Downstream Applications Based on DNA Quality Indicators Analysis. Biopreserv Biobank 14, 264–270. https://doi.org/10.1089/bio.2015.0064

Mabena, N.B., and Lephoto T.E. 2024. Characterization of EPNs and their bacterial symbionts. Univeristy of the Witwatersrand. https://wiredspace.wits.ac.za/items/87fe1874-0204-4577-bd2e-3cf3ee3e629c

Malan, A.P., Knoetze, R. and Moore, S.D., 2011 Isolation and identification of entomopathogenic nematodes from citrus orchards in South Africa and their biocontrol potential against false codling moth. *Journal of Invertebrate Pathology*, 108(2), pp. 115–125. Available at: https://doi.org/10.1016/j.jip.2011.07.006

Neira-Monsalve, E., Wilches-Ramírez, N.C., Terán, W., del Pilar Márquez, M., Mosquera-Espinosa, A.T., Sáenz-Aponte, A., 2020. Isolation, identification, and pathogenicity of *Steinernema carpocapsae* and its bacterial symbiont in Cauca-Colombia. *Journal of Nematology* 52, e2020-89. https://doi.org/10.21307/jofnem-2020-089

Nguyen KB, Malan AP, Gozel U. *Steinernema khoisanae* n. sp. (Rhabditida: Steinernematidae) a new entomopathogenic nematode from South Africa. *Nematology*. 2006;8:157–175.

Noosidum, A. *et al.*, 2010. Characterization of New Entomopathogenic Nematodes from Thailand: Foraging Behavior and Virulence to the Greater Wax Moth, *Galleria mellonella* L. (Lepidoptera: Pyralidae). *Journal of Nematology*, 42(4), pp. 281–291.

Nxitywa, A., Malan, A.P., 2021. Formulation of Entomopathogenic Nematodes for the Control of Key Pests of Grapevine: A Review. *South African Journal of Enology and Viticulture* 42, 123–135. https://doi.org/10.21548/42-2-4479

Ojha, K.K., Mishra, S. and Singh, V.K., 2022. Chapter 5 - Computational molecular phylogeny: concepts and applications. in D.B. Singh and R.K. Pathak (eds) *Bioinformatics*. *Academic Press*, pp. 67–89. Available at: https://doi.org/10.1016/B978-0-323-89775-4.00025-0

Park, Y., Kim, Y., Yi, Y. and Han, S., 1998. Optimal storage conditions of the entomopathogenic nematode, Steinernema carpocapsae. *Korean J. Appl. Entomol*, *3*, pp.10-16.

Platt, T., Stokwe, N.F., Malan, A.P., 2020. A Review of the Potential Use of Entomopathogenic Nematodes to Control Above-Ground Insect Pests in South Africa. *South African Journal of Enology and Viticulture* 41, 1–16. https://doi.org/10.21548/41-1-2424

Qi-zhi, L. *et al.* (2012) 'Re-description of *Oscheius chongmingensis* (Zhang et al., 2008) (Nematoda: Rhabditidae) and its entomopathogenicity', *Nematology*, 14, pp. 139–149. Available at: https://doi.org/10.1163/138855411X580777

Reboredo, G.R. and Camino, N.B., 2000. Two new rhabditida species (Nematoda: Rhabditidae) parasites of *Cyclocephala signaticollis* (Coleoptera: Scarabaeidae) in Argentina. *The Journal of*

Parasitology, 86(4), pp. 819–821. Available at: https://doi.org/10.1645/0022-3395(2000)086[0819:TNRSNR]2.0.CO;2

Reboredo G. R., Camino N. B. Two new species of nematodes (Rhabditida: Diplogasteridae and Rhabditidae) parasites of *Gryllodes laplatae* (Orthoptera: Gryllidae) in Argentina. *Memorias do Instituto Oswaldo Cruz.* 1998; 93:763–766.

Saitou N. and Nei M., **1987**. The neighbor-joining method: A new method for reconstructing phylogenetic trees. *Molecular Biology and Evolution* **4**:406-425.

Shapiro-Ilan DI, Gouge DH, Koppenhöfer AM., 2002. Factors affecting commercial success: case studies in cotton, turf and citrus. In: Gaugler R, editor. *Entomopathogenic Nematology*. New York, USA: CABI Publishing; pp. 333–356.

Sudhaus, W. 1976. Nomenklatorische Bemerkungen über Arten und Gattungen der Unterfamilie Rhabditinae sensu lato (Rhabditidae, Nematoda). *Nematologica* 22: 49–61, Available at: 10.1163/187529276X00049.

Sultana R and Pervez R., 2019. Description of *Cruznema minimus* sp. n. (Nematoda: Rhabditidae) and *Acrobeloides insignis* sp. n. (Nematoda; *Cephalobidae*) with a key to *Cruznema* species. *Annals of Plant Protection Sciences.* 27:3 pp. 394-399. DOI: 10.5958/0974-0163.2019.00087.9
Stern, D.L., 2013. The genetic causes of convergent evolution', *Nature Reviews Genetics*, 14(11), pp. 751–764. Available at: https://doi.org/10.1038/nrg3483

Stuart RJ, Barbercheck ME, Grewal PS, Taylor RAJ, Hoy CW., 2006. Population biology of entomopathogenic nematodes: Concepts, issues, and models. *Biological Control.* 38:80–102.
Tamura K. and Nei M., 1993. Estimation of the number of nucleotide substitutions in the control region of mitochondrial DNA in humans and chimpanzees. *Molecular Biology and Evolution* 10:512-526.

Tamura K., Nei M., and Kumar S., 2004. Prospects for inferring very large phylogenies by using the neighbor-joining method. *Proceedings of the National Academy of Sciences* (*USA*) 101:11030-11035.

Tamura K., Stecher G., and Kumar S., 2021. MEGA 11: Molecular Evolutionary Genetics Analysis Version 11. *Molecular Biology and Evolution* https://doi.org/10.1093/molbev/msab120

Vanlalhlimpuia *et al.*, 2018. Morphological and molecular characterization of entomopathogenic nematode, *Heterorhabditis baujardi* (Rhabditida, Heterorhabditidae) from Mizoram, northeastern India. *Journal of Parasitic Diseases: Official Organ of the Indian Society for Parasitology*, 42(3), pp. 341–349. Available at: https://doi.org/10.1007/s12639-018-1004-0

White GF. 1927. A method for obtaining infective nematode larvae from cultures. *Science,* 66:302–303. doi: 10.1126/science.66.1709.302-a.

Ye, W., Foye, S., MacGuidwin, A.E., Steffan, S., 2018. Incidence of *Oscheius onirici* (Nematoda: Rhabditidae), a potentially entomopathogenic nematode from the marshlands of Wisconsin, USA. J Nematol 50, 9–26. https://doi.org/10.21307/jofnem-2018-004

Zhang, K., Baiocchi, T., Lu, D., Chang, D.Z., Dillman, A.R., 2019. Differentiating between scavengers and entomopathogenic nematodes: Which is *Oscheius chongmingensis*? J Invertebr Pathol 167, 107245. https://doi.org/10.1016/j.jip.2019.107245

Zou, Y., Zhang, Z., Zeng, Y., Hu, H., Hao, Y., Huang, S., Li, B., 2024. Common Methods for Phylogenetic Tree Construction and Their Implementation in R. *Bioengineering (Basel)* 11, 480. https://doi.org/10.3390/bioengineering11050480

Chapter 4

Isolation and characterisation of symbiotic bacteria of *O.* sp. k KN-2024 isolate kv-2022

4.1 Introduction

The interactions between nematodes and bacteria can be mutualistic, parasitic or symbiotic (Kundu and Vyshali, 2022). In beneficial relationships, the nematodes or bacteria serve as food sources or mutual partners; enhancing growth, reproduction, defence, and nutrient acquisition (Murfin *et al.*, 2012). Bacterivorous nematodes, like *C. elegans*, opportunistically feed on bacteria or depend on specific bacterial partners. On the other hand, pathogenic interactions lead to disease (Poinar and Hansen, 1986; Hansen *et al.*, 2011; Murfin *et al.*, 2012). These relationships can be temporary, facultative, or evolve into long-term symbiosis (Murfin *et al.*, 2012).

EPNs forms stable symbiotic relationships with bacteria that are critical for insect larvae mortality (Chaston *et al.*, 2011). The obligate EPNs from genera *Steinernema*, *Heterorhabditis*, and *Oscheius* form symbiotic associations with bacteria of the family Enterobacteriaceae; *Xenorhabdus*, *Photorhabdus*, and *Serratia* genera, respectively (Pervez, Lone and Pattnaik, 2020). These symbiotic relationships are important as both organisms contribute essential functions for the successful infection of insect larvae (Ali *et al.*, 2005; Devi, 2023). The IJs stage of EPNs shelter the bacteria within their gut, providing protection from environmental stressors and predators while serving as dispersal vectors that deliver bacteria directly into the hemocoel of the insect host (Chaston *et al.*, 2011; Abd-Elgawad, 2022; Van, 2022). In turn, the bacteria produce toxins, exoenzymes, and antimicrobial compounds that digests its tissues, suppress competing microorganisms and rapidly kill the insect host, within 24 to 72 hours (Askary and Abd-Elgawad, 2021). This creates a suitable nutritional environment for nematode reproduction and development. While these core functions are conserved across all EPN-bacteria interactions, they are unique to each nematode species due to distinct physiological and metabolic mechanisms within species.

It is due to the combined action of the IJs and the virulence factors of the symbiotic bacteria (Ali *et al.*, 2005). Both the nematodes as well as the symbiotic bacteria proliferate within the insect cadaver until a new generation of IJs emerge, ready to infect a new insect host (Kaya and Gaugler, 1993). The rapid lethality observed in the insect pest is credited to the combined effects of both symbionts working synergistically (Pervez, Lone and Pattnaik, 2020). In addition to the symbiotic bacteria, EPNs form associations with several noncognate bacterial species, including members of the genera *Pseudomonas*, *Acinetobacter*, *Staphylococcus*, *Stenotrophomonas*, *Ochrobactrum*, and *Achromobacter* (Poinar., 1966; Mangowa and Serepa-Dlamini, 2020). However, their role in infectivity is not well understood, requiring further research. Our research aims to characterise the isolated bacteria from the nematode and determine its evolutionary relationship with other bacteria.

4.2 Materials and methods

4.2.1 Surface sterilisation of IJs and bacterial cultivation

IJs collected from White traps were transferred to 50 ml Falcon tubes and allowed to settle. The excess water was removed, and the nematodes were surface sterilised in 10 ml of 0.1% hypochlorite solution for 1 hour. The EPNs were subsequently rinsed three times with 5 ml ddH_2O at 1-hour intervals. To dilute any sterilising agents remaining on the IJs and prevent damage to the cuticle, they were further treated with 10 ml of Ringer's solution. The sterilised IJs were then transferred to a 1.5 ml microcentrifuge tube and mechanically crushed using a small pestle for about 30 minutes. 1 ml of nutrient broth was added to the microcentrifuge tube, which was sealed with Parafilm and incubated at 25°C with continuous agitation for 48 hours. This was then used for subsequent experiments for the isolation of pure colonies as well as for DNA extraction.

4.2.2 Bacterial colony growth on non-selective and selective agar for morphological identification

The bacterial broth from **Section 4.2.1** was initially spread aseptically onto non-selective nutrient agar (NA) to obtain isolated colonies. Once single colonies were obtained, these were subsequently quadrant streaked onto selective media: MacConkey agar and nutrient bromothymol triphenyltetrazolium agar (NBTA), prepared according to the protocol in

Appendix 7.3.3 (Dahal, 2024). All plates were sealed with parafilm and incubated at 25°C for 48 hours. After incubation, single colonies from the MacConkey agar plates were re-streaked to obtain pure cultures, with focus on MacConkey agar since symbiotic bacteria of infective juveniles (IJs) are typically Gram-negative. The colony morphology and colour were recorded 48 hours after the final streaking. The plates were then stored at 5°C for subsequent experiments.

4.2.3 Biochemical characterisation

Two key biochemical tests were performed to differentiate bacterial isolates based on their enzymatic activities. The detailed methodology for these tests is detailed in **Appendix 7.5**.

4.2.3.1 Catalase test

The catalase test was conducted to detect the presence of catalase enzyme, which converts hydrogen peroxide (H_2O_2) to water and oxygen. A single colony from each 48-hour culture was tested with 3% hydrogen peroxide solution. Immediate bubble formation indicated a positive result, signifying the presence of catalase enzyme. Results were recorded for all four bacterial isolates. Detailed protocol given in **(Appendix 7.5.1)**

4.2.3.2 Oxidase test

The oxidase test was performed to detect cytochrome c oxidase activity, an enzyme involved in aerobic respiration. The test employed Remel oxidase reagent on filter paper. Development of dark purple coloration within 10 seconds indicated a positive result, while no colour change after 2 minutes indicates a negative result. This test was performed to distinguish between bacteria of the family *Enterobacteriaceae* (oxidase-negative) and other genera such as *Pseudomonas, Aeromonas, Vibrio,* and *Neisseria* (oxidase-positive). Detailed protocol given in **(Appendix 7.5.2).**

4.2.4 Differential staining techniques

4.2.4.1 Gram staining

Bacterial isolates are classified based on their cell wall composition and characterised using standard Gram staining procedures (Bartholomew and Mittwer, 1952). Heat-fixed bacterial smears were sequentially treated with crystal violet (primary stain), Gram's iodine (mordant), ethanol (decolourising agent), and safranin (counterstain). Stained slides were observed under oil immersion at 1000× magnification using a light microscope. Bacteria were classified as Gram-positive (purple) or Gram-negative (pinkish red), and their cellular morphology was documented. Detailed protocol on the staining procedure used is provided in **Appendix 7.5.3.**

4.2.4.2 Endospore staining

To identify potential endospore-forming bacteria, isolates were subjected to endospore staining using malachite green as the primary stain and safranin as the counterstain. Slides were examined under oil immersion at 1000× magnification to detect the presence of endospores (green) within vegetative cells (pink or red). The detailed protocol on the staining procedure used is provided in **Appendix 7.5.4**.

4.2.5 Molecular characterisation of bacterial 16S rDNA gene

4.2.5.1 Bacterial DNA extraction

Prior to DNA extraction, the IJs were surface sterilised as described in **Section 4.2.1**. The DNA of all four bacterial isolates was extracted from pure cultures. The bacteria were cultured in Luria-Bertani (LB) broth overnight, and 3 ml was used for the extraction. The bacteria in the log phase were used for the extraction process to ensure high quality and quantity of DNA. The DNA was extracted using the E.Z.N.A Bacterial DNA Kit following the manufacturers protocol detailed in **Appendix 7.1**. The concentration and purity of the extracted DNA was assessed using the Nanodrop spectrophotometer as detailed in **Appendix 7.2** and stored at -80°C to prevent degradation prior to being sent to Inqaba Biotechnological Industries Pty (Ltd), South Africa for polymerase chain reaction (PCR) amplification and 16S rDNA genomic sequencing.

4.2.5.2 Polymerase chain reaction

The PCR step used to amplify the species-specific ITS region within the 16S rDNA was outsourced to Inqaba Biotechnological Industries Pty (Ltd), South Africa as has become common practise in laboratories. PCR amplification was performed using the NEB OneTaq 2X Master mix with standard buffer (Catalogue No. M0482S). Each reaction contained genomic DNA (10-30 ng/µl), 10 µM of both the forward and reverse primers, and nuclease free water (Catalogue No. E476) to adjust the final volume. The universal bacterial primers were used which are listed in **Table 1**.

The PCR conditions were as follows: an initial denaturation step at 94°C for 5 minutes, followed by 35 cycles of denaturation at 94°C for 30 seconds, annealing at 50°C for 30 seconds, and extension at 68°C for 1 minute. A final extension step was performed at 68°C for 10 minutes, after which the reaction was held at 4°C until further analysis. The integrity and presence of the PCR amplicons was assessed by agarose gel electrophoresis (1% agarose gel stained with EZ-vision Bluelight DNA Dye; with molecular weight marker: NEB Fast Ladder (N3238)).

Table 4.1: 16S rDNA gene universal primers used for bacterial identification

Name of Primer	Target	Sequence ($5^1 – 3^1$)
16S-27F	16S rDNA sequence	AGAGTTTGATCMTGGCTCAG
16S-1492R	16S rDNA sequence	CGGTTACCTTGTTACGACTT

Table 4.2: Sample requirements and quantities for PCR

Requirements	**Quantities**
Primers	≥ 10µl with a concentration of 10µM + 1µl for every reaction required
PCR products	≥ 15µl
Plasmids	≥ 12µl
Genomic DNA	≥ 15µl and concentration [≥30ng/µl]

4.2.5.3 Sanger sequencing

Following PCR amplification, the amplicons were enzymatically purified using the ExoSAP procedure (NEB M0293L; NEB M0371) to remove excess primers and unincorporated dNTPs before downstream applications. The purified amplicons were then subjected to sequencing using the ZR-96 DNA Sequencing Clean-up Kit™ (Zymo Research, Catalogue No. D4050) to further purify the DNA before sequencing reactions. Bidirectional sequencing was performed using BrilliantDye™ Terminator Cycle Sequencing Kit V3.1 (Nimagen, BRD3-100/1000) to generate both forward and reverse reads. Sequencing reactions were analysed using the ABI 3730x Genetic Analyzer (Applied Biosystems, Thermo Fisher Scientific), which utilises capillary electrophoresis to separate and detect fluorescently labelled DNA fragments. Raw sequence chromatograms were sent back for analysis.

4.2.5.4 Sequence trimming and visualisation

The sequences were visualised using BioEdit as this is a quality control tool for short sequences and further checked manually after which a BLAST search was performed. The first 20 to 30 sequences closely related to the first hit or with high affinity was used for further steps. These sequences were cut and pasted to a Microsoft Word document to check for mistakes. The bacterial isolates were then identified to species level by finding the similarities of the rDNA sequence to the already known sequences in the NCBI database.

4.2.6 Phylogenetic trees for evolutionary relationships

The aligned 16S rDNA sequences were used to create a phylogenetic tree on MEGA 12 (version 12.0.10). The tree was constructed with 4 unknown bacterial isolates, 17 known *Achromobacter* and 5 *Bordetella* species obtained from the NCBI database. *Alcaligenes faecalis* was used as the outgroup as it belongs to the same family (Alcaligenaceae) as *Achromobacter* and *Bordetella* but is phylogenetically distinct enough to provide a clear root for the evolutionary tree while still being closely related to accurately calibrate evolutionary distances. The phylogenetic tree for comparisons was constructed using the Kimura-2 model and Maximum Likelihood method and the parameters were set at 2,000 replications (bootstraps).

4.3 Results

Four different *Achromobacter* bacterial species recovered from *O*. sp k KN23 were isolated, sequenced and submitted to NCBI to obtain accession numbers. The isolated species with their accession numbers are: *Achromobacter* sp. strain A7 (PQ471029), *Achromobacter* sp. KN23 (PP782188), *Achromobacter kerstersii* strain Kav23 (PP779907) and *Achromobacter xylosoxidans* strain Kav2023 (PP753765). Biochemical and staining techniques were performed on the bacteria, which resulted in Gram negative strains.

4.3.1 Phenotypic characterisation

4.3.1.1 Bacterial morphology on selective agar

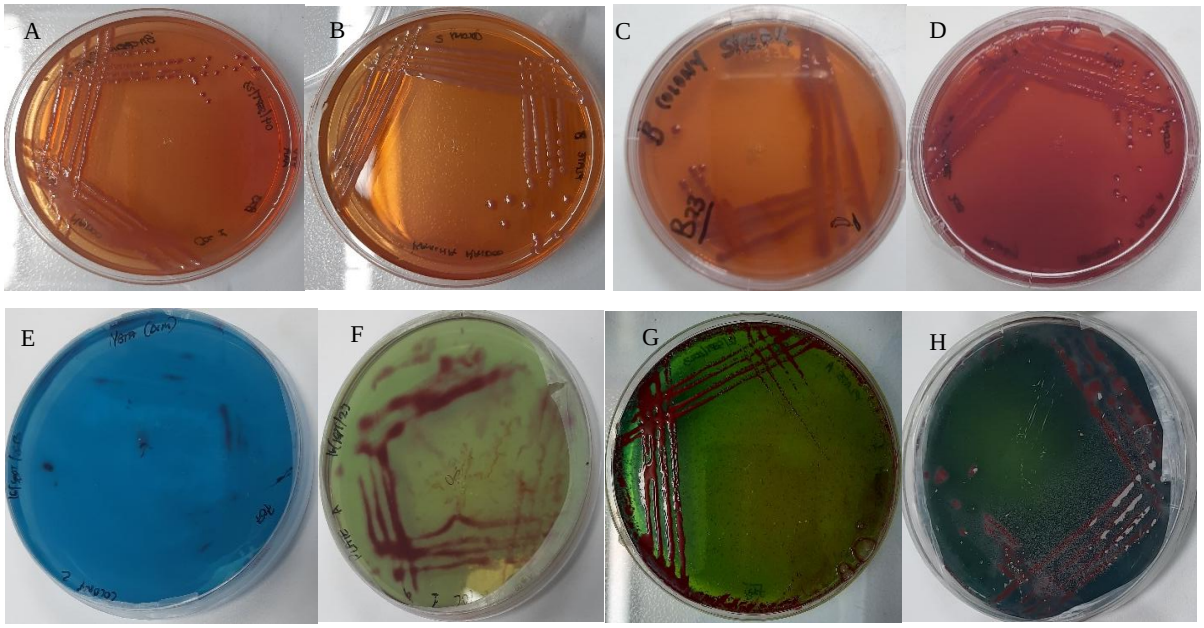

Figure 4.1| Colony morphology of *Achromobacter* isolates on selective media. A-D shows bacterial growth on MacConkey agar **E-H** show growth on NBTA (nutrient bromothymol blue tetrazolium agar) **A:** *Achromobacter* sp. strain A7 (PQ471029). **B:** *Achromobacter* sp. KN23 (PP782188). **C:** *Achromobacter kerstersii* strain Kav23 (PP779907). **D:** *Achromobacter xylosoxidans* strain Kav2023 (PP753765). The isolates on MacConkey agar (A-B) show non-lactose fermenting growth patterns, while NBTA media (C-F) reveals differential tetrazolium reduction and bromothymol blue absorption characteristics among the four strains.

4.3.1.2 Colony morphology

Colony growth on each agar was observed and recorded. On MacConkey agar, lactose-fermenting colonies appeared pink to red, while non-lactose fermenters remained colourless. On NBTA, phase I bacterial symbionts of EPNs were identified by their ability to absorb bromothymol blue, resulting in blue-green colonies. Phase II variants appeared red due to their inability to absorb the dye. These media-specific reactions provided preliminary biochemical characterisation of the bacterial isolates and insights into their potential symbiotic relationships with the nematodes.

Table 4.3. Colony morphology characteristics of *Achromobacter* isolates on selective differential media

Isolate	Accession	MacConkey Agar	NBTA Agar
Achromobacter sp. strain A7	PQ471029	Non-lactose fermenting **(A)**	Dark green medium with red bacterial growth along streak lines **(E)**
		Pink, shiny, elevated/ raised, circular colonies.	Dark pink, small, shiny and circular colonies.
Achromobacter sp. KN23	PP782188	Non-lactose fermenting **(B)**	Dark blue-green background with **(F)**
		Pale pink, uniform-sized, circular and shiny colonies.	Reddish pink, shiny, irregular shaped colonies.
Achromobacter kerstersii strain Kav23	PP779907	Non-lactose fermenting **(C)**	Bright blue medium **(G)**
		Dark-pink, uniform, circular shiny colonies.	No distinct colonies, However, the bacterial growth is non-pigmented/ white.
	PP753765	Non-lactose fermenting **(D)**	Green medium with reddish growth pattern **(H)**

Achromobacter xylosoxidans strain Kav2023		Dark pink, small, uniform, shiny colonies.	Red, shiny, non-uniform colonies.

4.3.2 Biochemical identification

Biochemical tests were performed to determine the presence of enzymes in the bacterial isolates.

4.3.2.1 Catalase test

A positive test was observed for all four bacterial isolates. Bubble formation was observed immediately upon the addition of 3% hydrogen peroxide. **Figure 4.2** below depicts the results obtained for the catalase test.

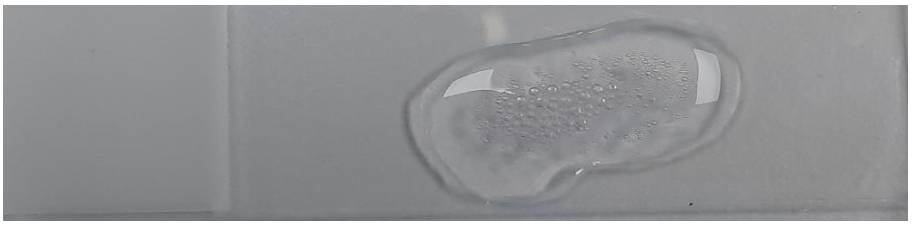

Figure 4.2 | Representative catalase test showing positive result characteristic of all four bacterial isolates. Effervescence was observed immediately upon the addition of 3% hydrogen peroxide.

4.3.2.2 Oxidase test

A positive oxidase test was observed for all four bacterial isolates. There was a colour change from white to dark purple within 30 seconds of treatment. A negative test is noted when colour change does not occur after two minutes. **Figure 4.3** below depicts the positive result.

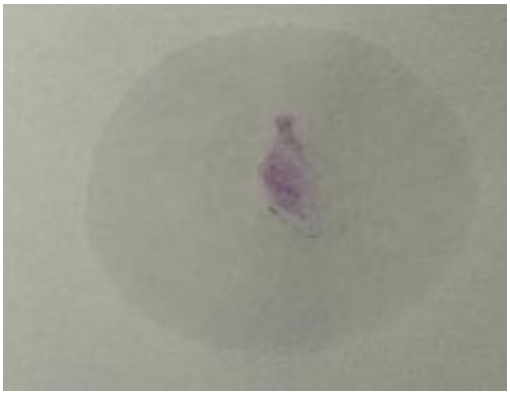

Figure 4.3 | Representative positive oxidase test result observed in all four bacterial isolates. All samples showed identical colour change from white to dark purple within 10 seconds of treatment.

4.3.3 Differential staining techniques

4.3.3.1 Gram staining

All four bacterial isolates were negative for Gram staining as they stained pink. **Figure 4.4** depicts the Gram results of the bacterial isolates.

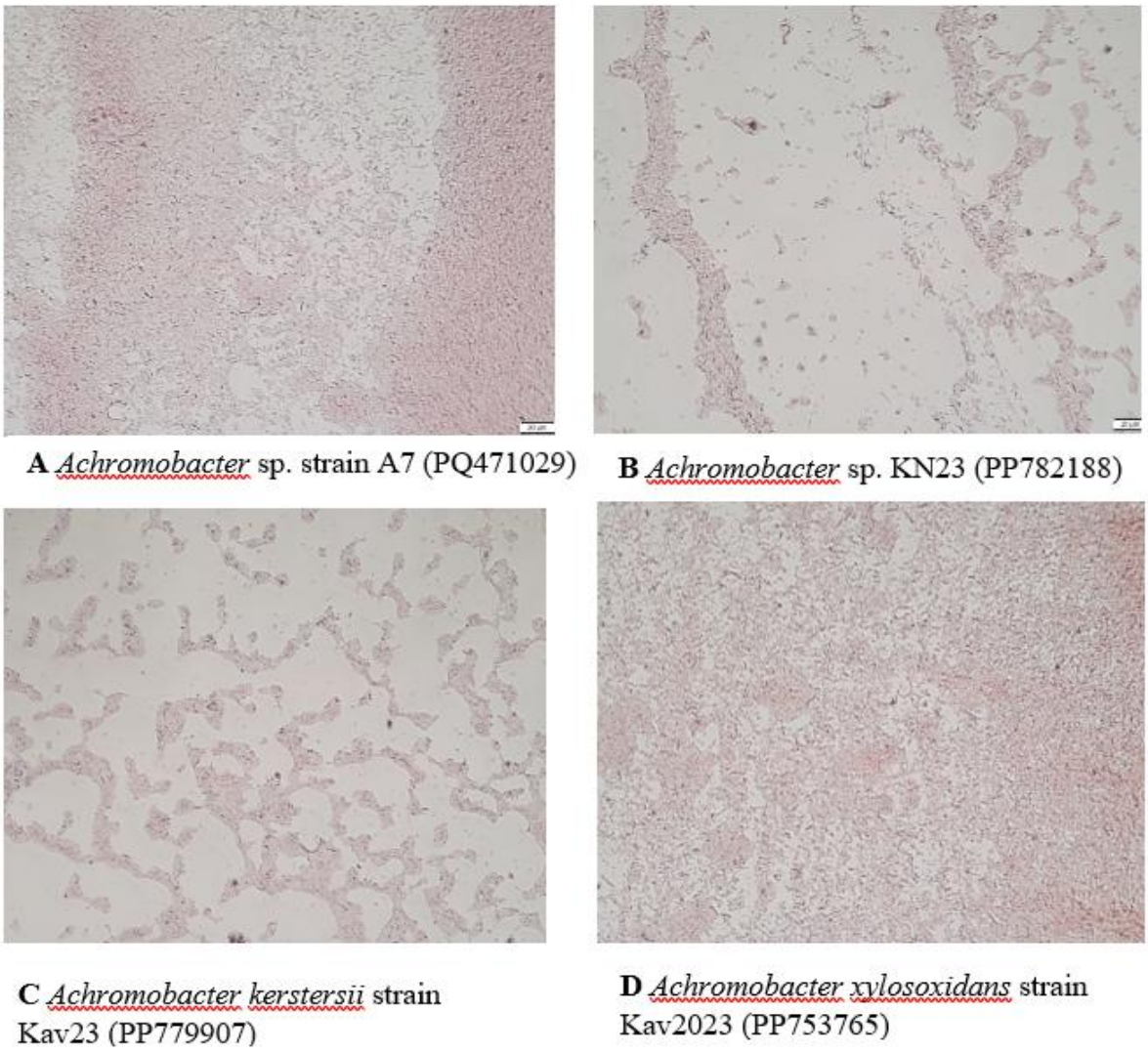

Figure 4.4 | Gram's reaction of the four bacterial isolates recovered from *O.* sp k KN-2024. All four bacterial isolates were observed to be Gram-negative rod-shaped cells, that stained pink after treatment with the Gram stain. Images observed at 40X under the Olympus BX 63 OM/ FM microscope.

4.3.3.2 Endospore staining

All four bacterial isolates were negative for endospore staining as no endospores were visible after staining and microscopic examination. **Figure 4.5** depicts the endospore results of the four bacterial isolates.

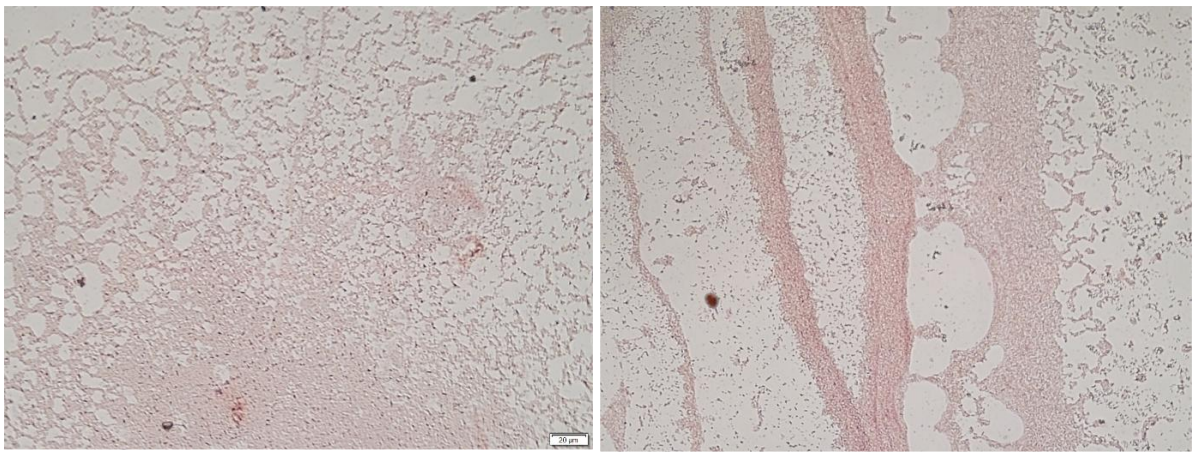

A *Achromobacter* sp. strain A7

B *Achromobacter* sp. KN23 (PP782188)

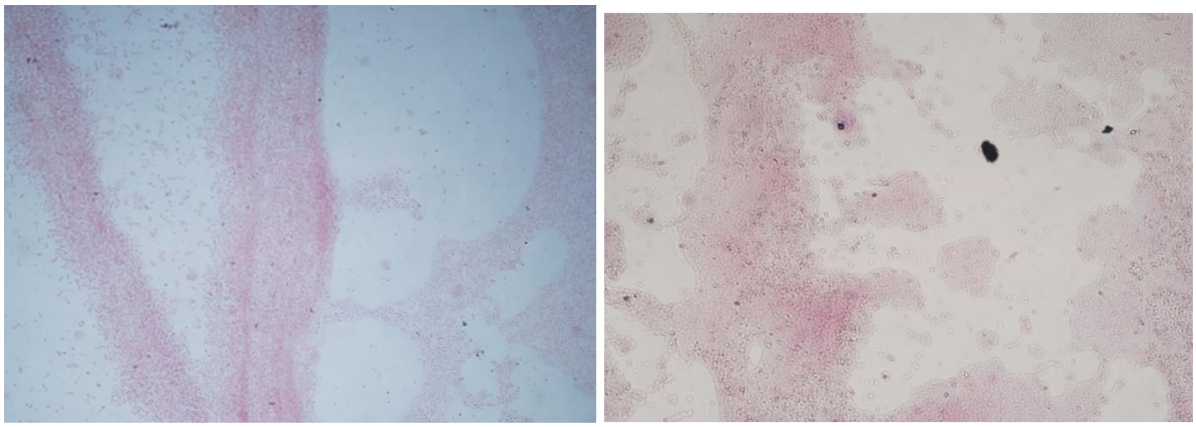

C *Achromobacter kerstersii* strain Kav23 (PP779907)

D *Achromobacter xylosoxidans* strain Kav2023 (PP753765)

Figure 4.5 | Endospore staining results for the four isolated species **A** *Achromobacter* sp. strain A7 (PQ471029) **B** *Achromobacter* sp. KN23 (PP782188) **C** *Achromobacter kerstersii* strain Kav23 (PP779907) and **D** *Achromobacter xylosoxidans* strain Kav2023 (PP753765). Microscopic examination revealed no endospore formation in all four isolated bacteria, confirming that they do not produce spores.

4.3.4 Molecular identification

To identify the isolated bacteria at the species level, the edited 16S rDNA gene were submitted to NCBI to obtain accession numbers. The Figures 4.6 to 4.9 show the consensus sequences of all four bacterial isolates that were trimmed and edited using BioEdit and submitted to NCBI.

4.3.4.1 Consensus sequences of the isolated bacteria

ATCTGTATGTTGTGAGAGAGGGAGCACACCCACTGTGGGTGTGACACGCGGC
CCAGTCTCCTGCGGGAGACCACAGTGGGGTATTTTGCACAATGGGGGAACCC
GTTATCCACCCATCCCGCGTGTGAGAAGAACGCTTTGGGGTTGTAAACCTCTT
TTGGCAGGAAAGAAACGTCAGGGTATAATCCCCCGGGAATGTGGCGGTACAT
ACAGAATAAGCCCCGTATATTTGCGTCACCACACCCGCGGTAATGAGTAGGGC
GCAAGCGTTAATGGGAATTAGTGGGCGTAAAGCGTGTGCAGGCGGTTCGGAA
AGAAAGATGTGAAATCCCAGAGCTTAACTTTGGATGCACATTTTTATGTACCG
ATATAGAGTGTGTCAGAGGGAGGTGGAATTCCGCGTGTCACAGTGAAATGTG
TAGATATGGGGAGGCACCCAGATGGAGAAGACATCCTCGTGGGATCACTGTC
ACGGTCACGCGAGAAAGCGGGGGGAGCACACAGGATTAGATCCCGTGGTAGT
CCACCCCATAAGAGATGTCAAGTATCTGTGGGGCCATTCGGCCCGCAGTAGCG
CAGCTAACGCGTGA

Figure 4.6 | Consensus sequences of the 16S rDNA gene of *Achromobacter* sp. strain A7 (PQ470129.1).

TGGGAGTGAGACGCGGCCCAGTCTCATGCGGGAGGCAGCAGTGGGGAATTTT
GCACAATGGGGGAAACCGTGATCCAGCCATCCCGCGTGTGAGATGAAGGCTT
TCGGGTTGTAAGCTCTTTTGGCAGGAAAGAAACGTCATGGTATAATACCCCGT
GAAACTGGCGGTACCTGCAGAATAAGCCCCGGCTATTTACGTCCCAGCAGCCG
CGGTAATGCGTAGGGTGCAAGCGTTAATCGGAATTAGTGGGCGTAAAGCGTG
CGCAGGCGGTTCGGAAAGAAAGATGTGAAATCCCAGAGCTTAACTTTGGAAG
CGCATTTTTATCTACCGATATAGAGTGTGTCAGAGGGAGGTGGAATTCCGCGT
GTAGCAGTGAAATGTGTAGATATGCGGAGGCACCCCGATGGAGAAGGCAGCC
TCGTGGGATAACACTCACGCTCACGCACGAAAGCGTGGGGAGCAAACAGGAT
TAGATCCCGTGGTAGTCCACCCCATAAGCGATGTCAAGTAGCTGGTGGGGCCT
TCGGCCCTTAGTAGCGCAGCTAACGC

Figure 4.7 | Consensus sequences of the 16S rDNA gene of *Achromobacter* sp. KN23 (PP782188.1).

GCTCACCAAGGCGACGATCCGTAGCTGGTTTGAGAGGACGACCAGCCACACT
GGGACTGAGACACGGCCCAGACTCCTACGGGAGGCAGCAGTGGGGAATTTTG
GACAATGGGGGAAACCCTGATCCAGCCATCCCGCGTGTGCGATGAAGGCCTT
CGGGTTGTAAAGCACTTTTGGCAGGAAAGAAACGTCATGGGCTAATACCCCGT
GAAACTGACGGTACCTGCAGAATAAGCACCGGCTAACTACGTGCCAGCAGCC
GCGGTAATACGTAGGGTGCAAGCGTTAATCGGAATTACTGGGCGTAAAGCGT
GCGCAGGCGGTTCGGAAAGAAAGATGTGAAATCCCAGAGCTTAACTTTGGAA
CTGCATTTTTAACTACCGAGCTAGAGTGTGTCAGAGGGAGGTGGAATTCCGCG
TGTAGCAGTGAAATGCGTAGATATGCGGAGGAACACCGATGGCGAAGGCAGC
CTCCTGGGATAACACTGACGCTCATGCACGAAAGCGTGGGGAGCAAACAGGA
TTAGATACCCTGGTAGTCCACGCCCTAAACGATGTCAACTAGCTGTTGGGGCC
TTCGGGCCTTAGTAGCGCAGCTAACGCGTGAAGTTGACCGCCTGGGGAGTACG
GTCGCAAGATTAAAACTCAAAGGAATTGACGGGGACCCGCACAAGCGGTGGA
TGATGTGGATTAATTCGATGCAACGCGAAAAACCTTACCTACCCTTGACATGT
CTGGAATTCCGAAGAGATTTGGAAGTGCTCGCAAGAGAACCGGAACACAGGT
GCTGCATGGCTGTCGTCAGCTCGTGTCGTGAGATGTTGGGTTAAGTCCCGCAA
CGAGCGCAACCCTTGTCATTAGTTGCTACGAAAGGGCACTCTAATGAGACTGC
CGGTGACAAACCGGAGGAAGGTGGGGATGACGTCAAGTCCTCATGGCCCTTA
TGGGTAGGGCTTCACACGTCATACAATGGTCGGGACAGAGGGTCGCCAACCC
GCGAGGGGGAGCCAATCCCAGAAACCCGATCGTAGTCCGGATCGCAGTCTGC
AACTCGACTGCGTGAAGTCGGAATCGCTAGTAATCGCGGATCAGCATGTCGCG
GTGAATACGTTCCCGGGTCTTGTACACACCGCCCGTCACACCATGGGAGTGGG
TTTTACCAGAAGTAGTTAGCCTAACCGCAAGGGGGGCGATACC

Figure 4.8 | Consensus sequences of the 16S rDNA gene of *Achromobacter kerstersii* strain Kav23 (PP779907.1).

GAGCTTAACTTTGGAACTGCATTTTTAACTACCGAGCTAGAGTGTGTCAGAGG
GAGGTGGAATTCCGCGTGTAGCAGTGAAATGCGTAGATATGCGGAGGAACAC
CGATGGCGAAGGCAGCCTCCTGGGATAACACTGACGCTCATGCACGAAAGCG
TGGGGAGCAAACAGGATTAGATACCCTGGTAGTCCACGCCCTAAACGATGTC
AACTAGCTGTTGGGGCCTTCGGGCCTTAGTAGCGCAGCTAACGCGTGAAGTTG
ACCGCCTGGGGAGTACGGTCGCAAGATTAAAACTCAAAGGAATTGACGGGGA
CCCGCACAAGCGGTGGATGATGTGGATTAATTCGATGCAACGCGAAAAACCT
TACCTACCCTTGACATGTCTGGAATTCCGAAGAGATTTGGAAGTGCTCGCAAG
AGAACCGGAACACAGGTGCTGCATGGCTGTCGTCAGCTCGTGTCGTGAGATGT
TGGGTTAAGTCCCGCAACGAGCGCAACCCTTGTCATTAGTTGCTACGAAAGGG
CACTCTAATGAGACTGCCGGTGACAAACCGGAGGAAGGTGGGGATGACGTCA
AGTCCTCATGGCCCTTATGGGTAGGGCTTCACACGTCATACAATGGTCGGGAC
AGAGGGTCGCCAACCCGCGAGGGGGAGCCAATCCCAGAAACCCGATCGTAGT
CCGGATCGCAGTCTGCAACTCGACTGCGTGAAGTCGGAATCGCTAGTAATCGC
GGATCAGCATGTCGCGGTGAATACGTTCCCGGGTCTTGTACACACCGCCCGTC
ACACCATGGGAGTGGGTTTTACCAGAAGTAGTTAGCCTAACCGCAAGGGGGG
CGATACCC

Figure 4.9 | The consensus sequences of the 16S rDNA gene of *Achromobacter xylosoxidans* strain Kav2023 (PP753765.1).

4.3.4.2 Evolutionary relationship of isolated *Achromobacter* spp.

The evolutionary relationships between the four isolated bacterial species and closely related species of the genus *Achromobacter* and *Bordetella*, were determined using a phylogenetic tree. This included the four isolated bacterial strains: *Achromobacter kerstersii* Kav23, *Achromobacter* sp. strain A7, *Achromobacter* sp. KN23 and *Achromobacter xylosoxidans* strain Kav2023.

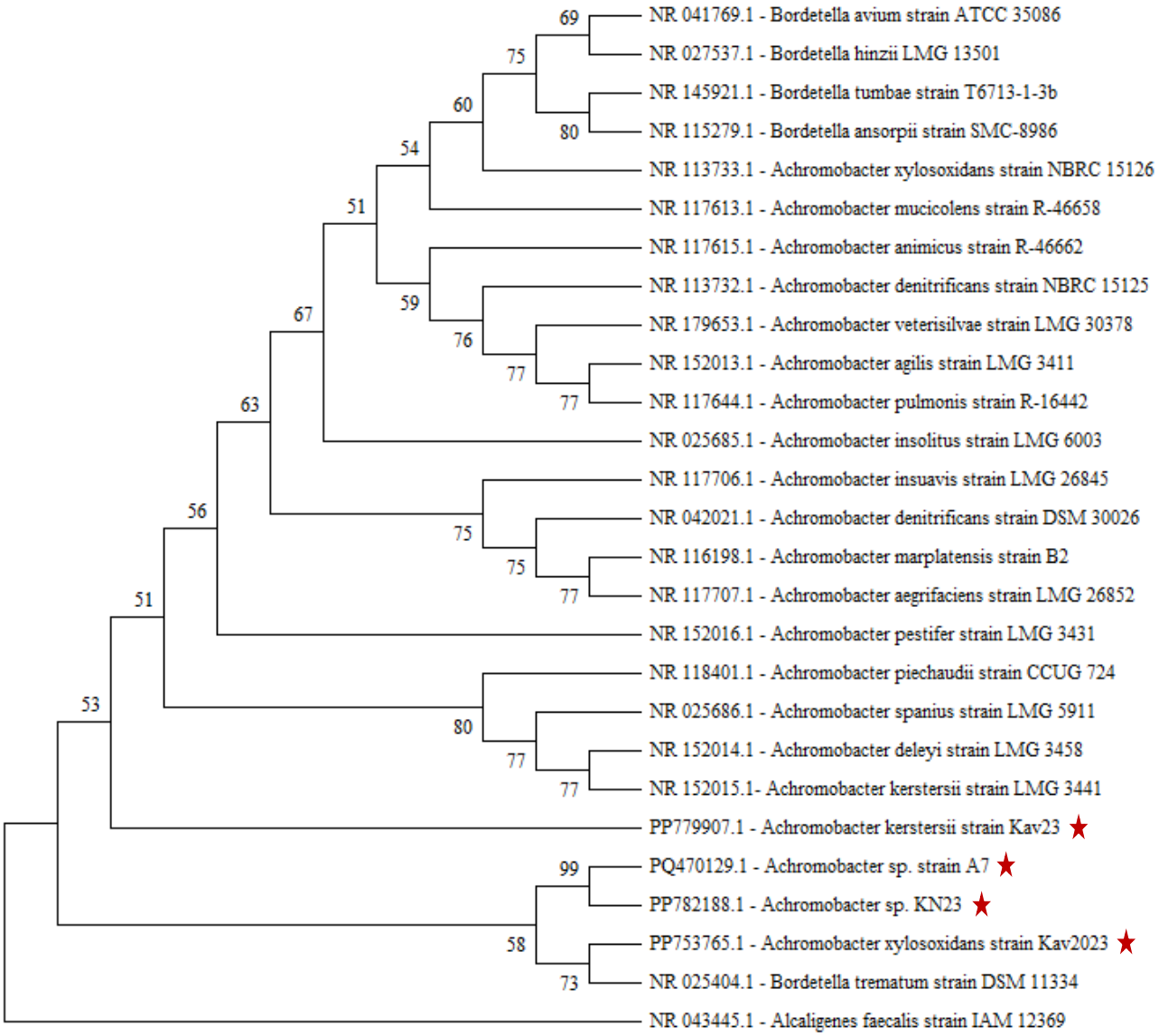

Figure 4.10 | Phylogenetic tree inferring the evolutionary relationship between species of *Achromobacter*. The relationships between the four isolated species and other closely related species were inferred. The tree was created using the Maximum Likelihood method with 2, 000 replicates in MEGA12 (version 12.0.10). The bootstrap values (in %) are shown below branches. The final dataset comprised of 27 nucleotide sequences with 551 positions. *Alcaligenes faecalis* (NR043445.1) was used as the outgroup. The four bacterial isolates are depicted with red stars.

Table 4.4 | Estimation of evolutionary divergence between species of *Achromobacter***.** The estimated evolutionary divergence between 27 *Achromobacter* spp. was provided based on nucleotide sequence comparisons. The values below the diagonal (indicated in black) indicate the number of base substitutions per site between sequences. Standard error estimates (above the diagonal, indicated in blue) were obtained using a bootstrap resampling approach with 2000 replicates. The analyses were conducted using the Tamura-Nei model in MEGA12. The accession numbers highlighted in green correspond to the isolated *Achromobacter* spp.

		1	2	3	4	5	6	7	8	9	10	11	12	13	14	15	16	17	18	19	20	21	22	23	24	25	26	27
1	PQ470129.1		0.021	0.021	0.021	0.021	0.021	0.021	0.021	0.021	0.021	0.021	0.021	0.021	0.021	0.021	0.021	0.015	0.021	0.022	0.022	0.022	0.030	0.031	0.031	0.022	0.026	0.021
2	NR_025686.1	0.192		0.000	0.000	0.000	0.003	0.003	0.003	0.003	0.003	0.004	0.004	0.004	0.004	0.004	0.005	0.012	0.002	0.006	0.006	0.006	0.004	0.004	0.006	0.006	0.013	0.004
3	NR_152014.1	0.190	0.000		0.000	0.000	0.003	0.002	0.002	0.002	0.003	0.004	0.004	0.004	0.004	0.004	0.005	0.012	0.002	0.006	0.006	0.006	0.004	0.004	0.006	0.006	0.013	0.004
4	NR_152015.1	0.192	0.000	0.000		0.000	0.003	0.003	0.003	0.003	0.003	0.004	0.004	0.004	0.004	0.004	0.005	0.012	0.002	0.006	0.006	0.006	0.004	0.004	0.006	0.006	0.013	0.004
5	NR_118401.1	0.192	0.000	0.000	0.000		0.003	0.003	0.003	0.003	0.003	0.004	0.004	0.004	0.004	0.004	0.005	0.012	0.002	0.006	0.006	0.006	0.004	0.004	0.006	0.006	0.013	0.004
6	NR_116198.1	0.192	0.005	0.004	0.005	0.005		0.003	0.002	0.002	0.004	0.004	0.004	0.004	0.004	0.004	0.005	0.012	0.003	0.006	0.006	0.006	0.004	0.004	0.000	0.007	0.013	0.004
7	NR_152016.1	0.194	0.004	0.002	0.004	0.004	0.005		0.003	0.003	0.003	0.004	0.004	0.004	0.004	0.004	0.005	0.012	0.003	0.006	0.006	0.006	0.004	0.004	0.006	0.006	0.013	0.004
8	NR_117706.1	0.194	0.004	0.002	0.004	0.004	0.002	0.004		0.000	0.003	0.004	0.004	0.003	0.004	0.004	0.004	0.012	0.003	0.007	0.006	0.006	0.006	0.000	0.004	0.006	0.014	0.004
9	NR_117707.1	0.193	0.004	0.002	0.004	0.004	0.002	0.004	0.000		0.003	0.004	0.004	0.003	0.004	0.004	0.004	0.012	0.003	0.007	0.006	0.006	0.006	0.000	0.004	0.006	0.014	0.004
10	NR_025685.1	0.194	0.005	0.004	0.005	0.005	0.007	0.005	0.005	0.005		0.003	0.004	0.003	0.003	0.003	0.004	0.013	0.004	0.006	0.006	0.006	0.004	0.004	0.006	0.006	0.014	0.003
11	NR_117615.1	0.196	0.009	0.007	0.009	0.009	0.011	0.009	0.009	0.009	0.004		0.004	0.002	0.002	0.002	0.003	0.013	0.004	0.006	0.005	0.007	0.004	0.004	0.006	0.006	0.014	0.003
12	NR_117613.1	0.194	0.009	0.007	0.009	0.009	0.011	0.009	0.009	0.009	0.007	0.007		0.004	0.004	0.004	0.005	0.013	0.004	0.006	0.006	0.006	0.004	0.004	0.006	0.006	0.014	0.004
13	NR_113732.1	0.197	0.009	0.007	0.009	0.009	0.007	0.009	0.005	0.006	0.004	0.002	0.009		0.000	0.000	0.003	0.013	0.004	0.006	0.005	0.006	0.006	0.000	0.004	0.006	0.014	0.003
14	NR_152013.1	0.199	0.011	0.009	0.011	0.011	0.009	0.011	0.007	0.007	0.005	0.002	0.009	0.000		0.000	0.003	0.013	0.005	0.006	0.005	0.006	0.006	0.000	0.004	0.006	0.014	0.003
15	NR_179653.1	0.199	0.011	0.009	0.011	0.011	0.009	0.011	0.007	0.007	0.005	0.002	0.009	0.000	0.000		0.003	0.013	0.005	0.006	0.005	0.006	0.006	0.000	0.004	0.006	0.014	0.003
16	NR_117644.1	0.201	0.015	0.013	0.015	0.015	0.013	0.015	0.011	0.007	0.009	0.005	0.013	0.004	0.004	0.004		0.013	0.005	0.006	0.006	0.007	0.008	0.006	0.006	0.006	0.014	0.004
17	PP782188.1	0.112	0.076	0.075	0.076	0.076	0.076	0.078	0.078	0.077	0.080	0.085	0.085	0.085	0.087	0.087	0.089		0.012	0.014	0.014	0.014	0.019	0.020	0.019	0.014	0.019	0.013
18	PP779907.1	0.190	0.002	0.002	0.002	0.002	0.004	0.005	0.005	0.005	0.007	0.011	0.011	0.011	0.013	0.013	0.017	0.074		0.006	0.006	0.007	0.000	0.006	0.004	0.007	0.013	0.005
19	NR_041769.1	0.206	0.020	0.020	0.020	0.020	0.022	0.020	0.024	0.024	0.018	0.017	0.022	0.018	0.018	0.018	0.022	0.095	0.018		0.004	0.007	0.000	0.006	0.004	0.006	0.014	0.006
20	NR_027537.1	0.213	0.020	0.020	0.020	0.020	0.022	0.020	0.020	0.020	0.018	0.017	0.022	0.015	0.015	0.015	0.018	0.099	0.022	0.011		0.006	0.006	0.000	0.004	0.006	0.014	0.005
21	NR_145921.1	0.211	0.022	0.020	0.022	0.022	0.022	0.022	0.020	0.020	0.022	0.024	0.022	0.020	0.022	0.022	0.026	0.097	0.024	0.024	0.017		0.007	0.004	0.006	0.006	0.014	0.006
22	PP753765.1	0.194	0.004	0.004	0.004	0.004	0.004	0.004	0.008	0.008	0.004	0.004	0.004	0.008	0.008	0.008	0.016	0.084	0.000	0.000	0.008	0.012		0.006	0.004	0.008	0.020	0.006
23	NR_042021.1	0.205	0.004	0.004	0.004	0.004	0.004	0.004	0.000	0.000	0.004	0.004	0.004	0.000	0.000	0.000	0.008	0.093	0.008	0.008	0.000	0.004	0.008		0.004	0.008	0.021	0.000
24	NR_025404.1	0.195	0.008	0.008	0.008	0.008	0.000	0.008	0.004	0.004	0.008	0.008	0.008	0.004	0.004	0.004	0.008	0.084	0.004	0.004	0.004	0.008	0.004	0.004		0.008	0.021	0.004
25	NR_115279.1	0.204	0.022	0.021	0.022	0.022	0.026	0.022	0.024	0.021	0.022	0.021	0.021	0.022	0.022	0.022	0.022	0.094	0.024	0.020	0.020	0.019	0.016	0.016	0.016		0.014	0.006
26	NR_043445.1	0.274	0.083	0.083	0.083	0.083	0.085	0.085	0.088	0.088	0.090	0.092	0.092	0.092	0.094	0.094	0.098	0.158	0.081	0.090	0.096	0.092	0.090	0.099	0.095	0.095		0.014
27	NR_113733.1	0.199	0.011	0.009	0.011	0.011	0.009	0.011	0.007	0.007	0.005	0.005	0.009	0.004	0.004	0.004	0.007	0.087	0.013	0.017	0.013	0.020	0.008	0.000	0.004	0.020	0.094	

4.4 Discussion

The morphological characteristics and molecular analyses were consistent, strongly indicating that all four bacterial isolates from *O.* sp. k KN-2024 isolate kv-2022 belong to the genus *Achromobacter* belonging to the family Alcaligenaceae, order Burkholderiales, and class Betaproteobacteria.

All isolates displayed negative Gram and endospore stains. The positive catalase and oxidase test results demonstrated important enzymatic capabilities in the bacterial isolates. The production of the catalase enzyme enables these bacteria to neutralise toxic hydrogen peroxide into water and oxygen, while the presence of cytochrome c oxidase indicates they can effectively utilize oxygen as a terminal electron acceptor in their respiratory chain. These enzymatic functions align with the aerobic nature of *Achromobacter* species and likely enhance their ability to thrive in soil environments. Such metabolic adaptations may benefit these

bacteria during their association with *Oscheius,* enabling survival in various oxygen conditions and providing protection against oxidative stress commonly encountered in soil microenvironments.

The 16S rDNA submitted to NCBI conclusively confirmed the identity of the bacterial isolates as *Achromobacter* spp, showing the reliability of both traditional microbiological methods and molecular techniques in bacterial identification.

The phylogenetic tree **Figure 4.10** demonstrates the evolutionary relationships between the four isolated *Achromobacter* strains and other related species. Particularly, the tree shows a high bootstrap value (99%) supporting the close relationship between *Achromobacter* sp. strain A7 and *Achromobacter* sp. KN23, suggesting these two strains are very closely related evolutionarily. The *A. xylosoxidans* strain Kav2023 branches separately but remains in the same clade with a bootstrap value of 58%, indicating a more distant relationship to the other two unidentified *Achromobacter* species. Also, *A. kerstersii* Kav23 appears to be more distantly related to the other three isolated strains, branching earlier in the phylogenetic tree.

The pairwise evolutionary distance analysis **Table 4.4** further supports these relationships, showing minimal genetic distances between closely related strains. For example, the distance between *A.* sp. strain A7 (PQ470129.1) and *A.* sp. KN23 (PP782188.1) is very small (likely around 0.01-0.02 substitutions per site based on the table), confirming their close evolutionary relationship. The distances between these strains and *A. xylosoxidans* strain Kav2023 (PP753763.1) are larger but still indicate relatedness within the same genus.

The association between *Achromobacter* spp. and EPNs has been documented in several studies, although the full extent of their ecological relationship remains incompletely understood. As noted by (Poinar., 1966), *Achromobacter nematophilus* Poinar & Thomas was found in the intestinal structures of two EPNs, and infective juveniles (IJs) containing *Achromobacter* led to the death of insect hosts through septicemia. However, contrasting findings by (Torres-Barragan *et al.,* 2011) showed that *A. xylosoxidans* isolated from *O. carolinensis* did not cause death in larvae after exposure, suggesting variability in the pathogenic potential of different *Achromobacter* strains or species-specific interactions with their hosts. Achromobacter has been classified as a non-cognate bacterial species, and its role in EPNs is not fully understood. However, it is noted that this species is found in EPNs of

Heterorhabdits, *Steinernema* and *Oscheius*, further proving that *O.* sp. k KN-2024 isolate kv-2022 is most likely an EPN.

The high bootstrap values observed in several branches of the phylogenetic tree (particularly values of 73-99% in the clade containing our isolates) indicate strong statistical support for these evolutionary relationships. The positioning of *Bordetella trematum* strain DSM 11334 near our isolated *Achromobacter* species is noteworthy and suggests possible horizontal gene transfer events or close evolutionary history between these genera.

The pairwise distance analysis provides additional insight into the genetic divergence among these strains. The relatively low substitution rates between some of our isolates (particularly the *Achromobacter* sp. strains A7 and KN23) suggest recent divergence or high conservation of the analysed gene regions. In contrast, higher substitution rates with respect to other *Achromobacter* species indicate greater evolutionary distance.

The isolation of the four different species of *Achromobacter* shows there are strong associations between *Achromobacter* and *Oscheius* which most likely represents a complex ecological relationship with multiple benefits. A study done by (Torres-Barragan *et al.,* 2011) isolated *Achromobacter xylosoxidans* from *Oscheius carolinensis* showing further association between the two genera. *Achromobacter* may assist *Oscheius* in its parasitic lifecycle by producing antimicrobial compounds, helping break down insect tissues, and contributing to insect pathogenesis through toxin production. Unlike the obligate symbioses seen between *Steinernema* and *Heterorhabditis* EPNs and their bacterial partners, *Oscheius* appears to form associations with various soil bacteria, including multiple *Achromobacter* species. This suggests a more opportunistic relationship that may involve metabolic complementation, where the bacteria provide capabilities the nematode lacks. The presence of multiple *Achromobacter* species within *Oscheius* indicates a dynamic microbiome that has potentially co-evolved with *Oscheius* to enhance both organisms' survival in their shared soil environment.

4.5 Conclusion

The phylogenetic analysis and pairwise distance calculations provide strong evidence for the taxonomic placement of the four isolated bacterial strains within the genus *Achromobacter*. The consistent morphological, biochemical, and molecular characteristics confirm their

identity and highlight the reliability of the integrated approach used for bacterial identification. The clustering patterns observed in the phylogenetic tree reveal that while all isolates belong to the same genus, they represent distinct evolutionary lineages, with *A. kerstersii* Kav23 being more distantly related to the other three isolates.

The association of these *Achromobacter* species with EPNs suggests they play important ecological roles in soil environments. Their co-existence likely contributes to the functioning of the soil microbiome and potentially enhances the effectiveness of EPNs as biological control agents against insect pests. The contrasting findings regarding pathogenicity in insect hosts indicate that the interactions between *Achromobacter* species, EPNs, and insects are complex and potentially strain or species-specific.

4.6 Recommendations and future works

Future research should focus on analysing the complete bacterial community associated with *O.* sp k KN-2024 using metagenomic approaches. While our current study has identified specific *Achromobacter* species through traditional culturing methods, a comprehensive analysis of the microbial community would provide valuable insights into population dynamics. By employing DNA sequencing techniques that capture unculturable bacteria, we can determine which bacteria—including the *Achromobacter* species—are numerically dominant in these environments.

The study would allow us to measure diversity within samples (alpha diversity) and compare bacterial communities across different locations or nematode species (beta diversity). This broader ecological perspective would help clarify the relative importance of our isolated *Achromobacter* strains within the overall microbial community and potentially identify additional bacterial species that contribute to EPN success in soil environments. These studies may assist in understanding the role noncognate bacterial isolates in EPNs success as biological control agents and could inform future applications in sustainable agriculture.

4.7 References

Abd-Elgawad, M.M.M., 2022. *Xenorhabdus* spp.: An Overview of the Useful Facets of Mutualistic Bacteria of Entomopathogenic Nematodes. *Life (Basel)* 12, 1360. https://doi.org/10.3390/life12091360

Ali, S.S., Ahmad, R., Hussain, M.A. and Pervez, R., 2005. Pest management in pulses through entomopathogenic nematodes. *Indian Institute of Pulses Research, Kanpur*, *59*.

Askary, T.H., Abd-Elgawad, M.M.M., 2021. Opportunities and challenges of entomopathogenic nematodes as biocontrol agents in their tripartite interactions. *Egyptian Journal of Biological Pest Control*, 31, 42. https://doi.org/10.1186/s41938-021-00391-9

Barreto, M.L., Teixeira, M.G. and Carmo, E.H. (2006) 'Infectious diseases epidemiology', *Journal of Epidemiology and Community Health*, 60(3), pp. 192–195. Available at: https://doi.org/10.1136/jech.2003.011593

Bartholomew, J.W., Mittwer, T., 1952. THE GRAM STAIN. *Bacteriology Reviews* 16, 1–29.

Bird, A.F. and Akhurst, R.J. 1983. The nature of the intestinal vesicle in nematodes of the family steinernematidae. *International Journal for Parasitology*, 13(6), pp. 599–606. Available at: https://doi.org/10.1016/S0020-7519(83)80032-0

Chaston, J.M., Suen, G., Tucker, S.L., Andersen, A.W., Bhasin, A., Bode, E., Bode, H.B., Brachmann, A.O., Cowles, C.E., Cowles, K.N., Darby, C., Léon, L. de, Drace, K., Du, Z., Givaudan, A., Tran, E.E.H., Jewell, K.A., Knack, J.J., Krasomil-Osterfeld, K.C., Kukor, R., Lanois, A., Latreille, P., Leimgruber, N.K., Lipke, C.M., Liu, R., Lu, X., Martens, E.C., Marri, P.R., Médigue, C., Menard, M.L., Miller, N.M., Morales-Soto, N., Norton, S., Ogier, J.-C., Orchard, S.S., Park, D., Park, Y., Qurollo, B.A., Sugar, D.R., Richards, G.R., Rouy, Z., Slominski, B., Slominski, K., Snyder, H., Tjaden, B.C., Hoeven, R. van der, Welch, R.D., Wheeler, C., Xiang, B., Barbazuk, B., Gaudriault, S., Goodner, B., Slater, S.C., Forst, S., Goldman, B.S., Goodrich-Blair, H., 2011. The Entomopathogenic Bacterial Endosymbionts *Xenorhabdus* and *Photorhabdus*: Convergent Lifestyles from Divergent Genomes. *PLOS ONE* 6, e27909. https://doi.org/10.1371/journal.pone.0027909

Devi, G., 2023. Entomopathogenic Nematodes and their Symbiotic Bacteria: Microorganism-Host Interactions: A Review. *International Journal of Environment and Climate Change*, 13, 3443–3455. https://doi.org/10.9734/ijecc/2023/v13i92597

Dahal, P., 2024. Streak Plate Method: Principle, Types, Methods, Uses [WWW Document]. URL https://microbenotes.com/streak-plate-method-principle-methods-significance-limitations/ (accessed 3.20.25).

Kaya, H.K. and Gaugler, R. (1993) 'Entomopathogenic Nematodes', *Annual Review of Entomology*, 38(Volume 38, 1993), pp. 181–206. Available at: https://doi.org/10.1146/annurev.en.38.010193.001145

Kundu, A., Vyshali, G., 2022. Current Status of Nematode-bacteria Interaction: A Mini Review *Agricultural Reviews*, URL https://arccjournals.com/journal/agricultural-reviews/R-2291 (accessed 3.19.25).

Maheshwari, P., Sankar, P.M., 2023. Chapter 42 - Culture-independent and culture-dependent approaches in symbiont analysis: in proteobacteria, in: Dharumadurai, D. (Ed.), Microbial Symbionts, Developments in Applied Microbiology and Biotechnology. *Academic Press*, pp. 743–763. https://doi.org/10.1016/B978-0-323-99334-0.00018-9

Mangowa, D., Serepa-Dlamini, M.H., 2020. Draft Genome Sequence of a Noncognate Bacterium, Achromobacter sp. Strain Bel, Associated with a Rhabditid Entomopathogenic Nematode. *Microbiology Resource Announcements* 9, e01247-20. https://doi.org/10.1128/MRA.01247-20

Murfin, K.E., Dillman, A.R., Foster, J.M., Bulgheresi, S., Slatko, B.E., Sternberg, P.W., Goodrich-Blair, H., 2012. Nematode-Bacterium Symbioses - Cooperation and Conflict Revealed in the "Omics" Age. *The Biological Bulletin*, 223, 85–102.

Pervez, R., Lone, S.A. and Pattnaik, S. (2020) 'Characterization of symbiotic and associated bacteria from entomopathogenic nematode Heterorhabditis sp. (nematode: Heterorhabditidae) isolated from India', *Egyptian Journal of Biological Pest Control*, 30(1), p. 144. Available at: https://doi.org/10.1186/s41938-020-00343-9

Poinar GO Jr, Thomas GM., 1966. Significance of *Achromobacter nematophilus* Poinar and Thomas (Achromobacteraceae: Eubacteriales) in the development of the nematode, DD-136 (*Neoaplectana* sp. Steinernematidae). *Parasitology*. 56(2):385-90. doi: 10.1017/s0031182000070980. PMID: 4960247.

Rizzatti, G. *et al*. 2017. Proteobacteria: A common factor in human diseases. *BioMed Research International*, 2017, p. 9351507. Available at: https://doi.org/10.1155/2017/9351507

Ruiu, L., 2015. Insect pathogenic bacteria in integrated pest management. *Insects*, 6(2), pp. 352–367. Available at: https://doi.org/10.3390/insects6020352

Silva, D. and Jacintho, L. 1997. The etymology of infection and infestation, *The Pediatric Infectious Disease Journal*, 16(12), p. 1188.

Tarasco, E., Fanelli, E., Salvemini, C., El-Khoury, Y., Troccoli, A., Vovlas, A., De Luca, F., 2023. Entomopathogenic nematodes and their symbiotic bacteria: from genes to field uses. , *Frontiers in Insect Science* 3, 1195254. https://doi.org/10.3389/finsc.2023.1195254

Torres-Barragan, A., Suazo, A., Buhler, W.G., Cardoza, Y.J., 2011. Studies on the entomopathogenicity and bacterial associates of the nematode *Oscheius carolinensis*. *Biological Control* 59, 123–129. https://doi.org/10.1016/j.biocontrol.2011.05.020

Ruiz-Vega, J., Cortés-Martínez, C.I. and García-Gutiérrez, C. (2018) 'Survival and Infectivity of Entomopathogenic Nematodes Formulated in Sodium Alginate Beads', *Journal of Nematology*, 50(3), pp. 273–280. Available at: https://doi.org/10.21307/jofnem-2018-037

Van, P., 2022. Note on entomopathogenic nematode and its life cycle. *International Journal of Nematology and Entomology* 9, 1–1.

Chapter 5

The thermal tolerance of two novel nematode species: *Oscheius* sp. k KN-2024 isolate kv-2022 and *Cruznema* sp. NTM-2021

5.1 Introduction

Different species of EPNs work best in different climatic zones; temperate, tropical, or sub-tropical (Lacey and Georgis, 2012). Hence, the use EPNs is not universal. The selection of EPNs as biological control agents is based on several factors, and these includes the host range, host foraging strategies, the EPNs tolerance to abiotic factors in the environment, as well as their effects on survival and efficacy. The environmental factors include temperature, desiccation, relative humidity (RH), soil temperature, soil type, salinity, exposure to ultraviolet light, the soils organic content and oxygen levels (Lacey and Georgis, 2012). The survival rate and infectivity of EPNs is negatively affected by exposure to extreme temperatures, both low and high (Gulzar *et al.,* 2020; Matuska-Lyżwa *et al.,* 2024).

Temperature has long-term effects on the stress tolerance, chemotaxis, and the proteome of EPNs resulting in reduced survival of EPNs which negatively impacts biocontrol efficacy (Gulzar *et al.*, 2020; Lillis *et al.*, 2023). It is one of the major factors affecting soil dwelling organisms including the IJ stages of EPNs. IJs occurs when host nutrients are exhausted. Their primary role is to seek out and parasitise new hosts. They possess adaptations to endure unfavourable environmental conditions, affecting their persistence in soil, infectivity, development, maturation, and reproductive capabilities. Temperature plays a crucial role in shaping these processes, with variations observed among species in their tolerance levels (Dunphy and Webster, 1986; Kaya, 1977). For instance, *Steinernematids* exhibit higher activity at lower temperatures compared to *Heterorhabditids*, indicating a temperate origin for the former (Grewal, Selvan and Gaugler, 1994). The distribution patterns of these nematodes, such as the prevalence of *Heterorhabditids* in warmer climates and the dominance of *Steinernematids* in temperate regions, further support this distinction.

An important aspect of nematology that notably influences the behaviour, distribution as well as survival capabilities of nematodes is their ability to tolerate extreme temperatures (Shapiro-Ilan, Han and Dolinksi, 2012). The ability of nematodes to withstand both cold and heat

temperatures influences their ecological resilience, applications in both biotechnology as well as agricultural pest management. Understanding their abilities to withstand high and low temperatures is mandatory to predict their responses to environmental changes, designing effective control strategies, and controlling their potential benefits in various fields. This chapter aims to explore nematodes efficacy at different temperature conditions as well as their thermal tolerance.

5.2 Methods and materials

5.2.1 Insects and nematodes

Both *O.* sp. k KN-2024 and *C.* sp. NTM-2021 were cultured in last instar *T. molitor* larvae obtained commercially (Steyn *et al.*, 2017). The infected *T. molitor* larvae were placed on White traps to collect emerging IJs for bioassays (Lee, Kim and Han., 2000). The IJs were stored at 4^{o}C and used within 10 days of their emergence. Both nematode species were used to compare interspecific variations.

5.2.2 Efficacy of *O.* sp. k KN-2024 and *C.* sp. NTM-2021 at a range of temperature conditions

The efficacy of the nematodes was determined at four different temperature conditions: 5, 25, 30 and 37°C. 50 IJs of each nematode species were placed in 90 mm petri dishes with 5 g of sterile loam soil hydrated to 10% moisture. The lids were replaced and sealed firmly with parafilm to prevent water loss. The experiment was acclimated by placing the petri dishes in the respective incubators for 2 hours prior to the addition of 10 last instar *T. molitor* larvae. The control was done with distilled water and no IJs. The experiment was performed in triplicates for both the treated and untreated samples. The petri dishes were incubated at different temperatures: 5, 25, 30 and 37°C, and were monitored every 48 hours over an 8-day period. The selection of temperature range was done in accordance with the prevailing average minimum and maximum temperatures of the region in which each nematode was collected. The dead larvae were removed every 48 hours. The larvae were considered dead upon observing a change in colour of the insect cadaver to dark brown, and no movement was detected upon probing with forceps. These cadavers were then placed in White traps to note

the emergence of IJs under a stereomicroscope and determine the nature of death (natural/ EPN-killed).

5.2.3 Statistical analysis

All statistical analyses were performed using Python (version 3.8.19) with the *statsmodels* and *scipy.stats* packages (see **Appendix 7**, **Table 7.1** for a summary of all Python libraries used and **Appendix 7.8.2** for Python code used for statistical analysis). These analyses assessed how temperature effects, species (*C.* sp. NTM-2021 vs *Oscheius* sp. KN-2024), exposure time (2, 4,6, and 8) days, and experimental condition (control versus treatment) influenced efficacy of the nematodes against the *T. molitor* larvae.

Before analysis, the data was tested for normality (Shapiro-Wilk test), homogeneity of variance (Levene's test), and homoscedasticity (Breusch-Pagan test). A four-way ANOVA was conducted to determine the main effects and interactions of temperature changes, species, time, and experimental condition on survival rates. For significant effects identified in the ANOVA, Tukey's Honest Significant Difference (HSD) test was performed to determine specific differences between groups.

The magnitude of effects was quantified using partial eta-squared (η^2_p) to assess the proportion of variance explained by each factor and their biological significance. Additionally, Cohen's *d* was calculated for pairwise comparisons between control and treatment groups to evaluate practical significance. Statistical significance was reported at three levels: *p < 0.05, **p < 0.01, and ***p < 0. 001.The overall model fitness was evaluated using the coefficient of determination (R^2), connecting statistical outcomes to the biological implications for nematode desiccation tolerance.

5.3 Results

The efficacy of *O.* sp. k KN-2024 and *C.* sp. NTM-2021 against *T. molitor* larvae varied significantly across temperatures. At 5°C, only *C.* sp. NTM-2021 showed limited effectiveness. As temperatures increased, the efficacy of both nematode species improved until reaching their respective optimal temperatures, after which effectiveness declined.

Oscheius sp. k KN-2024 demonstrated peak efficacy at 25°C, while *C*. sp. NTM-2021 performed optimally at 30°C. Statistical analysis revealed significant differences for *C*. sp. NTM-2021 at 30°C on days 4, 6, and 8 ($p < 0.05$), and at 25°C on day 8 only. At 30°C, control groups and *O*. sp. k KN-2024 treatments both exhibited some natural larval mortality. In *O*. sp. k KN-2024 treatments, larval death resulted from both natural causes and EPN infection. In contrast, all cadavers in *C*. sp. NTM-2021 treatments showed nematode emergence, with no purely natural mortality observed. At 37°C, neither nematode species showed efficacy against *T. molitor* larvae, with all observed mortality appearing to result from heat stress rather than infection.

Temporal analysis indicated that infection rates for both nematode species increased with time, reaching peak levels before eventually declining. Statistical analysis confirmed significant differences between treatments at 25°C, 30°C, and 37°C ($p < 0.05$ or $p < 0.01$) at various time points throughout the experiment.

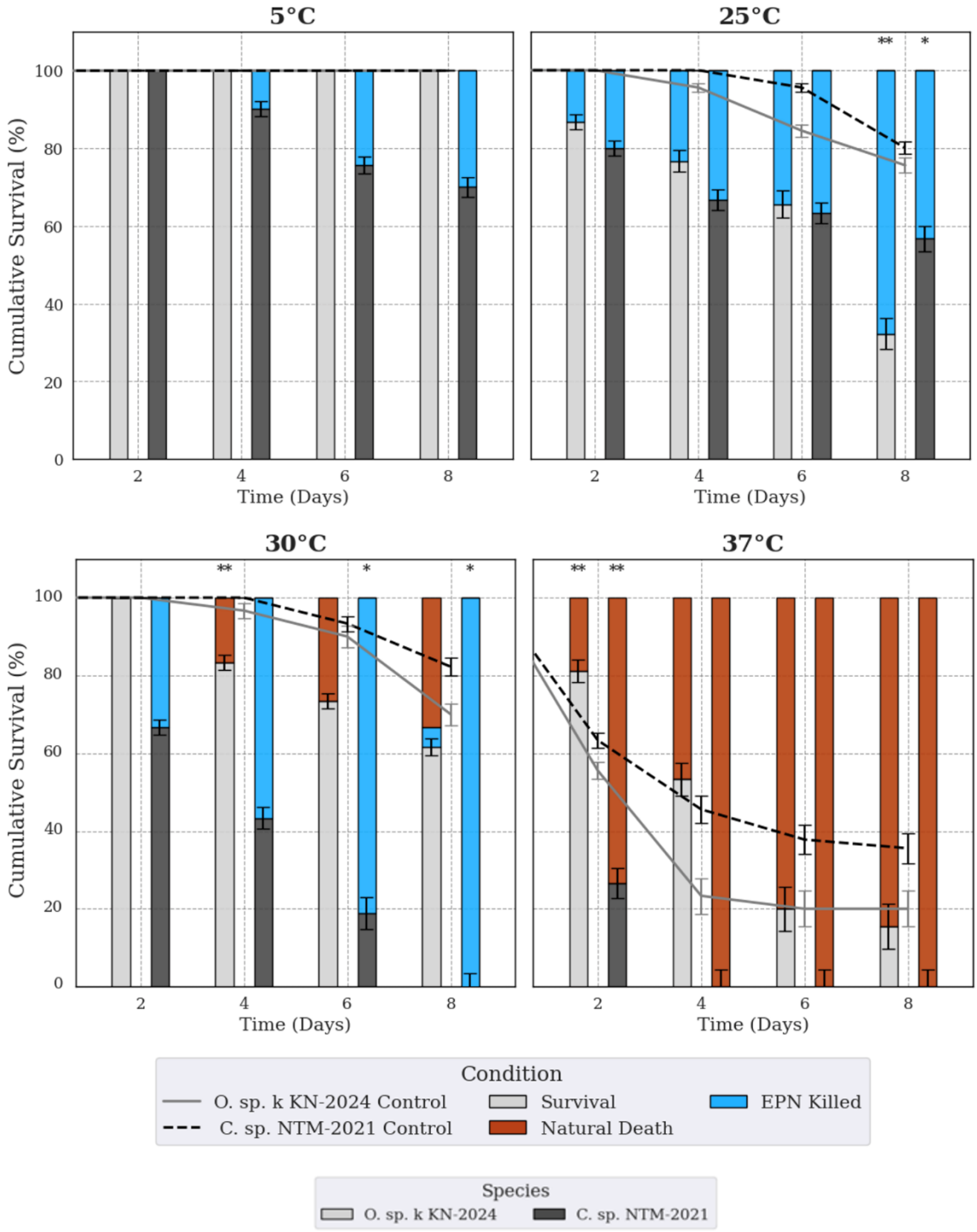

Figure 5.1 Temperature-dependent survival of *T. molitor* larvae exposed to *O.* sp k. KN-2024 and *C.* sp. NTM-2021 over 8 days. Stacked bar graphs display cumulative larval survival percentages at four temperature conditions (5, 25, 30, and 37°C) assessed at 2-day intervals. Light grey bars represent survival of larvae exposed to *O.* sp k. KN-2024, black bars indicate survival with *C.* sp. NTM-2021 exposure, blue sections show EPN-killed larvae, and red sections represent natural death. Controls are shown with trend lines: dashed for *C.* sp. NTM-

2021; solid for *O.* sp k. KN-2024). Statistical significance is indicated by asterisks (* $p < 0.05$, ** $p < 0.01$).

5.4 Discussion

The efficacy of EPNs against insect pests is known to be influenced by environmental factors, with temperature being particularly crucial for their survival and infectivity. Our results demonstrate distinct temperature-dependent efficacy profiles for *O.* sp. k KN-2024 and *C.* sp. NTM-2021 against *T. molitor* larvae, with implications for their potential application in biological control strategies.

The observed temperature-dependent efficacy patterns align with previous studies on EPNs, which typically show reduced activity at lower temperatures and increased pathogenicity as temperatures rise to species-specific optimum temperatures (Matuska-Łyżwa *et al.,* 2024). *Oscheius* sp. k KN-2024 exhibited optimal efficacy at 25°C, while *C.* sp. NTM-2021 performed best at 30°C, indicating different thermal preferences between these species. The complete ineffectiveness of both nematodes at 37°C suggests an upper thermal limit for their biological activity, likely due to physiological stress that impairs their mobility, host-finding ability, or reproduction (Matuska-Łyżwa *et al.*, 2024).

The ability of *C.* sp. NTM-2021 to maintain some effectiveness at 5°C, albeit limited, when *O.* sp. k KN-2024 showed no activity, indicates a broader temperature tolerance range for the former. This characteristic could be valuable for applications in cooler environments or seasons where temperature fluctuations occur.

Our findings at 30°C provide particularly interesting insights into the distinct pathogenicity mechanisms of these nematodes. The observation that all *C.* sp. NTM-2021-associated cadavers exhibited nematode emergence, whereas *O.* sp. k KN-2024 treatments showed both EPN-infected and naturally deceased larvae, supports the classification of *C.* sp. NTM-2021 as an opportunistic pathogen. This species appears capable of infecting both living larvae and recently deceased hosts, resulting in higher overall infection rates compared to *O.* sp. k KN-2024.

On the other hand, the pattern observed with *O*. sp. k KN-2024 at 30°C after 8 days provides compelling evidence of its true entomopathogenic nature. This species actively infected and killed living larvae rather than merely colonising already deceased hosts. The presence of both EPN-infected and naturally deceased larvae in these treatments demonstrates that *O*. sp. k KN-2024 does not opportunistically infect dead larvae to the same extent as *C*. sp. NTM-2021. This finding aligns with recent research demonstrating that *Oscheius* species exhibit entomopathogenic characteristics and should be classified as EPNs (Zhou *et al.*, 2017).

The time-dependent progression of infection rates reflects the biological cycle of these nematodes within their hosts. The observed increase in efficacy over time followed by eventual plateauing or decline aligns with typical EPN infection dynamics, where initial penetration is followed by reproduction within the host and subsequent emergence of infective juveniles. The statistically significant differences for *C*. sp. NTM-2021 at days 4, 6, and 8 at 30°C, compared to significance only at day 8 for 25°C, further illustrates how optimal temperature accelerates the infection process. This temporal pattern has important implications for field applications, suggesting that environmental conditions not only affect overall efficacy but also the speed at which pest control can be achieved.

These findings have practical implications for the selection and application of these nematode species in biological control programs. *Cruznema* sp. NTM-2021 offers versatility across a wider temperature range, making it potentially suitable for variable environmental conditions. In contrast, while *O*. sp. k KN-2024 has a narrower effective temperature range, it demonstrates superior efficacy at its optimal temperature, suggesting it could be more effective in controlled environments or when applied during periods with suitable temperatures.

The opportunistic pathogenicity of *C*. sp. NTM-2021 may be advantageous when target pest populations already experience some natural mortality, as it could amplify overall control by utilising both living and dead hosts for reproduction and population growth. However, its potential to colonise non-target dead organisms should be considered in ecological risk assessments before considering them as BCAs.

Conclusion

In conclusion, our results demonstrate that *O*. sp. k KN-2024 and *C*. sp. NTM-2021 exhibit distinct temperature-dependent efficacy profiles and pathogenicity mechanisms against *T. molitor* larvae. These differences highlight the importance of species-specific characterisation of EPNs for optimising their use in biological control strategies and suggest that these nematodes could complement each other if applied based on environmental conditions and specific control objectives.

5.5 References

Dunphy G. B. and Webster J. M. (1986) Temperature effects on the growth and virulence of *Steinernema feltiae* strains and *Heterorhabditis heliothidis*. J. Nematol. lg, 270-272.

Gaugler, R and Kaya H.K, (1990) (Eds.), Entomopathogenic Nematodes in Biological Control, CRC Press, Boca Raton, FL, pp. 93-116.

Geography (climate, wildlife and flora, provinces, population), n.d. . South African Embassy Paris, France. URL https://dirco.gov.za/paris/geography-climate-wildlife-and-flora-provinces-population/ (accessed 20.01.25).

Grewal, P.S., Selvan, S. and Gaugler, R. (1994) Thermal adaptation of entomopathogenic nematodes: Niche breadth for infection, establishment, and reproduction. *Journal of Thermal Biology*, 19(4), pp. 245–253. Available at: https://doi.org/10.1016/0306-4565(94)90047-7

Gulzar, S. *et al.* (2020) Environmental tolerance of entomopathogenic nematodes differs among nematodes arising from host cadavers versus aqueous suspension. *Journal of Invertebrate Pathology*, 175, p. 107452. Available at: https://doi.org/10.1016/j.jip.2020.107452

Kaya H. K. (1977) Development of the DD-136 strain of *Neoaplectana carpocapsae* at constant temperatures. *J. Nematol*. 9, 346-349.

Lacey, L.A. and Georgis, R. (2012) Entomopathogenic Nematodes for Control of Insect Pests Above and Below Ground with Comments on Commercial Production. *Journal of Nematology*, 44(2), pp. 218–225.

Lillis, P.E. *et al.* 2023. Low-temperature exposure has immediate and lasting effects on the stress tolerance, chemotaxis, and proteome of entomopathogenic nematodes. *Parasitology*, 150(1), pp. 15–28. Available at: https://doi.org/10.1017/S0031182022001445

Matuska-Łyżwa, J., Duda, S., Nowak, D., Kaca, W., 2024. Impact of Abiotic and Biotic Environmental Conditions on the Development and Infectivity of Entomopathogenic Nematodes in Agricultural Soils. *Insects* 15, 421. https://doi.org/10.3390/insects15060421

Shapiro-Ilan, D.I., Han, R. and Dolinksi, C. (2012) Entomopathogenic nematode production and application technology. *Journal of Nematology*, 44(2), pp. 206–217.

Zhou, G., Yang, H., Wang, F., Bao, H., Wang, G., Hou, X., Lin, J., Yedid, G., Zhang, K., 2017. Oscheius microvilli n. sp. (Nematoda: Rhabditidae): A Facultatively Pathogenic Nematode from Chongming Island, China. *J Nematol* 49, 33–41. https://doi.org/10.21307/jofnem-2017-044

Chapter 6

Comparison of desiccation tolerance among two nematode species: *Oscheius* sp. k KN2023 and *Cruznema* NTM 2021

6.1 Introduction

Nematodes are the most abundant multicellular organisms found on earth, inhabiting every ecosystem from oceans to deserts (Andrássy and Zombori, 1976; Platt, 1994; Sapir, 2021). Their success across various ecosystems and their large population size is due to their simple body structure and small size, resistant cuticle, and their ability to adapt (Coghlan, 2005). These characteristics contribute to the nematodes ability to endure environmental stressors including desiccation, and the ease of adapting acts as an important survival mechanism for many nematode species (Shapiro-Ilan *et al.,* 2014). When exposed to unfavourable conditions, nematodes may enter a Dauer or IJ stage, which are more resilient. The IJ stage of the specialised insect parasitic nematodes, EPNs, can better tolerate stress conditions, including desiccation, which is crucial for their mass production, storage, and field application as biocontrol agents (Kagimu *et al.,* 2017).

When exposed to desiccation stress, their survival and persistence are negatively impacted (Liu and Glazer, 2000; Shapiro-Ilan *et al*., 2021). They experience compromised physiological functions, reduced movement and host-seeking abilities, as well as decreased efficacy, preventing them from performing optimally as biocontrol agents in field applications. EPNs are exposed to moisture fluctuations in soil, particularly low moisture in the upper soil layers, where many of their insect hosts are found (Shapiro-Ilan *et al.,* 2021). The host-seeking IJs stage must survive these challenging conditions while maintaining its ability to infect insect hosts. As a result, research has investigated the physiological responses of EPNs to water loss, as there is considerable variation in desiccation tolerance among different species and strains (Yan *et al.,* 2019; San-Blas *et al.,* 2022).

Previous studies have primarily focused on commonly commercialised species such as *Steinernema feltiae* and *Heterorhabditis bacteriophora*, limiting the current understanding of the desiccation tolerance and commercial viability of locally isolated strains (Gao *et al.,* 2020). This study investigates the desiccation tolerance of two new nematode species: *O.* sp. k

KN2023 and *C.* NTM 2021, under controlled laboratory conditions, assessing their survival rates after exposure to different humidity levels. By understanding how they respond, this research aims to give valuable insights into their use as EPNs, enhancing their applications for biocontrol over the more commonly used commercial species of *Heterorhabditis* and *Steinernema*.

6.2 Methodology

6.2.1 Insects and nematodes

Both *O.* sp. k KN-2024 and *C.* sp. NTM-2021 were cultured in last instar *T. molitor* larvae obtained commercially (Steyn *et al.,* 2017). The infected *T. molitor* larvae were placed on White traps to collect emerging IJs for bioassays (Lee, Kim and Han., 2000). The IJs were stored at 4^{o}C and used within 10 days of their emergence. Both cultured nematode species were used to compare interspecific variations.

6.2.2 Testing nematode survival under controlled relative humidity conditions

EPNs isolated from White traps 3 to 5 days after emergence were used. The isolated EPNs were placed in 55 mm petri dishes and dried under the laminar flow (LAF) for approximately 1 hour to remove excess surface water. The desiccator was setup as seen in Figure The samples were then transferred into the desiccator with controlled environment. The RH conditions were maintained with saturated salt solutions at 25°C, and the data was continuously recorded (salts used shown in **Table 6.1**. For controls, EPNs suspended in 0.1% NaCl solution at room temperature were used. The samples were then collected and rehydrated after 24 and 48 hours. Samples were then taken to determine the percentage survival rate. This was performed by counting dead/ living IJs from approximately 100 IJs under a stereomicroscope at 1.5 x 10 magnification. An exclusionary dye was used to test mortality. A 1:1 ratio of Trypan blue was added to each sample, and the IJs that stained blue were counted as dead. This experiment was repeated with 3 replicates for each treatment and RH percentage. The results were plotted on the graph using matplotlib version 2024.06. Experimental procedure adapted from (Ramakrishnan *et al.,* 2022; Shapiro-Ilan *et al.,* 2014).

6.2.2.1 Desiccator setup

A controlled relative humidity environment was obtained using a desiccator chamber as shown in **Figure 6.1.** Various saturated salt solutions (**detailed in Table 6.1**) were prepared to maintain specific relative humidity (RH) levels: 33%, 53%, 75%, and 85%. The saturated salt solutions were placed in the bottom compartment of the desiccator, creating stable humidity conditions within the chamber at room temperature.

6.2.2.2 IJ quantification

To achieve 1000 IJs per petri dish, the number of IJs present in three 10 µl aliquot suspensions were counted under a stereomicroscope at 10 to 50x magnification. The average IJ count from these aliquots was used to calculate the concentration and the suspension volume was adjusted accordingly. Approximately 1000 IJs were used for each experimental and controls treatment, with each treatment performed in triplicate.

6.2.2.3 Sample preparation

Approximately 1000 IJs were transferred to 50 mm petri dishes using a 1 ml pipette and dried under the laminar flow (LAF) for 1 hour to remove excess surface water. This standardised initial condition created a uniform baseline for subsequent humidity exposure. For the controls, the IJs were pre-acclimated in 0.1% sodium chloride (NaCl) solution for 1 hour before being subjected to the same quantification and plating procedure as done for the experimental.

6.2.2.4 Desiccation treatment

The prepared experimental and control IJs were transferred to the corresponding desiccators. All treatments were maintained at a constant temperature of 25°C, and the experiments were run over 24 and 48-hours. Each humidity condition was performed in triplicates to ensure statistical validity of the results.

6.2.2.5 Assessment of viability

After exposure, the IJs survival was evaluated by rehydrating the samples for 12 hours with 1 ml of ddH_2O each. The survival rate was assessed using a 1:1 ratio of trypan blue stain. Live

IJs remained unstained due to intact cell membranes, while dead IJs absorbed the stain. IJs with over 50% of their bodies stained were counted as dead. The percentage of viable IJs were calculated by examining at least 200 IJs per sample under a stereomicroscope and determining the ratio of unstained (living) to total IJs counted.

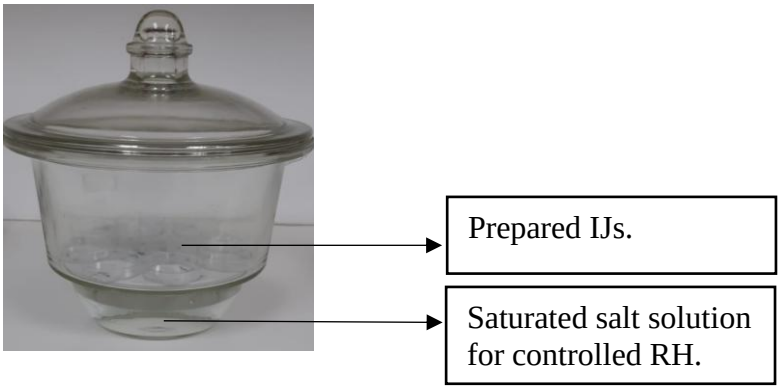

Figure 6.1 | The desiccator chamber setup under controlled conditions. The experimental and control samples were run over 24 and 48-hour period. The samples, experimental and controls, were placed in the chamber with a saturated salt solution at the bottom and stored in the 25ºC incubator. The lid was sealed and only opened to remove the samples after the experimental time had elapsed.

Table 6.1: Saturated salt solutions used to achieve controlled relative humidity levels

Relative humidity (%)	**Salt used**	**Molecular formula**
33	Magnesium chloride hexahydrate	$MgCl.\ 6H_2O$
53	Magnesium nitrate	$Mg\ (NO_3)_2.\ 6H_2O$
75	Sodium chloride	NaCl
85	Potassium chloride	KCl

6.2.3 Statistical analysis

All statistical analyses were performed using Python (version 3.8.19) with the *statsmodels* and *scipy.stats* packages (see **Appendix 7, Table 7.1** for a summary of all Python libraries used; and **Appendix 7.8.3** for Python code used for statistical analysis). These analyses assessed how relative humidity (RH), species (*C.* sp. NTM-2021 vs *Oscheius* sp. KN-2024), exposure time

(24h and 48h), and experimental condition (control versus treatment) influenced nematode survival in the desiccation experiment.

Prior to analysis, data were tested for normality (Shapiro-Wilk test), homogeneity of variance (Levene's test), and homoscedasticity (Breusch-Pagan test). A four-way ANOVA was conducted to determine the main effects and interactions of RH, species, time, and experimental condition on survival rates. For significant effects identified in the ANOVA, Tukey's Honest Significant Difference (HSD) test was performed to determine specific differences between groups.

The magnitude of effects was quantified using partial eta-squared (η^2_p) to assess the proportion of variance explained by each factor and their biological significance. Additionally, Cohen's *d* was calculated for pairwise comparisons between control and treatment groups to evaluate practical significance. Statistical significance was reported at three levels: *p < 0.05, **p < 0.01, and ***p < 0.001. The overall model fitness was evaluated using the coefficient of determination (R^2), connecting statistical outcomes to the biological implications for nematode desiccation tolerance.

6.3 Results

Survival rates of both *O.* sp. k KN-2024 and *C.* sp. NTM 2021 varied across different relative RH levels. At 33% RH, both species showed the lowest survival rates, with *C.* sp. NTM-2021 at approximately 30% and *O.* sp. k KN-2024 between 40-50%. Control groups at RH 33% exhibited divergent patterns, with *O.* sp. k KN-2024 controls at 50% survival and *C.* sp. NTM-2021 at 35%. At RH 53%, survival improved for both species, with *O.* sp. k KN-2024 reaching 90% in both treatment and control groups, while *C.* sp. NTM-2021 survival increased to around 50-60% for treatments and 60-70% for controls. Both species achieved their highest survival at RH 75% and 85%, consistently exceeding 80%, and the difference between treatment and control groups became minimal.

IJs of *O.* sp. k KN-2024 showed a higher survival rate compared to *C.* sp. NTM 2021 at all the tested RH conditions. A decline in survival from 24 to 48 hours was consistent for both species. Error bars were smaller at these higher humidity levels, indicating more consistent survival outcomes.

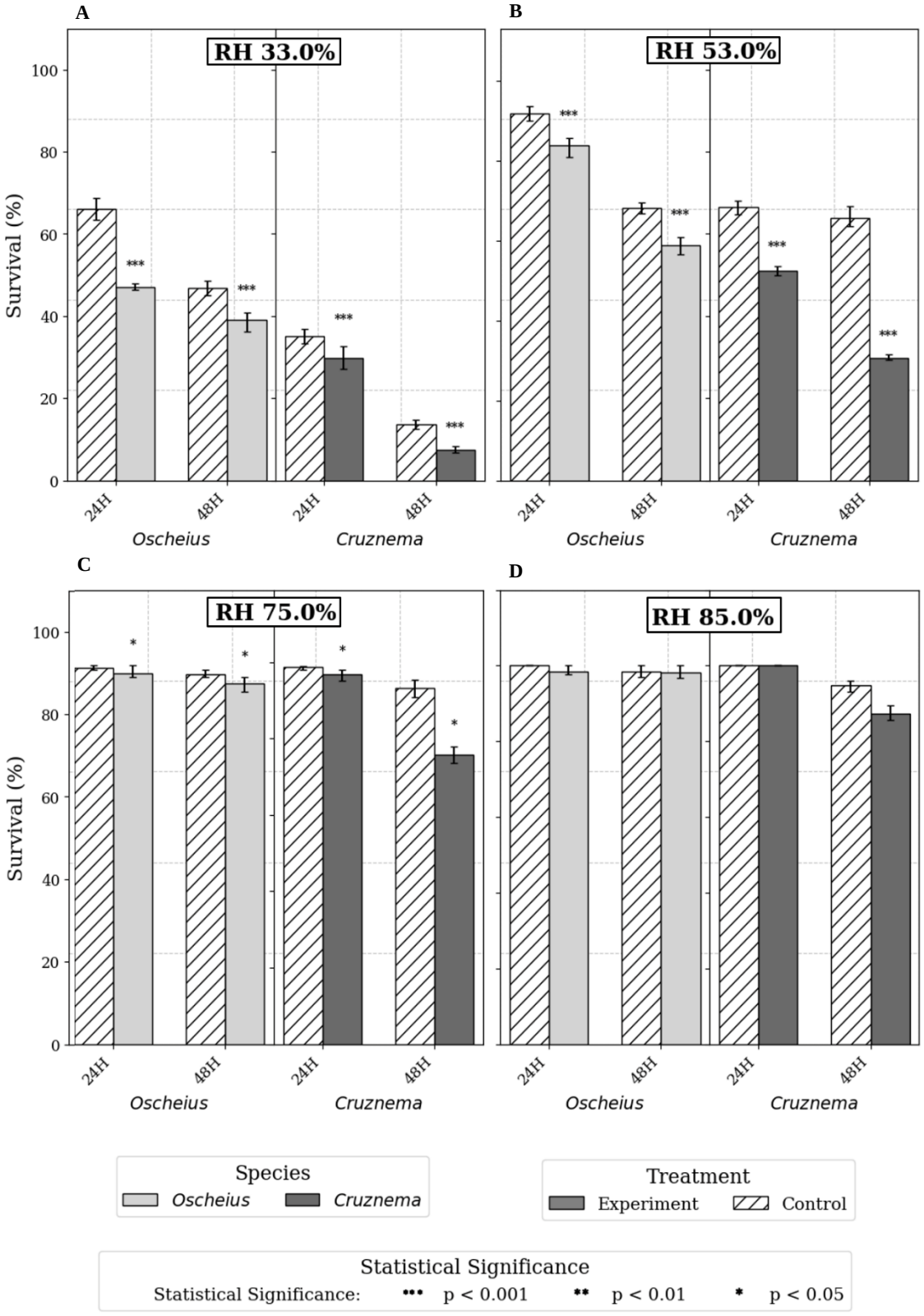
A
RH 33.0%
B
RH 53.0%
C
RH 75.0%
D
RH 85.0%
Survival (%)
0
20
40
60
80
100
24H
48H
Oscheius
Cruznema
Species
Oscheius
Cruznema
Treatment
Experiment
Control
Statistical Significance
Statistical Significance: *** p < 0.001 ** p < 0.01 * p < 0.05

Figure 6.2 | Mean percentage survival (±SEM) of IJs of *O*. sp. k KN-2024 (light grey bars) and *C.* sp. NTM-2021 (dark grey bars) exposed to four relative humidity (RH) conditions: **A**) 33, **B**) 53, **C**) 75, and **D**) 85%, for 24 and 48 hours. Both species showed reduced survival at lower RH levels (33% and 53%) compared to higher RH levels (75% and 85%), with *O.* sp. k KN-2024 demonstrating higher survival rates than *C.* sp. NTM-2021 across all tested RH conditions. The hatched bars represent control treatments (IJs pre-acclimated with 0.1% NaCl solution), while solid bars indicate experimental treatments (no prior- pre-acclimation). Statistical significance of experimental groups is indicated by asterisks (* = $p < 0.05$, ** = $p < 0.01$, *** = $p < 0.001$). Error bars represent standard error of the mean (SEM) from three biological replicates.

6.4 Discussion

The results show clear species-specific differences in desiccation tolerance between *O* sp. KN-2024 and *C* sp. NTM-2021 across varying RH conditions. *O* sp. KN-2024 consistently showed better desiccation tolerance compared to *C* sp. NTM-2021 across all tested humidity levels, with this difference being most evident at lower RH conditions (33% and 53%). The statistical significance ($p < 0.001$) confirms these differences are unlikely to have occurred by chance, with both species showing meaningful responses to desiccation stress. The four-way ANOVA and post-hoc Tukey HSD tests revealed that species identity explains a considerable portion of variance in survival outcomes, with interaction terms confirming that species-specific responses to RH become more pronounced with increased exposure time.

The species-specific differences observed between *O* sp. KN-2024 and *C* sp. NTM-2021 align with established patterns of interspecies variation in entomopathogenic nematodes. (Shapiro-Ilan *et al.*, 2009; Shapiro-Ilan *et al.*, 2014) demonstrated that desiccation tolerance varies greatly across EPN species, with *S. carpocapsae* exhibiting the highest tolerance, followed by *S. feltiae*, while *heterorhabditids* displayed the least tolerance. Similarly, (Morton and Garcia-del-Pino, 2009) observed greater desiccation tolerance in *S. carpocapsae* and *S. feltiae* compared with *H. bacteriophora*. These findings support our observation that species identity is a primary determinant of desiccation survival, with the greater performance of *O* sp. KN-2024 potentially displaying species-specific physiological adaptations like those documented in stress-tolerant steinernematids.

Survival rates for both species progressively increased from 33% to 85% RH, indicating a direct correlation between environmental moisture availability and nematode viability, with the survival gap between species narrowing at higher humidity levels where both achieved high survival rates (>80%). This relationship suggests that favourable moisture conditions mitigate species-specific physiological differences in desiccation resistance mechanisms. Pre-acclimation (in the control groups) significantly enhanced survival rates compared to non-acclimated samples, particularly at lower RH levels, though this advantage diminished as humidity increased, becoming minimal at 85% RH. This follows similar observations made by Shapiro-Ilan *et al.* (2014). This pattern indicates that favourable moisture conditions reduce the importance of pre-acclimation treatments. The impact of exposure time was evident, with 48h exposure generally resulting in reduced survival compared to 24h exposure, an effect more pronounced for *C* sp. NTM-2021 than for *O* sp. KN-2024, indicating that *O* sp. KN-2024 maintains better survival over extended desiccation periods, especially under severe stress conditions. The statistical significance indicators revealed that the most dramatic differences occurred at lower RH levels, where $p < 0.001$ was frequently observed between control and experimental groups, while at higher humidity (75% RH), differences became less significant ($p < 0.05$), and at 85% RH, many comparisons showed no significant difference.

Conclusions

The findings have significant implications for EPN field applications. *Oscheius* sp. k KN-2024 demonstrated superior desiccation tolerance compared to *C.* sp. NTM-2021 across all tested relative humidity levels, with this advantage becoming noticeable under more severe moisture stress conditions. This enhanced resilience to desiccation stress suggests *O* sp. k KN-2024 would maintain higher survival rates and thus greater biocontrol efficacy when deployed in variable environmental conditions. The persistence of *O.* sp. k KN-2024 under moisture-limited conditions makes it a good option for agricultural applications across diverse climatic zones, with humidity fluctuations. Pre-acclimation further enhanced this species survival capabilities, offering a practical method to optimise field performance. Based on these findings, *O.* sp. k KN-2024 is more suitable for biological control programs targeting moisture-limited agricultural environments, potentially extending the geographical and seasonal range where EPNs can be effectively used as sustainable pest management tools.

6.5 References

Andrássy, I., and Zombori, L., 1976. Evolution as a basis for the systematization of nematodes. (London: Pitman).

Coghlan, A., 2005. Nematode genome evolution, in: WormBook: The Online Review of *C. Elegans* Biology [Internet]. WormBook.

Crowe J., Hoekstra, F.A. and Crowe, L.M., 1992. Anhydrobiosis. *Annal. Review Physiology*. 54:579-599.

Grzyb, T., Skłodowska, A., 2022. Introduction to Bacterial Anhydrobiosis: A General Perspective and the Mechanisms of Desiccation-Associated Damage. *Microorganisms* 10, 432. https://doi.org/10.3390/microorganisms10020432

Lee, S., Kim, Y. and Han, S., 2000. An improved collecting method of the infective juveniles of the entomopathogenic nematode, *Steinernema carpocapsae* Weiser. *Korean J. Soil Zool*, *5*, pp.97-100.

Liu Q.Z., and I. Glazer., 2000. Desiccation survival of entomopathogenic nematodes of the genus *Heterorhabditis*. *Phytoparasitica*. 28(4):331-340.

Morton A, Garcia-del-Pino F., 2009. Ecological characterization of entomopathogenic nematodes isolated in stonefruit orchard soils of Mediterranean areas. *Journal of Invertebrate Pathology.*;102:203–213. https://doi.org/10.1016/j.jip.2009.08.002.

Nagwani, A.K., Melosik, I., Kaczmarek, Ł., Kmita, H., 2024. Recovery from anhydrobiosis in the tardigrade *Paramacrobiotus experimentalis*: Better to be young than old and in a group than alone. *Heliyon* 10. https://doi.org/10.1016/j.heliyon.2024.e26807

Platt, H.M., 1994. Foreward. In: The phylogenetic systematics of free-living nematodes, S. Lorenzen, ed. (London: The Ray Society).

Ramakrishnan, J., Salame, L., Nasser, A., Glazer, I., Ment, D., 2022. Survival and efficacy of entomopathogenic nematodes on exposed surfaces. *Sci Rep 12*, 4629. https://doi.org/10.1038/s41598-022-08605-2

Sapir, A., 2021. Why are nematodes so successful extremophiles? *Communicative & Integrative Biology*. 14, 24–26. https://doi.org/10.1080/19420889.2021.1884343

Shapiro-Ilan DI, Mbata GN, Nguyen KB, Peat SM, Blackburn D, Adams BJ., 2009. Characterization of biocontrol traits in the entomopathogenic nematode Heterorhabditis georgiana (Kesha strain), and phylogenetic analysis of the nematode's symbiotic bacteria. *Biological Control*; 51:377–387.

Shapiro-Ilan, D.I., Brown, I., Lewis, E.E., 2014. Freezing and Desiccation Tolerance in Entomopathogenic Nematodes: Diversity and Correlation of Traits. *The Journal of Nematology*. 46, 27–34.

Singh, S., Ambastha, V., Levine, A., Sopory, S.K., Yadava, P.K., Tripathy, B.C., Tiwari, B.S., 2015. Anhydrobiosis and programmed cell death in plants: Commonalities and Differences. *Current Plant Biology* 2, 12–20. https://doi.org/10.1016/j.cpb.2014.12.001

Steyn, W., Malan, A., Slabbert, M., 2017. Entomopathogenic nematodes <EPNs> for the control of Lepidopteran pests in litchi orchards in south Africa 23.

Chapter 7
Appendix

7.1 Nematode DNA extraction protocol

To the crushed nematodes, 350 µl of CTL buffer and 25 µl of Proteinase K solution was added and vortexed briefly to allow thorough mixing. The sample was then incubated overnight at 37°C and checked the next day to ensure that it was completely solubilised before the subsequent steps were performed. To the tube, 350 µl chloroform: isoamyl alcohol (24:1) was then added and vortexed to mix thoroughly. Sample was then centrifuged at 10, 000 x g for 2 minutes at room temperature. 500 µl of upper aqueous phase was carefully transferred to a clean 1.5 ml microcentrifuge tube avoiding the milky layer containing contaminants and inhibitors. This was followed by the addition of 500 µl of BL buffer and 2 µl RNase A. The tube was then vortexed at maximum speed for 15 seconds. The sample was then placed in the dry bath (heating block) preheated to 70°C for 10 minutes. To this, one volume. that is, 500 µl of 100% ethanol was then added and the sample was vortexed at maximum speed for 15 seconds.

A HiBind DNA mini column was inserted into a 2 ml collection tube. 750 µl of the cleared lysate, including the precipitates that had formed, was then transferred by careful aspirating into the HiBind DNA mini column. The tube was centrifuged for 60 seconds at maximum speed and the filtrate discarded. To the HiBind DNA mini column, 500 µl of HBC buffer was added and centrifuged at maximum speed for 30 seconds. The filtrate was discarded, and the 2 ml collection tube was reused. 700 µl of wash buffer was then added and centrifuged at maximum speed for 1 minute. The wash step was repeated. The empty HiBind DNA mini column was centrifuged at maximum speed for 2 minutes to dry the column matrix. The column was then transferred to a clean 1.5 ml microcentrifuge tube and 50 ml of elution buffer preheated to 70°C was added directly to the centre of the column membrane and let to sit at room temperature for 2 minutes. The tube was then centrifuged for 1 minute at maximum speed.

7.2 DNA concentration and purity assessment using a Nanodrop spectrophotometer

DNA quantification and quality assessment was performed using spectrophotometric analysis using NanoDrop technology. The NanoDrop software was opened by selecting "Nucleic Acids" from the desktop application. Prior to analysis, the instrument was initialised by cleaning both upper and lower pedestals with surface wipes and then placing 2 µl of NanoPure water on the lower pedestal, followed by lowering the sampling arm and selecting "OK." After initialisation, the pedestals were wiped clean. The instrument was then calibrated by applying 2 µl of elution buffer to the lower pedestal and selecting the "blank" option after which the pedestals were cleaned with surface wipes. Following calibration, DNA samples (2 µl) were individually measured by placing each sample on the pedestal, entering the sample identifier, and selecting "measure." All data were saved and documented with image captures for reference.

DNA quality was assessed using multiple parameters. Samples were considered of sequencing quality when meeting the following criteria: concentration above 80 ng/µl, A260/A280 ratio between 1.8-2.0 (indicating minimal protein contamination), and A260/A230 ratio between 2.0-2.2 (confirming absence of contaminants such as phenol, carbohydrates, or guanidine salts).

7.3 Non-selective and selective agar preparation

7.3.1 Preparation of nutrient agar

To prepare the agar, 28 grams of NA was suspended in 1 litre of distilled water with continuous shaking. The mixture was heated while stirring to ensure all the components were fully dissolved. The mixture was then autoclaved at 121°C for 15 minutes and allowed to cool but not solidify. Once cooled sufficiently, the agar was dispensed into 90 mm petri dishes under a lamina flow with a flame on until the agar solidified. The lids were partially covered to ensure no moisture droplets form on the lid. Once the agar solidified, the plates were replaced and sealed with parafilm. These were stored in the walk-in freezer/ cold room (5°C) for use in subsequent experiments.

7.3.2 Preparation of MacConkey agar

To prepare the agar, 52 grams of the MacConkey agar powder was dispensed in 1 litre of distilled water and brought to a boil to allow it to completely dissolve. The mixture was autoclaved at 121°C for 15 minutes and allowed to cool but not solidify. Once cooled sufficiently, the agar was dispensed into petri dishes under a lamina flow with a flame on (90 mm) until the agar solidified. The lids were partially covered to ensure no moisture droplets form on the lid. Once the agar solidified, the plates were replaced and sealed with parafilm. These were stored in the walk-in freezer/ cold room for use in subsequent experiments.

7.3.3 Preparation of NBTA

20 g of nutrient agar was added to 1 litre of distilled water, with 0.025 g bromothymol blue. The mixture was autoclaved at 121°C for 15 minutes and allowed to cool but not solidify. To this, 0.04 g of 2, 3, 5-triphenyltetrazolium chloride was added and allowed to cool further but not solidify. The agar was adjusted to a pH of 7. The agar was dispensed into petri dishes under a lamina flow close to a flame until the agar solidified. The lids were partially covered to ensure no moisture droplets form on the lid. Once the agar solidified, the plates were replaced and sealed with parafilm. These were stored in the walk-in freezer/ cold room for use in subsequent experiments.

7.3.4 Preparation of nutrient agar broth

NA broth was prepared using commercially available NA broth powder. The powder was dissolved in 800 mL of distilled water in a 2 L Erlenmeyer flask using a magnetic stirrer. After complete dissolution, the volume was adjusted to 1 L with distilled water. The broth was transferred to four 250 mL autoclavable glass bottles, labelled appropriately, and autoclaved at 121°C for 20 minutes. After cooling to room temperature, the bottles were sealed tightly and stored at 4°C for later use. Prior to use, each bottle was visually inspected for clarity to ensure no contamination occurred during storage.

7.3.5 Preparation of Luria-Bertani broth

LB broth was prepared using a commercially available LB broth powder containing 10 g of tryptone, 5 g of yeast extract, and 10 g of NaCl. The powder was added to 800 mL of distilled

water in a 2 L Erlenmeyer flask and stirred with a magnetic stir bar until completely dissolved. The solution was then brought to a final volume of 1 L with additional distilled water. The prepared broth was transferred to four 250 mL autoclavable glass bottles, each filled to approximately two-thirds capacity. The bottles were capped loosely and labelled with contents, preparation date, and initials of the preparer. The broth was sterilised by autoclaving at 121°C (15 psi) for 20 minutes. Following sterilisation, the bottles were allowed to cool to room temperature before the caps were tightened. The sterile LB broth was stored in a cold room at 4°C and used within two weeks of preparation. Prior to use, each bottle was visually inspected for clarity to ensure no contamination occurred during storage.

7.4 Bacterial DNA extraction protocol

About 3 ml of LB culture was centrifuged at 4, 000 x g for 10 minutes at room temperature. It was then aspirated, and the culture media was discarded. To this, 100 µl of TE buffer was added and vortexed to completely resuspend the pellet. 10 µl of Lysozyme resuspended with Elution Buffer was added and the tube was incubated at 37°C for 10 minutes. Following this, aspiration was performed, and the media was discarded. 100 µl of TL Buffer and 20 µl of Proteinase K solution was added and the tube was vortexed to mix thoroughly. The tube was incubated in a 55°C water bath with brief vortexing done every 20 minutes. 5 µl RNase A was then added and the tube was inverted several times to mix thoroughly, and the tube was allowed to sit at room temperature for 5 minutes. The tube was then centrifuged at 10, 000 x g for 2 minutes to allow for the formation of a pellet of all undigested materials. The supernatant was then transferred to a new 1.5 ml microcentrifuge tube gently without disturbing the pellet.

After this, an addition of 220 µl of BL Buffer was added and vortexed to mix thoroughly. The tube was incubated in a heating block for 10 minutes at 65°C. This was followed by the addition of 220 µl of ethanol and the tube was vortexed for 20 seconds at maximum speed to mix thoroughly. Any precipitates formed were broken down by pipetting up and down about 10 times.

A HiBind DNA Mini Column was then added into a 2 ml collection tube and the entire sample was transferred into the HiBind DNA Minin Column including the precipitates that had formed. The tube was centrifuged at 10, 000 x g for 1 minute and the filtrate and collection tube were discarded. The HiBind DNA Mini Column was inserted into a new 2 ml collection tube and to

this, 500 µl of HBC Buffer diluted with 100% isopropanol was added. The filtrate formed was discarded. 700 µl of DNA Wash Buffer diluted with 100% ethanol was then added. The tube was centrifuged at 10, 000 x for 1 minute and the filtrate was discarded, and the collection tube reused. A second was step was performed as done above. The empty HiBind Mini Column was then centrifuged at maximum speed of greater than 10, 000 x for 2 minutes to dry the column. This was a critical step in the bacterial DNA extraction, as it resulted in the complete removal of the ethanol that would have interfered with the downstream applications. The HiBind DNA Minin Column was then inserted into a new nuclease-free 1.5 ml microcentrifuge tube. 50 µl of Elution Buffer was added that was preheated to 65°C. The tube was allowed to sit at room temperature for 5 minutes after which it was centrifuged at 10, 000 x g for 1 minute to elute the DNA. A second elution step was performed with another 50 µl of Elution Buffer.

7.5 Protocols for biochemical characterisation

7.5.1 Catalase test protocol

A clean microscope slide is placed inside a 90 mm petri dish to contain any potentially hazardous aerosols. The petri dish is positioned on a dark background to enhance visibility of the reaction. Using a sterile inoculation loop, a single well-isolated 24-hour bacterial colony is transferred to the slide. One drop of 3% hydrogen peroxide is added to the bacterial sample using a Pasteur pipette, and the petri dish cover is immediately replaced. The preparation is observed for bubble formation (effervescence) within 5 seconds, which indicates the release of oxygen gas. A magnifying glass may be used if necessary to detect weak reactions. Results are recorded as positive when immediate bubble formation is observed, indicating the presence of catalase enzyme, or negative when no bubbles appear, signifying the absence of catalase.

7.5.2 Oxidase test protocol

A 55 mm filter paper is placed in a clean petri dish and moistened with 2 drops of Remel oxidase reagent. While the paper is still damp, a loopful of bacterial culture is transferred to the treated area using a sterile loop. The paper is observed for colour change within 30 seconds. A positive result is indicated by the development of a dark purple colour within 10 seconds, demonstrating the presence of cytochrome C oxidase. A negative result is recorded when no

colour change is observed after 2 minutes, with the paper remaining yellow. This test effectively differentiates bacteria based on their respiratory metabolism pathways.

7.5.3 Gram staining protocol

A thin bacterial smear is prepared on a clean microscope glass slide and heat-fixed by passing it through a flame 3-4 times to adhere the cells to the slide. Crystal violet solution is applied and allowed to stand for 1 minute as the primary stain. The slide is then gently rinsed with distilled water before applying Gram's iodine solution, which acts as a mordant, and letting it stand for 1 minute. After another gentle rinse with distilled water, the smear is decolorised with 95% ethanol for 10-20 seconds or until no more colour runs from the smear. The slide is immediately rinsed with distilled water to stop the decolourisation process, followed by counterstaining with safranin for 30 seconds. Following a final rinse with distilled water, the slide is blotted dry with bibulous paper. The prepared slide is examined under oil immersion at 1000× magnification, and cell morphology and Gram reaction are recorded. Gram-positive bacteria retain the crystal violet-iodine complex and appear purple, while Gram-negative bacteria lose this complex during decolourisation and appear pinkish red from the safranin counterstain.

7.5.4 Endospore staining protocol

A thin bacterial smear is prepared on a clean microscope glass slide and heat-fixed by passing it through a flame 3-4 times. The slide is placed on a staining rack positioned over a water bath for controlled heating. The bacterial smear is covered with malachite green staining solution and steamed gently for 7 minutes, with additional stain added as needed to prevent the preparation from drying out. Following the staining period, the slide is allowed to cool for 2 minutes before being thoroughly rinsed with distilled water to remove excess primary stain. The smear is then counterstained with safranin for 90 seconds, which colours the vegetative cells but not the endospores. After a final rinse with distilled water, the slide is blotted dry and examined under oil immersion at 1000× magnification. In a positive result, endospores appear green due to retention of the malachite green stain, while vegetative cells appear pink or red from the safranin counterstain. This differential staining technique allows for clear visualisation and identification of endospore-forming bacteria, which are typically members of the genera *Bacillus* and *Clostridium.*

7.6 Bacterial phylogenetic trees: Pairwise analysis description

```
Analysis ====================
  Analysis                                = ====================
  Scope                                   = Pairs of taxa
  Estimate Variance                       = ====================
     Variance Estimation Method           = Bootstrap method
        Bootstrap Replicates              = 2000
  Substitution Model                      = ====================
     Substitutions Type                   = Nucleotide
     Model/Method                         = Tamura-Nei model
     Substitutions to Include             = d: Transitions + Transversions
  Rates and Patterns                      = ====================
     Rates among Sites                    = Uniform Rates
     Pattern among Lineages               = Same (Homogeneous)
  Data Subset to Use                      = ====================
     Gaps/Missing Data                    = Pairwise deletion
```

7.7 Temperature tolerance efficacy experimental setup

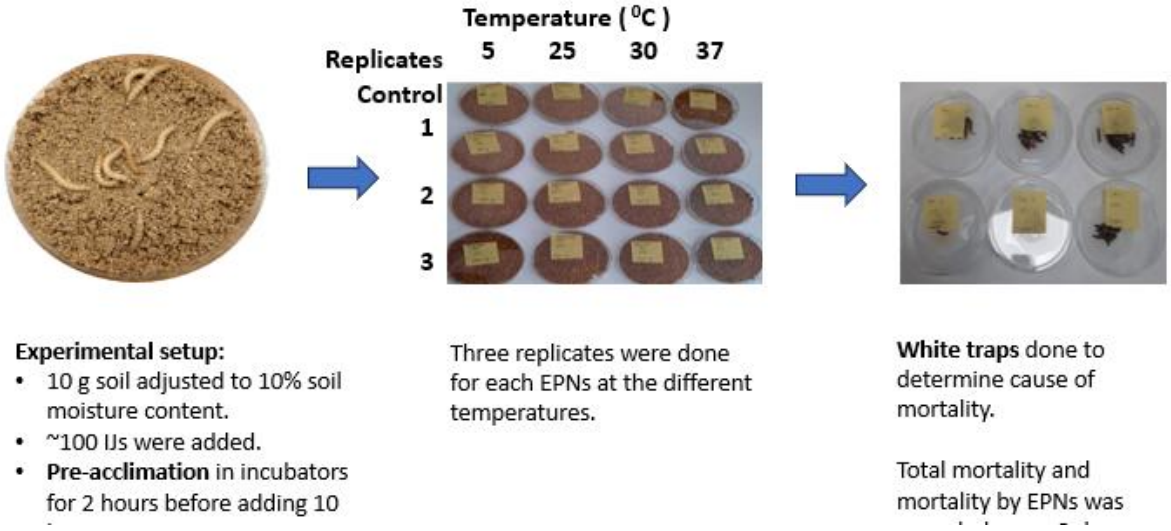

Figure 7.1 | Overview of the temperature efficacy testing protocol for *Oscheius* sp and *Cruznema* sp.

7.8 Python code for plotting and statistical analysis

7.8.1 LD80 python code

```python
from matplotlib.lines import Line2D
from scipy.stats import ttest_ind
import pandas as pd
import numpy as np
import matplotlib.pyplot as plt
import seaborn as sns

# Load data from CSV file and preprocess it by dropping unnecessary column and calculating percentage
src = pd.read_csv('../data/LD_50_OSCHEIUS.csv')
src['NUM_DEAD_PERCENT'] = (src['NUM_DEAD'] / 10) * 100  # Convert number of dead to percentage (assuming 10 is total)

# Group data by control status, time, and dose, then calculate mean mortality percentage
df = src.groupby(['CONTROL', 'TIME', 'IJS/LARVAE']).agg({'NUM_DEAD_PERCENT': 'mean'}).reset_index()
df = df.rename(columns={'NUM_DEAD_PERCENT': 'NUM_DEAD'})  # Rename column to reflect mean percentage
df = df.sort_values(by=['CONTROL', 'IJS/LARVAE'], ascending=[False, True])  # Sort for consistent ordering
df = df[['CONTROL', 'IJS/LARVAE', 'TIME', 'NUM_DEAD']]  # Reorder columns for clarity

# Define function to calculate standard error for each group
def calculate_se(group):
    n = len(group)  # Number of observations in the group
    return group['NUM_DEAD_PERCENT'].std() / np.sqrt(n) if n > 1 else 0  # SE = std / sqrt(n), 0 if n ⩽ 1

# Calculate standard error and merge with main dataframe
se = src.groupby(['CONTROL', 'TIME', 'IJS/LARVAE']).apply(calculate_se).reset_index()
se = se.rename(columns={0: 'SE'})  # Rename calculated SE column
df = pd.merge(df, se, on=['CONTROL', 'TIME', 'IJS/LARVAE'])  # Merge SE into main dataframe

# Define function to perform t-tests comparing experimental groups to control
def perform_ttest(time_dose_group, full_data):
    time, dose = time_dose_group.name  # Extract time and dose from group name
    if dose == 0:  # Skip control group (dose = 0)
        return np.nan
    experiment = time_dose_group['NUM_DEAD']  # Experimental group data
    control_data = full_data[(full_data['CONTROL'] == True) & (full_data['IJS/LARVAE'] == 0) & (full_data['TIME'] == time)]  # Matching control data
    control = control_data['NUM_DEAD']  # Control group data
    if len(control) > 1 and len(experiment) > 1:  # Ensure enough data for t-test
        t_stat, p_val = ttest_ind(control, experiment, equal_var=False)  # Welch's t-test (unequal variances)
        return p_val  # Return p-value
    return np.nan  # Return NaN if insufficient data

# Calculate p-values and merge with main dataframe
p_values = src.groupby(['TIME', 'IJS/LARVAE']).apply(lambda group: perform_ttest(group, src)).reset_index()
p_values = p_values.rename(columns={0: 'p_value'})  # Rename calculated p-value column
df = pd.merge(df, p_values, on=['TIME', 'IJS/LARVAE'], how='left')  # Left merge to retain all rows

```

```python

# Initialize plot with specified figure size
plt.figure(figsize=(15, 11))
df_filtered = df[df['TIME'] != 0].copy()  # Filter out time = 0 for plotting

# Define color palette for different doses
unique_doses = sorted(df_filtered['IJS/LARVAE'].unique())  # Get unique dose levels
blue_palette = sns.color_palette("Blues_r", n_colors=len(unique_doses) - 1)  # Blue shades for experimental doses
dose_color_map = {0: 'orange'}  # Control dose (0) in orange
for dose, color in zip([dose for dose in unique_doses if dose != 0], blue_palette):  # Assign colors to experimental doses
    dose_color_map[dose] = color

# Set up bar chart parameters
unique_times = sorted(df_filtered['TIME'].unique())  # Unique time points for x-axis
bar_width = 0.15  # Width of each bar
group_width = bar_width * len(unique_doses)  # Width of each time group
positions = np.arange(len(unique_times))  # Base positions for time points

# Dictionary to track positions of significance markers
marker_positions = {}

# Plot bars and error bars for each dose
for i, dose in enumerate(unique_doses):
    subset = df_filtered[df_filtered['IJS/LARVAE'] == dose]  # Subset data for current dose
    if not subset.empty:  # Proceed only if subset has data
        offset = (i - len(unique_doses) / 2) * bar_width + bar_width / 2  # Calculate offset for bar position
        bar_positions = positions + offset  # Adjust bar positions

        # Plot bars with appropriate labels and styling
        label = f"{dose} IJS/LARVAE ({'Control' if dose == 0 else 'Experiment'})"  # Label for legend
        edgecolor = 'black' if dose == 0 else None  # Black edge for control bars
        plt.bar(bar_positions, subset['NUM_DEAD'], width=bar_width, color=dose_color_map[dose],
                label=label if label not in plt.gca().get_legend_handles_labels()[1] else None,
                alpha=0.9, edgecolor=edgecolor, linewidth=1 if dose == 0 else 0)

        # Calculate error bar bounds (ensure lower bound doesn't go below 0)
        lower_err = np.minimum(subset['NUM_DEAD'], subset['SE'])
        upper_err = subset['SE']
        if dose == 0:  # Enhanced error bars for control group
            plt.errorbar(bar_positions, subset['NUM_DEAD'], yerr=[lower_err, upper_err], fmt='none',
                         ecolor='black', elinewidth=2.5, capsize=4, capthick=2)
        else:  # Standard error bars for experimental groups
            plt.errorbar(bar_positions, subset['NUM_DEAD'], yerr=[lower_err, upper_err], fmt='none',
                         ecolor='black', elinewidth=2, capsize=4, capthick=3)

```

```
89
90          # Add significance markers for experimental groups
91          if dose != 0:
92              for j, (index, row) in enumerate(subset.iterrows()):
93                  if pd.notna(row['p_value']):  # Check if p-value exists
94                      time = row['TIME']
95                      time_idx = unique_times.index(time)
96                      bar_pos = bar_positions[j]
97
98                      if (time, dose) not in marker_positions:  # Initialize marker count for this time-dose pair
99                          marker_positions[(time, dose)] = 0
100                     y_offset = 5 + (marker_positions[(time, dose)] * 5)  # Stack markers vertically
101                     y_pos = row['NUM_DEAD'] + row['SE'] + y_offset  # Position for marker
102
103                     if row['p_value'] < 0.01:  # Double asterisk for p < 0.01
104                         plt.text(bar_pos, y_pos, '**', ha='center', va='bottom',
105                                  fontsize=18, color='black', weight='bold', zorder=10)
106                         marker_positions[(time, dose)] += 1
107                     elif row['p_value'] < 0.05:  # Single asterisk for p < 0.05
108                         plt.text(bar_pos, y_pos, '*', ha='center', va='bottom',
109                                  fontsize=18, color='black', weight='bold', zorder=10)
110                         marker_positions[(time, dose)] += 1
111
112 # Customize plot appearance
113 plt.xlabel('Time (hours)', fontsize=16)  # X-axis label
114 plt.ylabel('Insect Mortality (%)', fontsize=16)  # Y-axis label
115 plt.tick_params(axis='both', which='major', labelsize=14)  # Tick label size
116 plt.grid(True, linestyle='--', alpha=0.7, axis='y')  # Add y-axis gridlines
117 plt.ylim(0, 120)  # Set y-axis range
118 plt.xticks(positions, unique_times)  # Set x-axis ticks to time points
119
120 # Create combined legend for doses and significance
121 dose_handles = [
122     Line2D([0], [0], color='orange', lw=4, label='0 IJS/LARVAE (Control)'),
123     Line2D([0], [0], color=dose_color_map[25], lw=4, label='25 IJS/LARVAE (Experiment)'),
124     Line2D([0], [0], color=dose_color_map[50], lw=4, label='50 IJS/LARVAE (Experiment)'),
125     Line2D([0], [0], color=dose_color_map[100], lw=4, label='100 IJS/LARVAE (Experiment)')
126 ]
127 sig_handles = [
128     Line2D([0], [0], linestyle='none', label='* p < 0.05'),  # Significance marker legend
129     Line2D([0], [0], linestyle='none', label='** p < 0.01')
130 ]
131 all_handles = dose_handles + sig_handles  # Combine all legend entries
132 plt.legend(handles=all_handles, title='Nematode Dose, Group, and Significance',
133            loc='lower center', bbox_to_anchor=(0.5, -0.25), ncol=3, fontsize=14, title_fontsize=14)  # Position legend below plot
134
135 plt.tight_layout()  # Adjust layout to prevent clipping
136 plt.savefig('../exports/lethal_dose.png', bbox_inches='tight')  # Save plot as PNG
137 plt.show()  # Display the plot
```

7.8.2 Temperature efficacy plotting and statistics (Python code)

```python
# Import matplotlib.pyplot for creating plots and visualizations
import matplotlib.pyplot as plt
# Import matplotlib.gridspec for creating a grid layout for subplots
import matplotlib.gridspec as gridspec
# Import numpy for numerical operations and array handling
import numpy as np
# Import matplotlib.patches for creating custom legend patches
import matplotlib.patches as mpatches
# Import matplotlib.lines for creating custom line elements in legends
from matplotlib.lines import Line2D
# Import pandas for data manipulation and analysis
import pandas as pd
# Import scipy.stats for statistical tests like Shapiro-Wilk and Levene's test
from scipy import stats
# Import statsmodels.api for statistical modeling tools
import statsmodels.api as sm
# Import ols from statsmodels.formula.api for ordinary least squares regression
from statsmodels.formula.api import ols
# Import MultiComparison for Tukey's HSD post-hoc tests
from statsmodels.stats.multicomp import MultiComparison
# Import anova_lm for performing ANOVA on fitted models
from statsmodels.stats.anova import anova_lm
# Import het_breuschpagan for testing heteroscedasticity in regression residuals
from statsmodels.stats.diagnostic import het_breuschpagan

# Analysis Function
def comprehensive_analysis(df):
    """
    Analyze how temperature, species, exposure time, and control vs. treatment affect nematode mortality.
    """
    # Create a copy of the DataFrame to avoid modifying the original data
    df = df.copy()
    # Define required columns for the analysis
    required_columns = ['SPECIES', 'TEMP', 'TIME', 'CONTROL', 'DEATH_EPN', 'PERCENT_DEAD']
    # Check if all required columns are present in the DataFrame
    if not all(col in df.columns for col in required_columns):
        raise ValueError(f"Missing required columns: {set(required_columns) - set(df.columns)}")

    # Fill NaN values in 'PERCENT_DEAD' with 0 and add small random noise to prevent zero variance issues
    df['PERCENT_DEAD'] = df['PERCENT_DEAD'].fillna(0) + np.random.normal(0, 0.001, len(df))

    # Warn if the sample size is small, which could affect statistical reliability
    if len(df) < 20:
        print("Warning: Small sample size may affect reliability (<20 observations)")

    # Step 1: Assumption Testing for statistical tests
    print("1. ASSUMPTION TESTING")
    print("-" * 50)

```

```
    # a) Test normality of data within each group using Shapiro-Wilk test
    print("\na) Normality Tests by Group:")
    for group, data in df.groupby(['TEMP', 'SPECIES', 'TIME', 'CONTROL']):
        n = len(data)
        std = data['PERCENT_DEAD'].std()
        # Perform Shapiro-Wilk test only if group size ≥ 3 and variance exists
        if n ≥ 3 and not np.isnan(std) and std > 0:
            stat, p = stats.shapiro(data['PERCENT_DEAD'])
            print(f"Group {group}: Shapiro-Wilk p={p:.4f} (n={n})")
        else:
            print(f"Group {group}: Skipped (n={n}, std={std:.4f})")

    # b) Test homogeneity of variance across groups using Levene's test
    print("\nb) Homogeneity of Variance:")
    groups = [group['PERCENT_DEAD'].dropna().values for _, group in
              df.groupby(['TEMP', 'SPECIES', 'TIME', 'CONTROL'])
              if len(group['PERCENT_DEAD'].dropna()) ≥ 3 and group['PERCENT_DEAD'].std() > 0]
    if len(groups) > 1:
        stat, p = stats.levene(*groups, center='median')
        print(f"Levene's test: p={p:.4f} (based on {len(groups)} groups)")
    else:
        print("Insufficient valid groups for Levene's test")

    # c) Test for heteroscedasticity using Breusch-Pagan test
    print("\nc) Heteroscedasticity Test:")
    try:
        # Fit a simple OLS model to test residuals
        model_simple = ols('PERCENT_DEAD ~ C(TEMP) + C(SPECIES) + C(TIME) + C(CONTROL)',
                           data=df.dropna()).fit()
        _, bp_p, _, _ = het_breuschpagan(model_simple.resid, model_simple.model.exog)
        print(f"Breusch-Pagan test: p={bp_p:.4f}")
        if bp_p < 0.05:
            print("Note: Heteroscedasticity detected; robust methods applied in ANOVA.")
    except Exception as e:
        print(f"Breusch-Pagan test failed: {e}")

    # Step 2: Perform ANOVA and Post-Hoc Tests
    print("\n2. ANOVA AND POST-HOC TESTS")
    print("-" * 50)
```

```
89
90      # a) Conduct a four-way ANOVA to assess main effects
91      print("\na) Four-way ANOVA Results:")
92      anova_table = None
93      full_model = None
94      formula = 'PERCENT_DEAD ~ C(TEMP) + C(SPECIES) + C(TIME) + C(CONTROL)'
95      try:
96          # Fit the full model with robust covariance (HC3) to handle potential heteroscedasticity
97          full_model = ols(formula, data=df.dropna()).fit(cov_type='HC3')
98          anova_table = anova_lm(full_model, typ=2, robust='hc3')
99          ss_residual = anova_table.loc['Residual', 'sum_sq']
100         # Calculate partial eta squared as an effect size metric
101         anova_table['partial_eta_sq'] = anova_table['sum_sq'] / (anova_table['sum_sq'] + ss_residual)
102         anova_table.loc['Residual', 'partial_eta_sq'] = np.nan
103         print(f"ANOVA Model: {formula}")
104         print(anova_table)
105     except np.linalg.LinAlgError:
106         # Fallback to a simpler model if the full model fails due to rank deficiency
107         print("Full model failed due to rank deficiency, trying simpler model")
108         formula = 'PERCENT_DEAD ~ C(TEMP) + C(SPECIES) + C(TIME) + C(CONTROL)'
109         try:
110             full_model = ols(formula, data=df.dropna()).fit(cov_type='HC3')
111             anova_table = anova_lm(full_model, typ=2, robust='hc3')
112             ss_residual = anova_table.loc['Residual', 'sum_sq']
113             anova_table['partial_eta_sq'] = anova_table['sum_sq'] / (anova_table['sum_sq'] + ss_residual)
114             anova_table.loc['Residual', 'partial_eta_sq'] = np.nan
115             print(f"Simplified ANOVA Model: {formula}")
116             print(anova_table)
117         except Exception as e:
118             print(f"Simplified ANOVA failed: {e}")
119     except Exception as e:
120         print(f"ANOVA failed: {e}")
121
122     # b) Perform Tukey HSD post-hoc tests for pairwise comparisons
123     print("\nb) Tukey HSD Tests:")
124     tukey_species_temp_results = {}
125
126     print("\nTEMP Comparisons:")
127     try:
128         # Compare 'PERCENT_DEAD' across different temperatures
129         temp_data = df[['TEMP', 'PERCENT_DEAD']].dropna()
130         mc_temp = MultiComparison(temp_data['PERCENT_DEAD'], temp_data['TEMP'])
131         tukey_temp_result = mc_temp.tukeyhsd()
132         print(tukey_temp_result)
133     except Exception as e:
134         print(f"TEMP Comparisons failed: {e}")
135
```

```
    print("\nSpecies within TEMP Comparisons:")
    # Compare species within each temperature level
    for temp in df['TEMP'].dropna().unique():
        temp_data = df[df['TEMP'] == temp].dropna(subset=['PERCENT_DEAD', 'SPECIES'])
        if len(temp_data['SPECIES'].unique()) > 1 and len(temp_data) >= 6:
            try:
                mc = MultiComparison(temp_data['PERCENT_DEAD'], temp_data['SPECIES'])
                result = mc.tukeyhsd()
                print(f"\nAt TEMP = {temp}°C:")
                print(result)
                tukey_species_temp_results[temp] = result
            except Exception as e:
                print(f"Error at TEMP = {temp}°C: {e}")

    # Step 3: Calculate Effect Sizes
    print("\n3. EFFECT SIZE ANALYSIS")
    print("-" * 50)

    # a) Calculate Cohen's d for control vs. treatment within each temp-species combination
    print("\na) Cohen's d Effect Sizes:")
    cohens_d_results = {}
    for temp in df['TEMP'].dropna().unique():
        for species in df['SPECIES'].unique():
            subset = df[(df['TEMP'] == temp) & (df['SPECIES'] == species)].dropna(subset=['PERCENT_DEAD'])
            control = subset[subset['CONTROL']]['PERCENT_DEAD']
            treatment = subset[~subset['CONTROL']]['PERCENT_DEAD']
            # Compute Cohen's d only if sufficient data and variance exist
            if len(control) >= 3 and len(treatment) >= 3 and control.std() > 0 and treatment.std() > 0:
                pooled_std = np.sqrt(((len(control)-1)*control.var() + (len(treatment)-1)*treatment.var()) /
                                     (len(control) + len(treatment) - 2))
                cohens_d = (treatment.mean() - control.mean()) / pooled_std
                print(f"TEMP={temp}, Species={species}: Cohen's d = {cohens_d:.2f} "
                      f"(n_control={len(control)}, n_treatment={len(treatment)})")
                cohens_d_results[(temp, species)] = cohens_d
            else:
                print(f"TEMP={temp}, Species={species}: Skipped "
                      f"(n_control={len(control)}, n_treatment={len(treatment)}, "
                      f"std_control={control.std():.4f}, std_treatment={treatment.std():.4f})")

    # Return results for further use
    return anova_table, full_model, tukey_species_temp_results, cohens_d_results
```

```
177
178 def get_statistical_summary(df, anova_results, model):
179     # Provide a summary of the ANOVA results if available
180     if anova_results is None or model is None:
181         return "ANOVA failed, no summary available.", []
182
183     # Compile model fit statistics
184     summary = [f"Model Fit: R² = {model.rsquared:.3f}, Adjusted R² = {model.rsquared_adj:.3f}"]
185     significant_effects = []
186
187     # Identify significant effects from ANOVA table
188     for idx, row in anova_results.iterrows():
189         if idx != 'Residual' and not pd.isna(row['PR(>F)']):
190             p_val = row['PR(>F)']
191             eta_sq = row['partial_eta_sq']
192             if p_val < 0.05:
193                 sig = '***' if p_val < 0.001 else '**' if p_val < 0.01 else '*'
194                 significant_effects.append(f"{idx} (p={p_val:.3f}{sig}, n²={eta_sq:.3f})")
195
196     summary.append("\nSignificant Effects (p < 0.05):")
197     summary.extend(significant_effects if significant_effects else ["None detected"])
198     return "\n".join(summary), significant_effects
199
200 # Load data from CSV file
201 src = pd.read_csv('../data/EFF_FINAL.csv')
202 # Run the comprehensive analysis
203 anova_results, model, tukey_species_temp_results, cohens_d_results = comprehensive_analysis(src)
204 # Generate and print the statistical summary
205 summary_text, significant_effects = get_statistical_summary(src, anova_results, model)
206 print("\n=== Statistical Results ===")
207 print("-" * 50)
208 print("Four-way ANOVA Results:")
209 print(anova_results.to_string() if anova_results is not None else "ANOVA failed.")
210 print("\nModel Fit and Significant Effects:")
211 print(summary_text)
212 print("\nTukey HSD Tests for Species within TEMP:")
213 for temp, result in tukey_species_temp_results.items():
214     print(f"\nAt TEMP = {temp}°C:")
215     print(result)
216 print("\nCohen's d Effect Sizes:")
217 for (temp, species), d in cohens_d_results.items():
218     print(f"TEMP={temp}, Species={species}: Cohen's d = {d:.2f}")
219 print("-" * 50)
220
221
```

```
221
222 def plot_species_efficacy(df, temp_levels):
223     """
224     Plot efficacy charts with control lines and stacked bars for treatment survival, natural death, and EPN killed.
225     Includes error bars, significance asterisks above bars based on t-tests, and CI in legend.
226     Handles precision loss in t-tests by checking sample size and variance.
227     """
228     ### Define colors and styles
229     # Define colors for each species for consistent visualization
230     species_colors = {'Oscheius': '#D3D3D3', 'Cruznema': '#4a4a4a'}
231     # Define line styles for control lines of each species
232     species_styles = {'Oscheius': '-', 'Cruznema': '--'}
233     # Define colors for treatment survival bars
234     treatment_colors = {'Oscheius': '#D3D3D3', 'Cruznema': '#4a4a4a'}
235     # Define color for EPN-killed portion in stacked bars
236     epn_killed_color = '#1EB0FF'
237     # Define color for natural death portion in stacked bars
238     natural_death_color = '#B7410E'
239
240     ### Define time points
241     # Specify the time points to display on the x-axis
242     display_times = [2, 4, 6, 8]
243
244     ### Enable LaTeX-like rendering
245     # Disable LaTeX rendering and set font to serif for better readability
246     plt.rc('text', usetex=False)
247     plt.rc('font', family='serif')
248
249     ### Set up the figure with subplots
250     # Create a figure with specified size and white background
251     fig = plt.figure(figsize=(20, 8.5))
252     fig.patch.set_facecolor('white')
253     # Define a grid layout with varying width and height ratios for subplots
254     gs = gridspec.GridSpec(4, len(temp_levels) + 1, width_ratios=[0.01] + [1]*len(temp_levels),
255                            height_ratios=[0.8, 0.1, 0.1, 0.1])
256
257     ### Add y-axis label
258     # Create a subplot for the y-axis label only (no axes)
259     ax_ylabel = fig.add_subplot(gs[0, 0])
260     ax_ylabel.axis('off')
261     ax_ylabel.set_ylabel('Cumulative Survival (%)', fontsize=18)
262
263     ### Define species list
264     # List of species to analyze and plot
265     species_list = ['Oscheius', 'Cruznema']
266
```

```
    ### Plot for each temperature
    for temp_idx, temp in enumerate(temp_levels):
        # Create a subplot for each temperature level
        ax_temp = fig.add_subplot(gs[0, temp_idx + 1])
        ax_temp.set_title(f'{temp}°C', fontsize=18, fontweight='bold')
        # Add a grid for visual reference
        ax_temp.grid(True, linestyle='--', alpha=0.7)
        ax_temp.tick_params(axis='y', labelsize=12)
        ax_temp.patch.set_alpha(0)

        ### Filter data for this temperature
        # Extract data specific to the current temperature
        temp_data = df[df['TEMP'] == temp]

        ### Plot control lines for each species (cumulative) with error bars
        for species in species_list:
            # Filter control data for the current species
            control_data = temp_data[(temp_data['SPECIES'] == species) & (temp_data['CONTROL'] == True)]
            if not control_data.empty:
                # Aggregate control data by time for mean, std, and count
                aggregated_data = control_data.groupby('TIME')['PERCENT_DEAD'].agg(['mean', 'std', 'count']).reset_index()
                times = aggregated_data['TIME'].values
                percent_dead_mean = aggregated_data['mean'].values
                percent_dead_se = aggregated_data['std'].values / np.sqrt(aggregated_data['count'].values)
                # Add initial time point (0) with zero death
                times = np.concatenate([[0], times])
                percent_dead_mean = np.concatenate([[0], percent_dead_mean])
                percent_dead_se = np.concatenate([[0], percent_dead_se])
                # Sort data by time to ensure correct order
                sorted_indices = np.argsort(times)
                times = times[sorted_indices]
                percent_dead_mean = percent_dead_mean[sorted_indices]
                percent_dead_se = percent_dead_se[sorted_indices]
                # Calculate cumulative death and survival
                cumulative_dead = np.cumsum(percent_dead_mean)
                cumulative_se = np.sqrt(np.cumsum(percent_dead_se ** 2))
                survival = 100 - cumulative_dead
                survival_se = cumulative_se
                # Interpolate survival across all time points (0-8)
                full_times = np.arange(0, 9)
                survival_full = np.interp(full_times, times, survival)
                # Set color based on species
                color = 'black' if species == 'Cruznema' else 'gray'
                # Plot control line
                ax_temp.plot(full_times, survival_full, color=color,
                             linestyle=species_styles[species], linewidth=2,
                             label=f'${{ {species} }}$ Control', zorder=10)
                # Add error bars at display times
                survival_at_display = np.interp(display_times, times, survival)
                se_at_display = np.interp(display_times, times, survival_se)
                ax_temp.errorbar(display_times, survival_at_display, yerr=se_at_display,
                                 fmt='none', color=color, capsize=5, capthick=1, zorder=11)
```

```
        ### Prepare bar data with spacing
        # Define bar width and gap between species bars
        bar_width = 0.35
        small_gap = 0.4
        x_positions = np.array(display_times)

        ### Calculate and plot stacked bars with significance
        for species_idx, species in enumerate(species_list):
            # Filter data for the current species
            species_data = temp_data[temp_data['SPECIES'] == species]
            natural_death_means = []
            epn_killed_means = []
            survival_means = []
            survival_ses = []
            survival_cis = []
            significance = []

            ### Calculate control survival for comparison
            control_data = temp_data[(temp_data['SPECIES'] == species) & (temp_data['CONTROL'] == True)]

            for time in display_times:
                # Filter treatment and control data for the current time
                treat_data = species_data[(species_data['TIME'] == time) & (species_data['CONTROL'] == False)]
                ctrl_data = control_data[control_data['TIME'] == time]
                if not treat_data.empty:
                    # Calculate mean EPN-killed and natural death percentages
                    epn_data = treat_data[treat_data['DEATH_EPN'] == True]
                    epn_killed_mean = epn_data['PERCENT_DEAD'].mean() if not epn_data.empty else 0
                    nat_data = treat_data[treat_data['DEATH_EPN'] == False]
                    natural_death_mean = nat_data['PERCENT_DEAD'].mean() if not nat_data.empty else 0
                    total_dead_mean = treat_data['PERCENT_DEAD'].mean()
                    total_dead_se = treat_data['PERCENT_DEAD'].std() / np.sqrt(len(treat_data)) if len(treat_data) > 1 else 0
                    survival_mean = 100 - total_dead_mean
                    survival_se = total_dead_se
                    # Calculate 95% Confidence Interval
                    ci = stats.t.interval(confidence=0.95, df=len(treat_data)-1, loc=survival_mean, scale=survival_se) if len(treat_data) > 1 and t
                    survival_ci = (ci[1] - ci[0]) / 2

                    # Perform t-test for significance vs control with safeguards
                    if (not ctrl_data.empty and len(treat_data) >= 2 and len(ctrl_data) >= 2 and
                        treat_data['PERCENT_DEAD'].std() > 0 and ctrl_data['PERCENT_DEAD'].std() > 0):
                        t_stat, p_val = stats.ttest_ind(treat_data['PERCENT_DEAD'], ctrl_data['PERCENT_DEAD'], equal_var=False)
                        sig = '***' if p_val < 0.001 else '**' if p_val < 0.01 else '*' if p_val < 0.05 else ''
                    else:
                        sig = ''  # No significance if data is insufficient or variance is zero
                else:
                    # Default values if no treatment data is available
                    natural_death_mean = 0
                    epn_killed_mean = 0
                    survival_mean = 100
                    survival_se = 0
                    survival_ci = 0
                    sig = ''
```

```
            natural_death_means.append(natural_death_mean)
            epn_killed_means.append(epn_killed_mean)
            survival_means.append(survival_mean)
            survival_ses.append(survival_se)
            survival_cis.append(survival_ci)
            significance.append(sig)

        ### Calculate cumulative values
        # Compute cumulative means and standard errors for stacking
        natural_death_means = np.cumsum(natural_death_means)
        epn_killed_means = np.cumsum(epn_killed_means)
        survival_means = 100 - (epn_killed_means + natural_death_means)
        survival_ses = np.sqrt(np.cumsum(np.array(survival_ses) ** 2))
        survival_cis = np.sqrt(np.cumsum(np.array(survival_cis) ** 2))

        ### Plot stacked bars
        # Calculate offset for species bars
        offset = species_idx * (bar_width + small_gap) - (bar_width + small_gap) / 2
        # Plot survival bars with error bars
        bars = ax_temp.bar(x_positions + offset, survival_means,
                           bar_width, color=treatment_colors[species],
                           edgecolor='black',
                           label=f'${{ {species} }}$ Survival (CI ±{survival_cis[-1]:.1f}%)',
                           yerr=survival_ses, error_kw={'capsize': 5, 'capthick': 1}, zorder=5)
        # Plot EPN-killed bars stacked on survival
        ax_temp.bar(x_positions + offset, epn_killed_means,
                    bar_width, bottom=survival_means, color=epn_killed_color,
                    edgecolor='black',
                    label=f'${{ {species} }}$ EPN Killed' if species_idx == 0 else "", zorder=5)
        # Plot natural death bars stacked on top
        ax_temp.bar(x_positions + offset, natural_death_means,
                    bar_width, bottom=[i + j for i, j in zip(survival_means, epn_killed_means)],
                    color=natural_death_color, edgecolor='black',
                    label=f'${{ {species} }}$ Natural Death' if species_idx == 0 else "", zorder=5)

        ### Add significance asterisks above bars
        for bar, sig in zip(bars, significance):
            height = bar.get_height()
            total_height = height + epn_killed_means[bars.index(bar)] + natural_death_means[bars.index(bar)]
            ax_temp.text(bar.get_x() + bar.get_width() / 2, total_height + 5,
                         sig, ha='center', va='bottom', fontsize=12, fontweight='bold')

```

```
        ### Customize axes
        # Set x-ticks and labels
        ax_temp.set_xticks(display_times)
        ax_temp.set_xticklabels([f'{t}' for t in display_times], fontsize=12)
        ax_temp.set_xlabel('Time (Days)', fontsize=14)
        ax_temp.set_ylim(0, 110)
        # Show y-label only on the leftmost plot
        if temp_idx == 0:
            ax_temp.set_ylabel('Cumulative Survival (%)', fontsize=16)
        else:
            ax_temp.set_yticklabels([])
        # Set x-axis limits with padding
        ax_temp.set_xlim(min(display_times) - 0.5 - bar_width - small_gap,
                         max(display_times) + 0.5 + bar_width + small_gap)

    ### Add legends
    # Species legend
    ax_species_legend = fig.add_subplot(gs[2, :len(temp_levels)//2+1])
    ax_species_legend.axis('off')
    ax_species_legend.patch.set_alpha(0)
    species_legend_elements = [
        mpatches.Patch(facecolor=species_colors[species], edgecolor='black',
                       label=f'${{ {species} }}$')
        for species in species_list
    ]
    ax_species_legend.legend(handles=species_legend_elements, loc='center',
                             ncol=len(species_list), fontsize=14, title='Species',
                             title_fontsize=16)

    # Treatment condition legend
    ax_treatment_legend = fig.add_subplot(gs[2, len(temp_levels)//2+1:])
    ax_treatment_legend.axis('off')
    ax_treatment_legend.patch.set_alpha(0)
    treatment_legend_elements = [
        mpatches.Patch(facecolor=treatment_colors['Oscheius'], edgecolor='black', label='Survival'),
        mpatches.Patch(facecolor=natural_death_color, edgecolor='black', label='Natural Death'),
        mpatches.Patch(facecolor=epn_killed_color, edgecolor='black', label='EPN Killed')
    ]
    ax_treatment_legend.legend(handles=treatment_legend_elements, loc='center', ncol=3,
                               fontsize=14, title='Condition', title_fontsize=16)


    ### Add significance legend
    ax_sig_legend = fig.add_subplot(gs[3, :])
    ax_sig_legend.axis('off')
    ax_sig_legend.patch.set_alpha(0)
    sig_legend_elements = [
        Line2D([0], [0], marker='None', label='Statistical Significance:', linestyle=''),
        Line2D([0], [0], marker='$***$', label='p < 0.001', markersize=15, linestyle='', color='black'),
        Line2D([0], [0], marker='$**$', label='p < 0.01', markersize=11, linestyle='', color='black'),
        Line2D([0], [0], marker='$*$', label='p < 0.05', markersize=8, linestyle='', color='black')
    ]
    ax_sig_legend.legend(handles=sig_legend_elements, loc='center', ncol=4,
                         fontsize=12, title_fontsize=14)

    ### Adjust layout
    # Tighten layout and adjust spacing between subplots
    plt.tight_layout()
    plt.subplots_adjust(wspace=0.05, hspace=0.2)
    plt.show()

### Main execution
# Get unique temperature levels from the DataFrame and sort them
temp_levels = sorted(src['TEMP'].unique())
# Call the plotting function with the data and temperature levels
plot_species_efficacy(src, temp_levels)
```

7.8.3 Desiccation plotting python code

```python
import pandas as pd  # For handling data tables (like your nematode survival data)
import numpy as np  # For numerical calculations (e.g., averages, variances)
from scipy import stats  # For tests like Shapiro-Wilk to check normality
import statsmodels.api as sm  # For ANOVA and regression models
from statsmodels.formula.api import ols  # For setting up the ANOVA formula
from statsmodels.stats.multicomp import MultiComparison  # For Tukey HSD comparisons
from statsmodels.stats.diagnostic import het_breuschpagan  # For checking error patterns
import matplotlib.pyplot as plt  # For creating plots
import matplotlib.gridspec as gridspec  # For arranging subplots neatly
import matplotlib.patches as mpatches  # For legend patches (e.g., species colors)
from matplotlib.lines import Line2D  # For significance markers in the legend

def comprehensive_analysis(df):
    """
    Analyze how relative humidity (RH), species (Oscheius and Cruznema), exposure time (24h and 48h),
    and control vs. treatment conditions affect nematode survival, as described in the methodology.
    """
    # Prepare the data for analysis by making a copy and setting the right data types
    df = df.copy()
    df['CONTROL'] = df['CONTROL'].astype(bool)  # Convert CONTROL column to boolean (TRUE/FALSE) for control or treatment
    df['RH'] = df['RH'].astype(float)  # Convert RH levels (33, 53, 75, 85) to floating-point numbers
    df['TIME'] = df['TIME'].astype(float)  # Convert exposure time (24h, 48h) to floating-point numbers
    df['PERCENT_SURVIVAL'] = df['PERCENT_SURVIVAL'].astype(float)  # Convert survival percentage (0-100) to floating-point
    df['SPECIES'] = df['SPECIES'].astype(str)  # Ensure species names (Oscheius, Cruznema) are strings

    # Step 1: Check if survival percentages are suitable for our main analysis (ANOVA)
    print("1. ASSUMPTION TESTING")
    print("-" * 50)

    # Test if data follows a normal distribution using Shapiro-Wilk test
    print("\na) Normality Tests by Group:")
    for group, data in df.groupby(['RH', 'SPECIES', 'TIME', 'CONTROL']):
        if data['PERCENT_SURVIVAL'].std() > 0:  # Only test normality if there's variation in the data
            stat, p = stats.shapiro(data['PERCENT_SURVIVAL'].values)  # Perform Shapiro-Wilk test on survival values
            if p <= 0 or p != p:  # Handle invalid p-values (negative, zero, or NaN) often due to small sample sizes
                p = 0.001  # Substitute with a small positive value as a fallback
                print(f"Warning: Invalid p-value (e.g., {p:.4f}) for group {group}. Likely due to small sample size. Using 0.001 as substitute.")
            print(f"Group {group}: Shapiro-Wilk p={p:.4f}")  # Display p-value; p > 0.05 suggests data is normal enough

    # Check if variances are similar across groups with Levene's test
    print("\nb) Homogeneity of Variance Tests:")
    groups = [group['PERCENT_SURVIVAL'].values for _, group in
              df.groupby(['RH', 'SPECIES', 'TIME', 'CONTROL'])]  # Extract survival data for each group
    levene_stat, levene_p = stats.levene(*groups)  # Perform Levene's test for equal variances
    print(f"Levene's test: p={levene_p:.4f}")  # Display p-value; p > 0.05 indicates variances are similar

    # Check if error patterns are consistent using Breusch-Pagan test
    print("\nc) Heteroscedasticity Test:")
    model = ols('PERCENT_SURVIVAL ~ C(RH) + C(SPECIES) + C(TIME) + C(CONTROL)', data=df).fit()  # Fit a basic OLS model
    _, bp_p, _, _ = het_breuschpagan(model.resid, model.model.exog)  # Test for consistent error variance
    print(f"Breusch-Pagan test: p={bp_p:.4f}")  # Display p-value; p > 0.05 suggests errors are consistent

```

```
52
53      # Step 2: Use four-way ANOVA to explore effects of RH, species, time, and control/treatment
54      print("\n2. ANOVA AND POST-HOC TESTS")
55      print("-" * 50)
56
57      print("\na) Four-way ANOVA Results:")
58      # Set up ANOVA with main effects and their interactions (e.g., RH and species together)
59      full_model = ols('PERCENT_SURVIVAL ~ C(RH) + C(SPECIES) + C(TIME) + C(CONTROL) + ' +
60                       'C(RH):C(SPECIES) + C(RH):C(TIME) + C(RH):C(CONTROL) + ' +
61                       'C(SPECIES):C(TIME) + C(SPECIES):C(CONTROL) + C(TIME):C(CONTROL)',
62                       data=df).fit()  # Fit the full ANOVA model including interactions
63      anova_table = sm.stats.anova_lm(full_model, typ=2)  # Generate ANOVA table (Type 2 for balanced interaction terms)
64
65      # Measure the size of effects with partial eta-squared to show biological importance
66      anova_table['partial_eta_sq'] = np.nan  # Initialize a column for effect sizes
67      ss_residual = anova_table.loc['Residual', 'sum_sq']  # Get residual sum of squares (unexplained variance)
68      for idx in anova_table.index:
69          if idx != 'Residual':
70              ss_effect = anova_table.loc[idx, 'sum_sq']  # Get sum of squares for this factor or interaction
71              anova_table.loc[idx, 'partial_eta_sq'] = ss_effect / (ss_effect + ss_residual)  # Calculate partial eta-squared
72      print(anova_table)  # Display ANOVA table with p-values and effect sizes
73
74      print("\nb) Tukey HSD Tests:")
75      print("\nRH Comparisons:")
76      # Check if each RH group has enough variation and samples to compare
77      rh_groups = df.groupby('RH')['PERCENT_SURVIVAL'].apply(lambda x: len(x.unique()) > 1 and len(x) > 1)
78      valid_rh = rh_groups[rh_groups].index  # Identify RH levels with sufficient data for comparison
79      if len(valid_rh) > 1:  # Ensure there are at least 2 valid RH levels to compare
80          mc_rh = MultiComparison(df[df['RH'].isin(valid_rh)]['PERCENT_SURVIVAL'], df[df['RH'].isin(valid_rh)]['RH'])
81          tukey_rh_result = mc_rh.tukeyhsd()  # Perform Tukey HSD test to compare RH levels
82          print(tukey_rh_result)  # Display results showing which RH levels differ significantly
83      else:
84          print("Warning: Insufficient variation or samples for RH comparisons. Tukey HSD skipped.")  # Warn if data is inadequate
85
86      print("\nSpecies within RH Comparisons:")
87      tukey_species_rh_results = {}  # Dictionary to store Tukey HSD results for plotting
88      for rh in df['RH'].unique():
89          rh_data = df[df['RH'] == rh]  # Filter data for the current RH level
90          if len(rh_data) > 1 and len(rh_data['SPECIES'].unique()) > 1:  # Check for multiple species and samples
91              mc = MultiComparison(rh_data['PERCENT_SURVIVAL'], rh_data['SPECIES'])  # Set up species comparison
92              try:
93                  print(f"\nAt RH = {rh}%:")
94                  result = mc.tukeyhsd()  # Perform Tukey HSD test for species at this RH
95                  print(result)  # Display results
96                  tukey_species_rh_results[rh] = result  # Store results for later use (e.g., plotting)
97              except Exception as e:
98                  print(f"Error at RH = {rh}%: {e}")  # Handle any errors during Tukey HSD calculation
99
100     # Step 4: Calculate Cohen's d to measure practical survival differences
101     print("\n3. EFFECT SIZE ANALYSIS")
102     print("-" * 50)
103
```

```
    print("\na) Cohen's d Effect Sizes:")
    cohens_d_results = {}  # Dictionary to store Cohen's d values for reporting or plotting
    for rh in df['RH'].unique():
        for species in df['SPECIES'].unique():
            subset = df[(df['RH'] == rh) & (df['SPECIES'] == species)]  # Filter data by RH and species
            if len(subset) > 0:
                control = subset[subset['CONTROL']]['PERCENT_SURVIVAL']  # Extract survival for control group
                treatment = subset[~subset['CONTROL']]['PERCENT_SURVIVAL']  # Extract survival for treatment group
                if len(control) > 0 and len(treatment) > 0:  # Ensure both groups have data
                    pooled_std = np.sqrt((np.var(control) + np.var(treatment)) / 2)  # Calculate pooled standard deviation
                    if pooled_std > 0:  # Avoid division by zero
                        cohens_d = (np.mean(control) - np.mean(treatment)) / pooled_std  # Compute Cohen's d
                        print(f"RH={rh}, Species={species}: Cohen's d = {cohens_d:.2f}")
                        cohens_d_results[(rh, species)] = cohens_d  # Store result

    return anova_table, full_model, tukey_species_rh_results, cohens_d_results  # Return results for further use

def get_statistical_summary(df, anova_results, model):
    """Summarize results with a fit score (R²) and highlight significant effects with p-values and effect sizes,
    linking numbers to real effects on nematode desiccation tolerance."""
    summary = []
    r2 = model.rsquared  # Proportion of variance explained by the model
    adj_r2 = model.rsquared_adj  # Adjusted R² accounting for the number of predictors
    summary.append(f"Model Fit: R² = {r2:.3f}, Adjusted R² = {adj_r2:.3f}")

    significant_effects = []  # List to collect significant effects
    for idx, row in anova_results.iterrows():
        if idx != 'Residual':
            p_val = row['PR(>F)']  # Extract p-value for this factor or interaction
            eta_sq = row['partial_eta_sq']  # Extract effect size (partial eta-squared)
            if p_val < 0.05:  # Check if the effect is statistically significant
                sig = '***' if p_val < 0.001 else '**' if p_val < 0.01 else '*'  # Assign significance stars
                significant_effects.append(f"{idx} (p={p_val:.2e}{sig}, n²={eta_sq:.3f})")  # Format significant effect

    summary.append("\nSignificant Effects:")
    summary.extend(significant_effects)  # Add significant effects to summary
    return f"\n{summary}\n\n\n", significant_effects  # Return formatted summary and list of significant effects

def plot_with_summary(df, significant_effects, tukey_species_rh_results, cohens_d_results):
    """Plot survival data with significance markers from Tukey HSD, reflecting the methodology's validation step."""
    def calculate_stats(group):
        # Calculate mean and standard error for a group of survival data
        stats = {
            'MEAN': group['PERCENT_SURVIVAL'].mean(),  # Average survival percentage
            'SE': group['PERCENT_SURVIVAL'].std() / np.sqrt(len(group)) if len(group) > 1 else 0  # Standard error
        }
        return pd.Series(stats)


    # Calculate average and standard error for each group
    stats = df.groupby(['SPECIES', 'CONTROL', 'TIME', 'RH']).apply(calculate_stats).reset_index()
    stats['TIME'] = stats['TIME'].astype(int)  # Convert TIME back to integer for plotting

    # Get unique values for plotting
    species_list = ['Oscheius', 'Cruznema']  # List of species
    rh_levels = sorted(stats['RH'].unique())  # Sorted unique RH levels (e.g., 33, 53, 75, 85)
    time_points = sorted(stats['TIME'].unique())  # Sorted unique time points (e.g., 24, 48)

    # Enable LaTeX rendering for italic text (simulated with Matplotlib's mathtext)
    plt.rc('text', usetex=False)  # Disable LaTeX, use mathtext instead
    plt.rc('font', family='serif')  # Set font to serif for a professional look

    # Set up the figure with subplots
    fig = plt.figure(figsize=(20, 8.5))  # Create a figure with specified size
    gs = gridspec.GridSpec(4, len(rh_levels) + 1, width_ratios=[0.01] + [1]*len(rh_levels), height_ratios=[0.8, 0.1, 0.1, 0.1])  # Define grid layout

    # Define colors for species
    species_colors = {'Oscheius': '#D3D3D3', 'Cruznema': '#6a6a6a'}  # Light gray and dark gray for species

    # Add y-axis label
    ax_ylabel = fig.add_subplot(gs[0, 0])  # Create subplot for y-axis label
    ax_ylabel.axis('off')  # Hide axes
    ax_ylabel.set_ylabel('Survival (%)', fontsize=18)  # Add y-axis label

    # Parse significant effects for potential use (e.g., main effects)
    significant_effects_dict = {}
    for effect in significant_effects:
        key = effect.split(' ')[0]  # Extract factor name (e.g., "C(RH)")
        p_val_str = effect.split('p=')[1].split(',')[0]  # Extract p-value with stars (e.g., "1.26e-60***")
        significant_effects_dict[key] = p_val_str
```

```
183
184     for rh_idx, rh in enumerate(rh_levels):
185         ax_rh = fig.add_subplot(gs[0, rh_idx + 1])  # Create subplot for each RH level
186         ax_rh.set_title(f'RH {rh}%', fontsize=18, fontweight='bold')  # Set title with RH percentage
187         ax_rh.axis('on')  # Keep axes visible
188         ax_rh.tick_params(axis='both', which='both', bottom=False, top=False, left=False, right=False, labelbottom=False, labelleft=False)  # Hide ticks
189         ax_rh.grid(True, linestyle='--', alpha=0.7)  # Add a dashed grid for readability
190
191         for species_idx, species in enumerate(species_list):
192             ax = ax_rh.inset_axes([species_idx/len(species_list), 0, 1/len(species_list), 1], transform=ax_rh.transAxes)  # Create inset axes for each s
193             species_data = stats[(stats['SPECIES'] == species) & (stats['RH'] == rh)]  # Filter data for this species and RH
194
195             x = np.arange(len(time_points))  # X positions for time points
196             width = 0.35  # Width of bars
197
198             max_height = 0  # Track maximum height for y-axis scaling
199             for is_control in [False, True]:  # Plot treatment then control
200                 data = species_data[species_data['CONTROL'] == is_control]  # Filter by control/treatment
201                 means = [data[data['TIME'] == time]['MEAN'].values[0] if not data[data['TIME'] == time].empty else 0 for time in time_points]  # Get mea
202                 ses = [data[data['TIME'] == time]['SE'].values[0] if not data[data['TIME'] == time].empty else 0 for time in time_points]  # Get standar
203
204                 yerr = ses  # Use standard error for error bars
205                 max_height = max(max_height, max([mean + se for mean, se in zip(means, ses)]))  # Update max height
206
207                 offset = width/2 if not is_control else -width/2  # Offset bars for treatment/control
208                 ax.bar(x + offset, means, width, color='white' if is_control else species_colors[species],
209                        edgecolor='black', hatch='//' if is_control else None,
210                        label='Control' if is_control else 'Treatment')  # Plot bars
211                 ax.errorbar(x + offset, means, yerr=yerr, fmt='none', ecolor='black', capsize=3)  # Add error bars
212
213                 # Add significance markers from Tukey HSD to validate species differences within RH
214                 if not is_control and rh in tukey_species_rh_results:
215                     tukey_result = tukey_species_rh_results[rh]  # Get Tukey HSD result for this RH
216                     for row in tukey_result._results_table.data[1:]:  # Skip header row
217                         group1, group2, _, p_adj, *_ = row  # Extract comparison details
218                         if {group1, group2} == {'Cruznema', 'Oscheius'} and p_adj < 0.05:  # Check if significant
219                             sig = '***' if p_adj < 0.001 else '**' if p_adj < 0.01 else '*'  # Assign significance stars
220                             for j, time in enumerate(time_points):
221                                 y_pos = means[j] + ses[j] + 2  # Position above error bar
222                                 ax.text(j + offset, y_pos, sig, ha='center', va='bottom', fontweight='bold')  # Add marker
223
```

```
            ax.set_xticks(x)  # Set x-axis ticks
            ax.set_xticklabels([f'{t}H' for t in time_points], fontsize=12, rotation=45, ha='right')  # Label time points (e.g., 24H, 48H)
            y_max = max(110, max_height * 1.1 + 10)  # Set y-axis limit with buffer
            ax.set_ylim(0, y_max)  # Apply y-axis limits

            if rh_idx == 0 and species_idx == 0:  # Add y-label only to the first subplot
                ax.set_ylabel('Survival (%)', fontsize=16)
            else:
                ax.set_ylabel('')  # No y-label for others
                ax.set_yticklabels([])  # Hide y-tick labels

            ax.tick_params(axis='y', labelsize=12)  # Set y-tick font size
            ax.patch.set_alpha(0)  # Make background transparent

        # Add species labels below the time points in *italics*
        ax_species = fig.add_subplot(gs[1, rh_idx + 1])  # Create subplot for species labels
        ax_species.axis('off')  # Hide axes
        for species_idx, species in enumerate(species_list):
            ax_species.text(species_idx / len(species_list) + 0.5 / len(species_list), 0.5, f'${{ {species} }}$',
                            ha='center', va='center', fontsize=14, transform=ax_species.transAxes)  # Add italicized species name

    # Add legend for species colors with *italics*
    ax_species_legend = fig.add_subplot(gs[2, :len(rh_levels)//2+1])  # Create subplot for species legend
    ax_species_legend.axis('off')  # Hide axes
    legend_elements = [mpatches.Patch(facecolor=color, edgecolor='black', label=f'${{ {species} }}$')
                       for species, color in species_colors.items()]  # Create legend patches
    ax_species_legend.legend(handles=legend_elements, loc='center', ncol=len(species_list),
                             fontsize=14, title='Species', title_fontsize=16)  # Add species legend

    # Add legend for treatment and control
    ax_treatment_legend = fig.add_subplot(gs[2, len(rh_levels)//2+1:])  # Create subplot for treatment legend
    ax_treatment_legend.axis('off')  # Hide axes
    treatment_legend_elements = [
        mpatches.Patch(facecolor='gray', edgecolor='black', label='Experiment'),  # Treatment patch
        mpatches.Patch(facecolor='white', edgecolor='black', hatch='//', label='Control')  # Control patch
    ]
    ax_treatment_legend.legend(handles=treatment_legend_elements, loc='center', ncol=2,
                               fontsize=14, title='Treatment', title_fontsize=16)  # Add treatment legend

    # Add legend for significance markers from Tukey HSD
    ax_sig_legend = fig.add_subplot(gs[3, :])  # Create subplot for significance legend
    ax_sig_legend.axis('off')  # Hide axes
    sig_legend_elements = [
        Line2D([0], [0], marker='None', label='Statistical Significance:', linestyle=''),  # Title entry
        Line2D([0], [0], marker='$***$', label='p < 0.001', markersize=15, linestyle='', color='black'),  # *** marker
        Line2D([0], [0], marker='$**$', label='p < 0.01', markersize=11, linestyle='', color='black'),  # ** marker
        Line2D([0], [0], marker='$*$', label='p < 0.05', markersize=8, linestyle='', color='black')  # * marker
    ]
    ax_sig_legend.legend(handles=sig_legend_elements, loc='center', ncol=4,
                         fontsize=14, title='Statistical Significance', title_fontsize=16)  # Add significance legend

    plt.tight_layout()  # Adjust layout to prevent overlap
    plt.subplots_adjust(wspace=0.05, hspace=0.2)  # Fine-tune spacing between subplots
    plt.show()  # Display the plot

# Run the analysis and plot
df = pd.read_csv('../data/DESC.csv')  # Load the nematode survival data from a CSV file
anova_results, model, tukey_species_rh_results, cohens_d_results = comprehensive_analysis(df)  # Perform comprehensive analysis
summary_text, significant_effects = get_statistical_summary(df, anova_results, model)  # Generate statistical summary
plot_with_summary(df, significant_effects, tukey_species_rh_results, cohens_d_results)  # Create and display the plot
```

7.8.4 Summary of Python libraries

Table 7.1: Summary of Python libraries used in the research code

Name	Version	Name	Version	Name	Version
altair	5.0.1	jupyterlab	4.2.5	prompt_toolkit	3.0.43
anyio	4.2.0	jupyterlab_pygments	0.1.2	psutil	5.9.0
appnope	0.1.2	jupyterlab_server	2.27.3	ptyprocess	0.7.0
argon2-cffi	21.3.0	jupyterlab_widgets	3.0.10	pure_eval	0.2.2
argon2-cffi-bindings	21.2.0	kiwisolver	1.4.4	pycparser	2.21
arrow	1.3.0	krb5	1.20.1	pygments	2.15.1
asttokens	2.0.5	lcms2	2.12	pyparsing	3.0.9
async-lru	2.0.4	lerc	3	pyqt	5.15.10
attrs	23.1.0	libbrotlicommon	1.0.9	pyqt5-sip	12.13.0
babel	2.11.0	libbrotlidec	1.0.9	pysocks	1.7.1
backcall	0.2.0	libbrotlienc	1.0.9	python	3.8.19
beautifulsoup4	4.12.3	libclang	14.0.6	python-dateutil	2.9.0post0
blas	1	libclang13	14.0.6	python-fastjsonschema	2.16.2
bleach	4.1.0	libcxx	14.0.6	python-json-logger	2.0.7
bottleneck	1.3.7	libdeflate	1.17	python-tzdata	2023.3
brotli	1.0.9	libedit	3.1.20230828	pytz	2024.1
brotli-bin	1.0.9	libffi	3.4.4	pyyaml	6.0.1
brotli-python	1.0.9	libgfortran	5.0.0	pyzmq	25.1.2
bzip2	1.0.8	libgfortran5	11.3.0	qt-main	5.15.2
ca-certificates	2024.7.2	libglib	2.78.4	qtconsole	5.6.0
certifi	2024.8.30	libiconv	1.16	qtpy	2.4.1
cffi	1.17.1	libllvm14	14.0.6	readline	8.2
charset-normalizer	3.3.2	libopenblas	0.3.21	referencing	0.30.2
comm	0.2.1	libpng	1.6.39	requests	2.32.3
contourpy	1.0.5	libpq	12.17	rfc3339-validator	0.1.4
cycler	0.11.0	libsodium	1.0.18	rfc3986-validator	0.1.1
cyrus-sasl	2.1.28	libtiff	4.5.1	rpds-py	0.10.6
debugpy	1.6.7	libwebp-base	1.3.2	scikit-learn	1.3.2
decorator	5.1.1	libxml2	2.13.1	scipy	1.10.1
defusedxml	0.7.1	llvm-openmp	14.0.6	seaborn	0.13.2
exceptiongroup	1.2.0	lz4-c	1.9.4	send2trash	1.8.2
executing	0.8.3	markupsafe	2.1.3	setuptools	75.1.0
fonttools	4.51.0	matplotlib	3.7.2	sip	6.7.12
fqdn	1.5.1	matplotlib-base	3.7.2	six	1.16.0
freetype	2.12.1	matplotlib-inline	0.1.6	sniffio	1.3.0
gettext	0.21.0	mistune	2.0.4	soupsieve	2.5
glib	2.78.4	mysql	5.7.24	sqlite	3.45.3
glib-tools	2.78.4	nbclient	0.8.0	stack_data	0.2.0
gst-plugins-base	1.14.1	nbconvert	7.10.0	statsmodels	0.14.1
gstreamer	1.14.1	nbformat	5.9.2	tabulate	0.9.0
h11	0.14.0	ncurses	6.4	terminado	0.17.1
httpcore	1.0.2	nest-asyncio	1.6.0	threadpoolctl	3.5.0
httpx	0.27.0	notebook	7.2.2	tinycss2	1.2.1
icu	73.1	notebook-shim	0.2.3	tk	8.6.14
idna	3.7	numexpr	2.8.4	tomli	2.0.1
importlib-metadata	7.0.1	numpy	1.24.3	toolz	0.12.0
importlib_metadata	7.0.1	numpy-base	1.24.3	tornado	6.4.1
importlib_resources	6.4.0	openjpeg	2.5.2	traitlets	5.14.3
ipykernel	6.28.0	openssl	3.0.15	types-python-dateutil	2.9.0.20241206
ipython	8.12.2	overrides	7.4.0	typing-extensions	4.11.0
ipywidgets	8.1.2	packaging	24.1	typing_extensions	4.11.0
isoduration	20.11.0	pandas	2.0.3	unicodedata2	15.1.0
jedi	0.19.1	pandas-flavor	0.6.0	uri-template	1.3.0
jinja2	3.1.4	pandocfilters	1.5.0	urllib3	2.2.2
joblib	1.4.2	parso	0.8.3	wcwidth	0.2.5
jpeg	9e	patsy	1.0.1	webcolors	24.8.0
json5	0.9.6	pcre2	10.42	webencodings	0.5.1
jsonpointer	3.0.0	pexpect	4.8.0	websocket-client	1.8.0
jsonschema	4.19.2	pickleshare	0.7.5	wheel	0.44.0
jsonschema-specifications	2023.7.1	pillow	10.4.0	widgetsnbextension	4.0.10
jupyter	1.0.0	pingouin	0.5.5	xarray	2023.1.0
jupyter-lsp	2.2.0	pip	24.2	xz	5.4.6
jupyter_client	8.6.0	pkgutil-resolve-name	1.3.10	yaml	0.2.5
jupyter_console	6.6.3	platformdirs	3.10.0	zeromq	4.3.5
jupyter_core	5.7.2	ply	3.11	zipp	3.17.0
jupyter_events	0.10.0	pooch	1.7.0	zlib	1.2.13
jupyter_server	2.14.1	prometheus_client	0.14.1	zstd	1.5.5
jupyter_server_terminals	0.4.4	prompt-toolkit	3.0.43		